Chapter 3
Enhancing the Speed of Rotation for Symmetrical Molecular Motors

In this chapter the smallest light-driven molecular motor that has been made so far is presented. This new motor molecule consists of only 28 carbon and 24 hydrogen atoms. It is shown that the concept of control over the direction of movement at the molecular level by introduction of substituents adjacent to the double bond of a sterically overcrowded alkene does not only hold for molecular motors with six-membered rings, but is also applicable to achieve unidirectional movement for molecular motors having five-membered rings. Despite the planar nature of the five-membered rings in the molecule, the energy differences between the (pseudo-)diaxial and (pseudo-)diequatorial orientation are large enough to direct the rotation of one half of the molecule with respect to the other half in a clockwise fashion. Like the molecular motors with a six-membered ring, the full rotary cycle is performed in four consecutive steps. Two energetically uphill photochemical isomerizations are each followed by a thermal helix inversion process. The entire rotary process is fueled by the light energy consumed in the two photochemical steps. The unidirectionality of the entire process is ensured by the preference of the substituents to adopt a (pseudo-)diaxial orientation in the irreversible thermal steps. Compared to the original molecular motor described in the previous chapter, the energy barrier for the rate determining thermal step has decreased dramatically. The half-life of the fastest step has been lowered to only 18 s at room temperature. The sterically more hindered molecular motor having five-membered rings and t-butyl groups attached to the stereogenic centers was also successfully synthesized. One of the four isomers of this alkene could not be detected experimentally. The molecule can be switched selectively between three different isomers. Unidirectional rotation around the central double bond could, unfortunately, not be proven unequivocally.

Part of this chapter has been published: M. K. J. ter Wiel, R. A. van Delden, A. Meetsma, B. L. Feringa, *J. Am. Chem. Soc.* **2003**, *125*, 15076-15086.

3.1 Molecular Design

In the previous chapter, the synthesis and properties of a family of the first generation molecular motors was described.[1] The molecular motor **3.1**, shown in figure 3.1, was the first molecule for which a unidirectional 360° rotation around the central double bond was demonstrated and it has been used as a prototype for the design of new molecular motors.[2] Despite the progress that has been made in the control over the rotary behavior of the motor molecules, these compounds are still far from being applicable in nanotechnological devices. Although these molecules allowed a valuable proof of principle there remains room for improvement of their properties and in particular the rate-determining step in all the rotational processes, the thermally driven helix inversion.

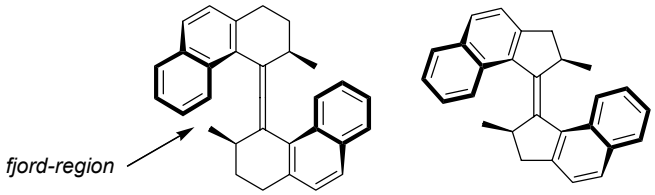

3.1 **3.2**

Figure 3.1 *First-generation molecular motor **3.1** and the new molecular motor **3.2**.*

For all molecular motors investigated sofar, the thermal helix inversion has been shown to be the rate determining step of the rotary process. Despite all the improvements that have been made to lower the barrier for this step, the fastest molecular motor still has an half-life of 2400 s at room temperature.[2a] Hence, the question is how this barrier can be decreased further without affecting the unidirectionality of rotation around the central double bond. Especially relevant to the design and improvement of the molecular motors are the geometry and conformation around the central double bond and the steric hindrance at the "*fjord region*" of the molecules. So far, all motor molecules capable of a 360° rotation consisted of one or two six-membered rings, which contained a stereogenic center to ensure the unidirectionality of the movement. A six-membered ring introduces a considerable amount of steric hindrance into the molecules. It is expected that in a molecular motor made of two smaller five-membered rings bearing the stereogenic centers as in **3.2** (figure 3.1) less steric hindrance is introduced. However, it remains a pertinent question whether lowering of the steric hindrance around the double bond would indeed result in a faster 360° unidirectional rotation in such a molecule. In this context, an interesting example is a molecular motor in which the tetrahydrophenanthrene moiety in the upper half of the molecule has been replaced by a tetrahydronaphthalene moiety (see chapter 1).[3] For this motor molecule it has been shown clearly that lowering of the steric hindrance does not necessarily lead to a faster molecular rotation. In this case a considerable increase of the half-life of the unstable form and, as a consequence, a slower rotation is observed.

3.1.1 Retrosynthesis and Synthesis

As is the case for all overcrowded alkenes, the introduction of the sterically demanding double bond is the major synthetic challenge. Every (retro-)synthesis of an overcrowded alkene is therefore dominated by the crucial step for the formation of this double bond (scheme 3.1). One of the most powerful methods to create sterically demanding olefins is the McMurry reaction (see paragraph 2.2 for a more detailed discussion of the McMurry reaction). Via this reductive coupling, using a low-valent titanium reagent, two ketones are connected to form a double bond. In the previous chapter, which deals with molecular motors with two six-membered rings, it was shown that the yields obtained in the McMurry reaction to form sterically overcrowded alkenes are low. Since the two symmetric halves of the molecule are connected by a highly strained double bond between two five-membered rings for the newly designed molecular motor, similar problems in the McMurry reaction of ketone **3.3** can be anticipated. Nevertheless, model studies indicate that the steric hindrance is slightly smaller than in the six-membered ring analogues and therefore a higher yield might be expected. The introduction of a methyl substituent (and other substituents) in **3.3** can either proceed after (route A) or prior to (route B) the ring closure to the ketone. Therefore, ketone **3.3** is obtainable either by methylation of ketone **3.4** or by a Friedel-Crafts reaction with the linear derivative **3.6**. It is important that the Friedel-Crafts reaction occurs regioselectively at the 1-position of the naphthalene moiety and the undesired side-reaction at the 3-position should be avoided. Both ketones **3.3** and **3.4** may be derived from relatively simple naphthalene based precursors such as **3.5** and **3.6**, which can be prepared using standard synthetic methodology.

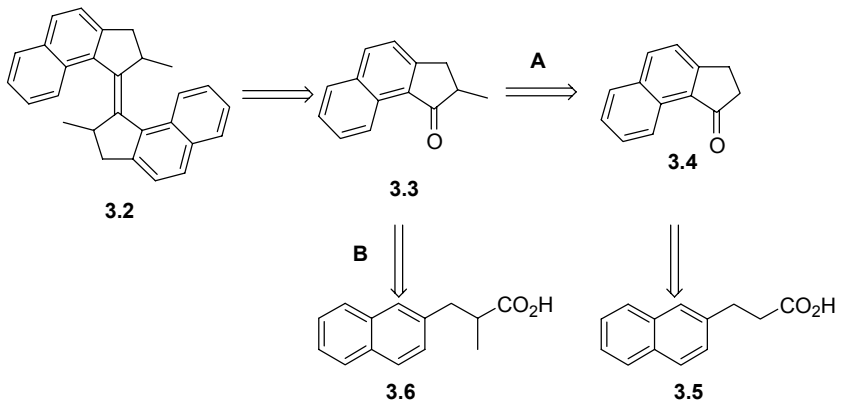

Scheme 3.1 *Retrosynthetic scheme for the synthesis of the new motor molecule **3.2**.*

The first attempt to synthesize motor **3.2** was *via* route A (scheme 3.1). An advantage of this route is that ketone **3.4** is known from the literature and therefore no problems concerning the regioselectivity of the Friedel-Crafts reaction are to be expected.[4] Naphthalen-2-yl-acetic acid **3.7** was reduced with lithium aluminium hydride in boiling THF to give alcohol **3.8** in moderate yield.[5] The alcohol **3.8** was then converted to the bromide **3.9**,[5] which after reaction with KCN in DMSO gave the cyanide **3.10**.[6] Refluxing **3.10** overnight in 30% HCl gave smoothly acid **3.5**[7], which was converted into the desired

ketone **3.4** in a two step procedure involving a Friedel-Crafts reaction. Formation of the enolate of ketone **3.4** using LDA in THF at low temperature and subsequent reaction with methyl iodide gave a mixture of three compounds: mono- and di-alkylated products **3.3** and **3.11** besides the starting material **3.4**. From this mixture, the desired ketone **3.3** was isolated only in low yield.

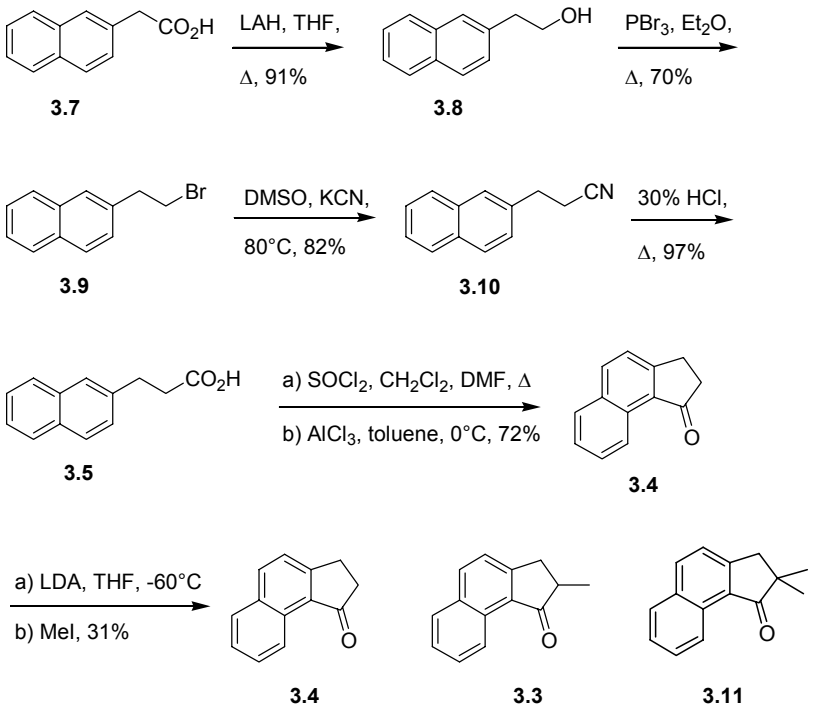

Scheme 3.2 *Initial synthetic route towards ketone **3.3**.*

Obviously, a more efficient synthetic route was needed in which the methyl substituent could be introduced in a controllable manner and the number of reaction steps would be decreased. Therefore, it was chosen to perform the alkylation reaction in an earlier stage of the synthesis, as is depicted in scheme 3.1 as route B. In this approach, the enolate of methyl propionate **3.12** was generated at low temperature using freshly prepared LDA in THF and then allowed to react with bromide **3.13**[8] to give the ester **3.14** in moderate yield (scheme 3.3). The ester was hydrolyzed by reaction with KOH in an ethanol/water mixture yielding acid **3.6**. This acid was treated with $SOCl_2$ to provide acid chloride **3.15**, which was subjected to a Friedel-Crafts reaction using $AlCl_3$ in dichloroethane to give ketone **3.3** in 86% yield. Noteworthy is that the reaction proceeds selectively at the 1-position of the naphthalene ring. Reaction at the 3-position, leading to an isomeric ketone, was not observed in this case. Finally, ketone **3.3** was reductively coupled using the McMurry reaction with $TiCl_4$ and zinc powder as the reducing agent in dry THF. The overcrowded alkene **3.2** was obtained as a mixture of both the *trans*- and *cis*-isomers in an approximate

ratio of 2:5 and a combined yield of 76%. A remarkable feature, that has also been observed in for the motors with a six-membered ring, is that only a diastereomerically pure mixture of (*R*,*R*)- and (*S*,*S*)-olefins is obtained after the McMurry reaction. Since racemic ketone **3.3** is used, the resultant olefin would be expected to be a statistical mixture of (*R*,*R*), (*S*,*S*), (*S*,*R*) and (*R*,*S*) coupled products, but the (*R*,*S*)- and (*S*,*R*)-isomers are not formed. By recrystallization of the mixture of olefins **3.2** from ethyl acetate, *trans*-**3.2** was obtained pure as slightly yellow crystals in 14% yield. The purification of the *cis*-isomer was significantly more difficult, since multiple recrystallizations, first from ethyl acetate and then from ethanol, were needed to obtain *cis*-**3.2** pure as slightly yellow crystals.

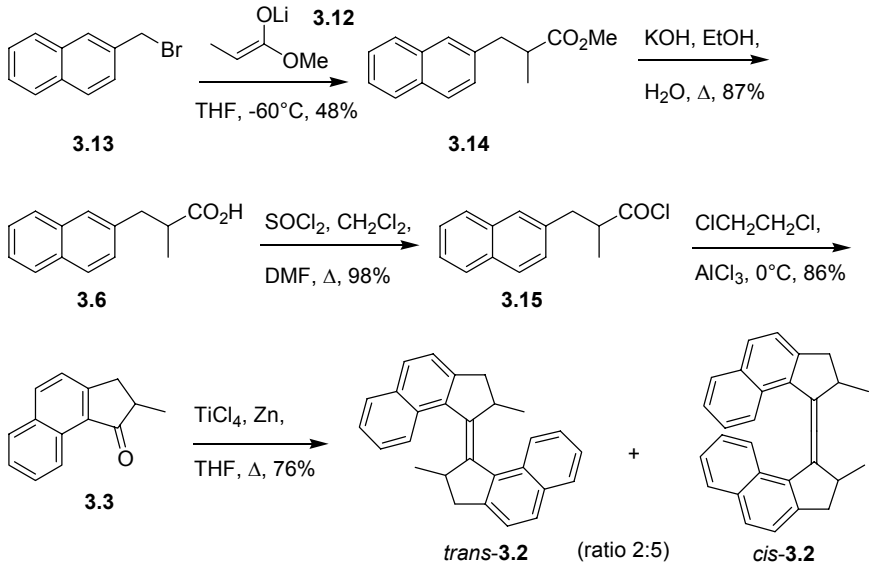

Scheme 3.3 *Synthesis of Molecular Motor **3.2**.*

At this point, it is important to note two major differences compared to the original motor molecule **3.1**. First, the reductive coupling of the two ketone moieties in the last step in the synthesis of the molecular motor with six-membered rings proceeds in very low yields. From the coupling of two ketones with a five-membered ring, a combined yield of 76% is obtained. Second, particularly remarkable is the preferred formation of the *cis*-isomer over the *trans*-isomer. For the original motor molecules, not even a trace of the *cis*-isomer was observed after the McMurry reaction. The implication of this observation is that *cis*-**3.2** is possibly more stable than *trans*-**3.2**. Apparently, the stereoselectivity in the formation of the pinacolate titanium-intermediate (see chapter 2) is affected to a considerable extent by the ring-size of the ketones. However, these molecular models do not provide sufficient insight into the difference between the two intermediate pinacolates and no firm conclusion can be drawn explaining the preferred formation of *cis*-**3.2**. Both alkenes *cis*-**3.2** and *trans*-**3.2** were prepared in their racemic forms. To prove the rotary cycle by CD spectroscopy, enantiopure material is required and therefore the enantiomers of both isomers were separated using preparative chiral HPLC. Separation of the enantiomers of the *trans*-**3.2**

alkene was achieved on a Daicel Chiralcel OD column using a highly apolar eluent (heptane : *i*-propanol = 99.9 : 0.1). Based on comparison of the CD data with those of similar compounds, the absolute configuration of the first eluted fraction of *trans*-**3.2** was assigned to be (2*R*,2'*R*)-(*P*,*P*)-*trans*-**3.2**. HPLC separation of the enantiomers of *cis*-**3.2** was accomplished using heptane : *i*-propanol = 99.5 : 0.5 as an eluent on a Daicel Chiralcel OD column. The configuration of the first eluted fraction of *cis*-**3.2** was assigned to be (2*R*,2'*R*)-(*P*,*P*)-*cis*-**3.2** by comparison with CD data of related compounds (*vide infra*).

3.1.2 Asymmetric Synthesis

In order to avoid the time consuming and costly preparative chromatographic resolution of the enantiomerically pure alkenes *cis*-**3.2** and *trans*-**3.2**, an alternative synthetic method was envisioned in which the methyl substituent of the alkenes is introduced *via* an asymmetric synthesis route. This synthetic route could, in combination with CD spectroscopy, provide valuable information concerning the absolute configuration at the stereocenters of these molecules. As has already been outlined in the previous chapter, many methods have been developed for the stereoselective introduction of an alkyl substituent adjacent to a carbonyl functional group. Particularly relevant methodology, which has already proven its value in the stereoselective synthesis of the six-membered molecular motors,[9] is based on the oxazolidinone protocol developed by Evans.[10,11] The advantage of this methodology over, for example, the Enders hydrazone method,[12] is that it makes use of a less sterically demanding acid derivative.

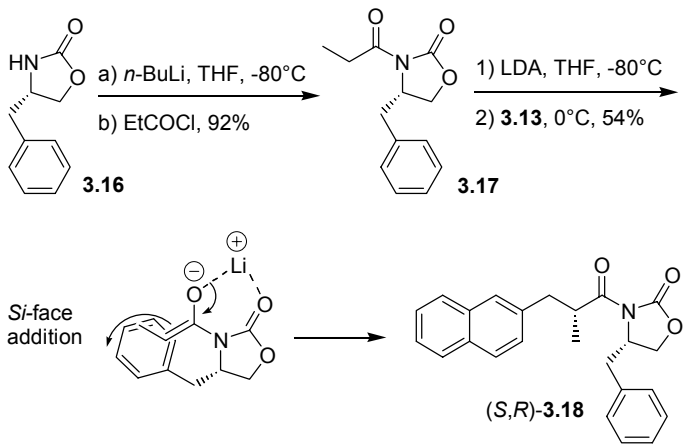

Scheme 3.4 *Diastereoselective alkylation using the Evans protocol.*

The asymmetric synthesis (scheme 3.4) starts with chiral oxazolidinone **3.16**, which can be prepared in a two step procedure starting from L-phenylalanine by standard methodology.[13] By lithiation of **3.16** at low temperature, followed by reaction with propionyl chloride, the oxazolidinone **3.17** was obtained in good yield according to a literature procedure.[14] Generation of the enolate of **3.17** using LDA followed by quenching with 2-(bromomethyl)naphthalene **3.13** gives **3.18** in moderate yield (54%). Important in this

reaction is the exclusive formation of the *Z*-enolate and the shielding of the *Re*-face of the molecule so that reaction of the bromide only occurs at the *Si*-face resulting in a newly created stereocenter of (*R*)-absolute configuration. Since in principle it is possible to form two diastereomers in the alkylation reaction, the reaction mixture was carefully analyzed to ascertain the presence of only the desired (*S*,*R*)-**3.18** diastereomer. The (*S*,*S*)-**3.20** diastereomer, which should be formed in only a small amount during the reaction, was prepared independently in a two step synthetic sequence starting with racemic acid **3.6** (scheme 3.5). This acid was converted into its acid chloride and then allowed to react with **3.19**. After workup, the diastereomers (*S*,*S*)-**3.20** and (*S*,*R*)-**3.18** were readily separated by column chromatography and analyzed by ^{1}H NMR. The analysis revealed that during the stereoselective synthesis, as depicted in scheme 3.4, no detectable amount of diastereomer (*S*,*S*)-**3.20** was produced.

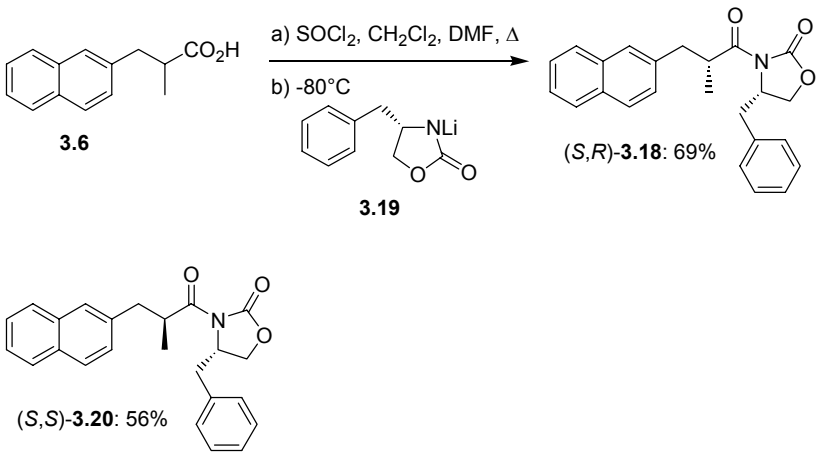

Scheme 3.5 *Independent preparation of diastereomers **3.18** and **3.20**.*

Diastereomerically pure **3.18** was deprotected using LiOH and H_2O_2 in a THF/water mixture resulting in the enantiomerically pure carboxylic acid (*R*)-**3.6** in high yield (90%). The enantiomeric excess proved to be higher than 99%, as was determined by conversion of the acid (*R*)-**3.6** into the methyl ester (*R*)-**3.14**, which could be separated by HPLC (Daicel Chiralcel OB-H column, heptane : *i*-propanol = 99:1). Ring closure of the enantiomerically pure acid (*R*)-**3.6**, by conversion to acid chloride (*R*)-**3.16** and subsequent Friedel-Crafts reaction with $AlCl_3$ afforded the enantiomerically pure ketone (*R*)-**3.3** in high yield. The chiral ketone (*R*)-**3.3** is prone to racemization if the workup of the reaction mixture is not performed under neutral conditions. According to HPLC analysis, the ketone (*R*)-**3.3** was obtained with an e.e. > 99% (Daicel Chiralcel OB-H column, heptane : *i*-propanol = 99:1). Finally, the McMurry procedure was used to couple reductively the two halves. A protocol using $TiCl_4$ in combination with zinc powder was employed, providing **3.2** as *cis*-*trans* mixture in a 5:2 ratio. However, chiral HPLC analysis revealed that both isomers were obtained as racemates. Unfortunately, under the reaction conditions used, the chiral ketone (*R*)-**3.3** racemizes completely rendering this elegant route, aiming at an

asymmetric synthesis of the *cis*- and *trans*-alkenes **3.2**, useless for the stereoselective formation of enantiomerically pure *cis*- and *trans*-**3.2**.

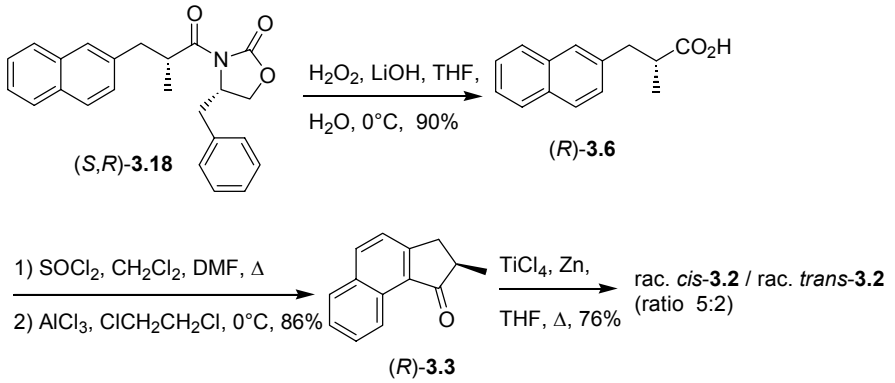

Scheme 3.6 *Attempted asymmetric synthesis route toward motor molecule **3.2**.*

3.1.3 Structural Analysis

The ^{1}H and ^{13}C NMR spectra immediately reveal a C_2-symmetric nature for both *trans*-**3.2** and *cis*-**3.2** in solution. The NMR data obtained are in complete agreement with the assigned structures and the individual absorptions in the ^{1}H NMR spectrum were assigned using COSY and NOESY experiments. The ^{1}H NMR spectra of both isomers of the five-membered ring molecule closely resemble their six-membered ring counterparts described in chapter 2 as shifts in both types of motors follow the same trends.

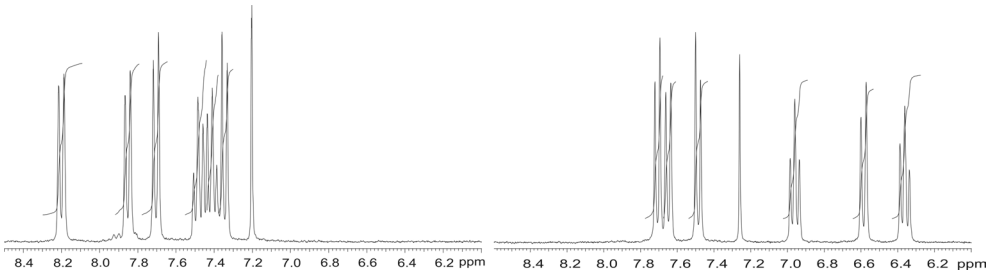

Figure 3.2 *^{1}H NMR spectra of the aromatic region of trans-**3.2** (left) and cis-**3.2** (right).*

In the aromatic region the ^{1}H absorptions for *trans*-**3.2** are found between δ 7.4 and 8.3 ppm (figure 3.2, left side). A confirmation of the assignment of the *trans* geometry was found in the observation of a NOE signal between Me_2 and $H_{9'}$ and between $Me_{2'}$ and H_9 (for numbering of the individual atoms in *trans*-**3.2** see figure 3.3). The protons in the aromatic region of the ^{1}H NMR spectrum of *cis*-**3.2** were found at relatively high field as high as δ 6.3 ppm (figure 3.2, right side). This is due to the ring current anisotropy experienced by the protons because of the close proximity of the naphthalene moiety in the opposite half of the molecule. This upward shift in the spectrum is in full accordance with

data of the previously described *cis*-isomer of **3.1**. In the NOESY spectrum of *cis*-**3.2** no interaction was observed between Me_2 or H_2 and $H_{9'}$ (see for numbering of the individual atoms in *cis*-**3.2** figure 3.4). In order to demonstrate unequivocally the assigned geometry of the two isomers and to determine the preferred conformation of the stable forms of these molecules, crystals were grown for X-ray crystallographic analysis. Crystals from *trans*-**3.2**, obtained by recrystallization from ethyl acetate, were found to be suitable for X-ray crystallographic analysis. The crystal used was found to be orthorhombic with space group *Pbca* (No. 61) and contained one molecule of *trans*-**3.2** in the asymmetric unit cell. Two views of the *trans*-**3.2** are depicted in figure 3.3.

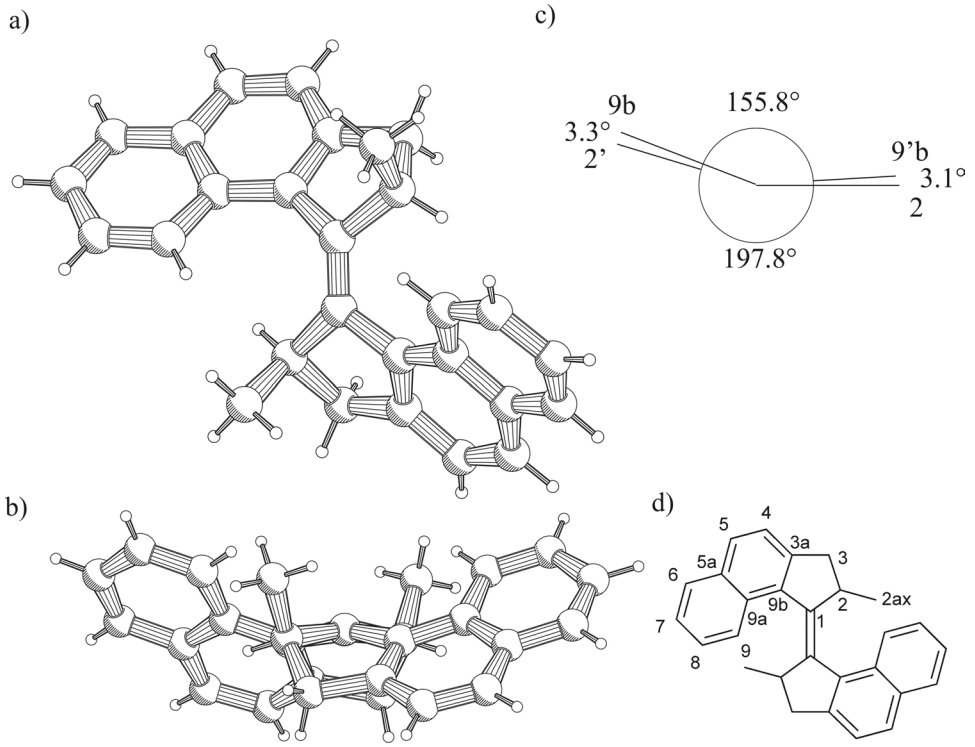

Figure 3.3 *PLUTO drawings of one enantiomer of racemic (2R*,2'R*)-(P*,P*)-trans-(±)-2,2'-dimethyl-2,2',3,3'-tetrahydro-1,1'-bicyclopenta[a]naphthalenylidene* ***3.2*** *viewed perpendicular onto the central double bond (a) and along the central double bond (b). The structures do not express the absolute stereochemistry of the molecule. The Newman projection of the central double bond (c) as well as the numbering scheme employed for the molecule (d) are depicted.*

Compared with the C_2-symmetric nature in solution, as was revealed by NMR spectroscopy, the structure of the molecule in the crystal is slightly distorted due to crystal packing effects but can be regarded pseudo-C_2-symmetric. Most important structural features of *trans*-**3.2** in the solid state are the overall double helical shape and the (pseudo-)

axial orientation of both methyl substituents at the stereogenic centers. As can clearly be seen from figure 3.3, the naphthalene moiety and the methyl substituent in one half of the molecule point in the same direction.

The central double bond in *trans*-**3.2** was found to be only slightly elongated with a length of 1.3497 Å compared to the literature value of 1.33 Å for a common olefinic bond.[15] The bond angles around C_1 and $C_{1'}$ are: C_2-C_1-C_{9b} = 104.1°, C_2-C_1-$C_{1'}$ = 126.0° and C_{9b}-C_1-$C_{1'}$ = 127.4° making the average total angle around C_1 and $C_{1'}$ 357.5° (values are an average of the values found in the two parts of the residue since the structure is being regarded as pseudo-C_2-symmetric). Remarkably, in *trans*-**3.2** the central olefinic bond is more twisted than its six-membered analogue **3.1** (chapter 2). The values for the torsion angles around the double bond are C_2-C_1-$C_{1'}$-$C_{2'}$= -162.2°, C_{9b}-C_1-$C_{1'}$-$C_{9'b}$ = 155.8° and C_2-C_1-$C_{1'}$-$C_{9'b}$ = -3.2° (average). The angle between the least-square planes of the atoms in both naphthalene moieties (85.2°) in *trans*-**3.2** show that the naphthalene chromophores are nearly perpendicularly arranged with respect to each other. The twist of the naphthalene moiety itself in *trans*-**3.2**, with respect to the least-square plane of the atoms C_2-C_1-C_{9b}-$C_{9'b}$-$C_{1'}$-$C_{2'}$, is on average 42.6°, a value that is also reflected in the torsion angle C_1-$C_{1'}$-$C_{9'b}$-$C_{9'a}$, which is on average 44.5° for both halves of *trans*-**3.2**. The five-membered ring itself is remarkably flat and the ring deviates only slightly from the least-square plane through the atoms C_1-C_2-C_3-C_{3a}-C_{9b}. The atoms C_2 and $C_{2'}$ (average 0.220Å) and C_1 and $C_{1'}$ (average 0.200Å) show the largest deviations from this plane. Nevertheless, the methyl substituents at the stereogenic centers clearly adopt a (pseudo-)axial orientation (C_1-$C_{1'}$-$C_{2'}$-$Me_{2'ax}$ is -116.2° (average)) and the most stable conformation of *trans*-**3.2** shows a helicity similar to that found for *trans*-**3.1**.

Crystals suitable for X-ray structure determination of the racemic *cis*-**3.2** isomer were obtained by recrystallization from ethanol. The crystal used was found to be monoclinic with space group $P2_1$ (No. 4) and contained two enantiomers of *cis*-**3.2** in the asymmetric unit cell. The two residues (from here on arbitrarily named enantiomer 1 and 2), are, apart from minor distortions due to crystal packing effects, enantiomers. Similar to *trans*-**3.2**, the structure of *cis*-**3.2** is C_2-symmetric at first sight, but both residues are slightly distorted. The helical shape and the (pseudo-)axial orientation of the methyl substituents at the stereogenic centers are evident from the structure depicted in figure 3.4. The naphthalene moiety and the methyl substituent in each half point in the same direction, implying that this geometry is the most stable for *cis*-**3.2**. The central double bonds in both enantiomers of *cis*-**3.2** (1.365 and 1.352 Å) were found to be more elongated and more planar than the central double bond in *trans*-**3.2** (1.3497 Å).[15] This can be seen clearly in the Newman projection in figure 3.4 (compare figure 3.3). The bond angles around C_1 and $C_{1'}$ in enantiomer 1 are: C_2-C_1-C_{9b} = 105.0°, C_2-C_1-$C_{1'}$ = 121.6° and C_{9b}-C_1-$C_{1'}$ = 133.2° (average total angle around C_1 and $C_{1'}$= 359.8°) and in enantiomer 2: C_2-C_1-C_{9b} = 104.6°, C_2-C_1-$C_{1'}$ = 122.0° and C_{9b}-C_1-$C_{1'}$ = 133.3° (average total angle around C_1 and $C_{1'}$= 359.9°) (values are an average of the values found in the two parts of the residue since the structure is pseudo-C_2-symmetric). The values for the torsion angles around the double bond are: C_2-C_1-$C_{1'}$-C_2 = 11.0°, C_{9b}-C_1-$C_{1'}$-$C_{9'b}$ = -3.2° and C_2-C_1-$C_{1'}$-$C_{9'b}$ = -176.1° (average) for enantiomer 1 and C_2-C_1-$C_{1'}$-C_2 = -10.9°, C_{9b}-C_1-$C_{1'}$-$C_{9'b}$ = -1.4° and C_2-C_1-$C_{1'}$-$C_{9'b}$ =

175.3° for enantiomer 2. This means that the deviation from planarity of the central double bond for *cis*-**3.2** is smaller than that was found for both *trans*-**3.1** and *trans*-**3.2**. In *cis*-**3.2** the angle between the least-square planes of the atoms in both naphthalene moieties (average 31.5°) was much smaller than for *trans*-**3.2** (85.2°). This is reflected in the torsion angles in both enantiomers between $C_{1'}$-C_1-C_{9b}-C_{9a} which are 31.3° and –32.7°, respectively, in *cis*-**3.2**. Again, the five-membered ring itself is remarkably flat and its atoms deviate only slightly from the plane through C_1-C_2-C_3-C_{3a}-C_{9b} in both moieties; the largest deviations are associated with the atoms C_1, C_2, $C_{1'}$ and $C_{2'}$.

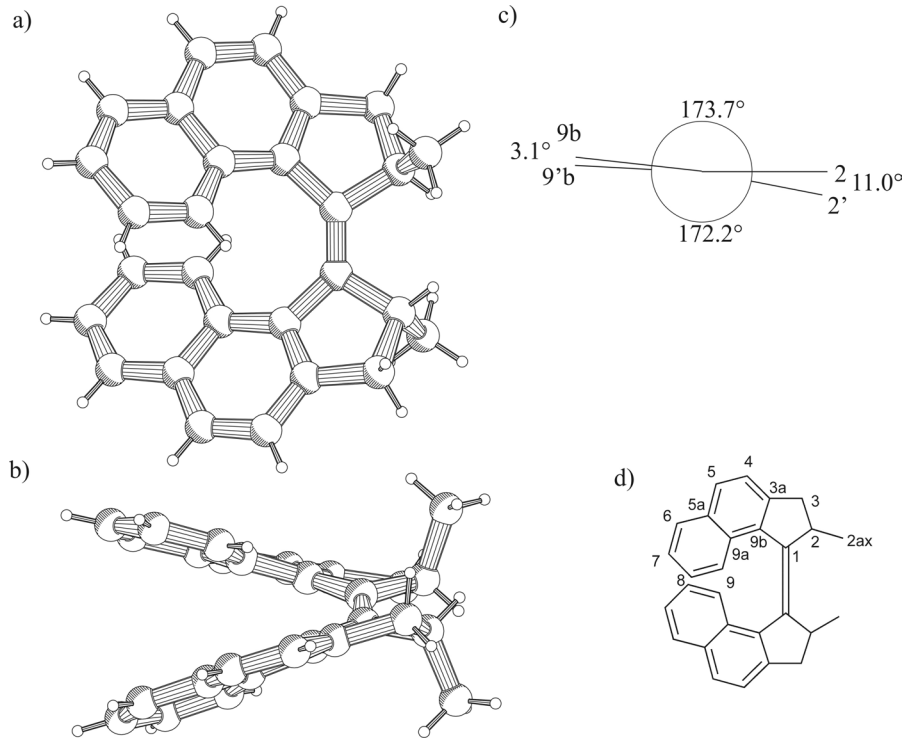

Figure 3.4 *PLUTO drawings of one enantiomer of racemic (2R*,2'R*)-(P*,P*)-cis-(±)-2,2'-dimethyl-2,2',3,3'-tetrahydro-1,1'-bicyclopenta[a]naphthalenylidene* ***3.2*** *viewed perpendicular onto the central double bond (a) and along the central double bond (b). The structures do not express the absolute stereochemistry of the molecule. The Newman projection of the central double bond (c) as well as the numbering scheme employed for the molecule (d) are depicted.*

The five membered ring in *cis*-**3.2** is even more planar than that of *trans*-**3.2**; the average deviation from the five-membered rings of C_1 and $C_{1'}$ in both residues being 0.172Å and of C_2 and $C_{2'}$ 0.185Å. Also for *cis*-**3.2**, it is clear that the methyl substituents at the stereogenic center adopt a (pseudo-)axial orientation (C_1-$C_{1'}$-$C_{2'}$-$Me_{2'ax}$ are on the average -96.4° and 96.9°).

3.1.4 Photochemical Experiments

In order to show whether the molecule is able to perform a unidirectional rotation around the central double bond, photochemical experiments were performed. Enantiomerically pure (2*R*,2'*R*)-(*P*,*P*)-*cis*-**3.2**, obtained by preparative chiral HPLC, was irradiated ($\lambda \geq$ 280 nm, T= -40°C) in *n*-hexane and subsequently heated at room temperature resulting in a mixture of (2*R*,2'*R*)-(*P*,*P*)-*cis*-**3.2** and (2*R*,2'*R*)-(*P*,*P*)-*trans*-**3.2** (*vide infra*). These two isomers were readily separated by chiral HPLC on a preparative Daicel Chiralcel OD column using a mixture of heptane : *i*-propanol in a ratio of 99.9 : 0.1 as the eluent.

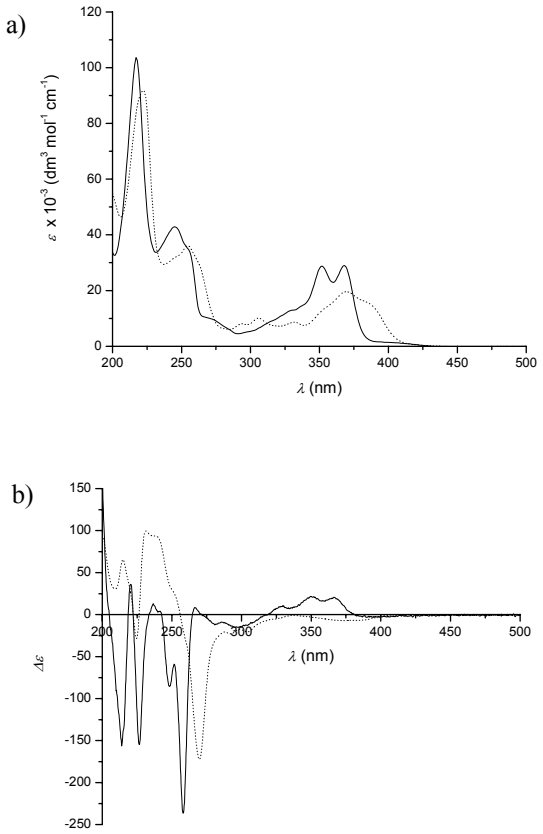

Figure 3.5 *a) UV-Vis spectra (n-hexane) of the stable olefins: cis-**3.2** (dotted line) and trans-**3.2** (solid line); b) CD spectra (n-hexane) of the stable olefins: (2R,2'R)-(P,P)-cis-**3.2** (dotted line) and (2R,2'R)-(P,P)-trans-**3.2** (solid line).*

The UV-Vis spectra of pure *cis*-**3.2** and *trans*-**3.2** are shown in figure 3.5a and the circular dichroism (CD) spectra of enantiomerically pure (2*R*,2'*R*)-(*P*,*P*)-*cis*-**3.2** and (2*R*,2'*R*)-(*P*,*P*)-*trans*-**3.2** are shown in figure 3.5b. The absolute configuration of (2*R*,2'*R*)-(*P*,*P*)-*cis*-

3.2 and (2*R*,2'*R*)-(*P*,*P*)-*trans*-**3.2** could be assigned by comparison with the CD spectra of (3*R*,3'*R*)-(*P*,*P*)-*cis*-**3.1** and (3*R*,3'*R*)-(*P*,*P*)-*trans*-**3.1**. The assignments were confirmed by calculations (figure 3.13). From X-ray structural analysis of *cis*-**3.2** and *trans*-**3.2** (*vide supra*) it is evident that the orientation of methyl substituents at the stereogenic centers is (pseudo-)axial.

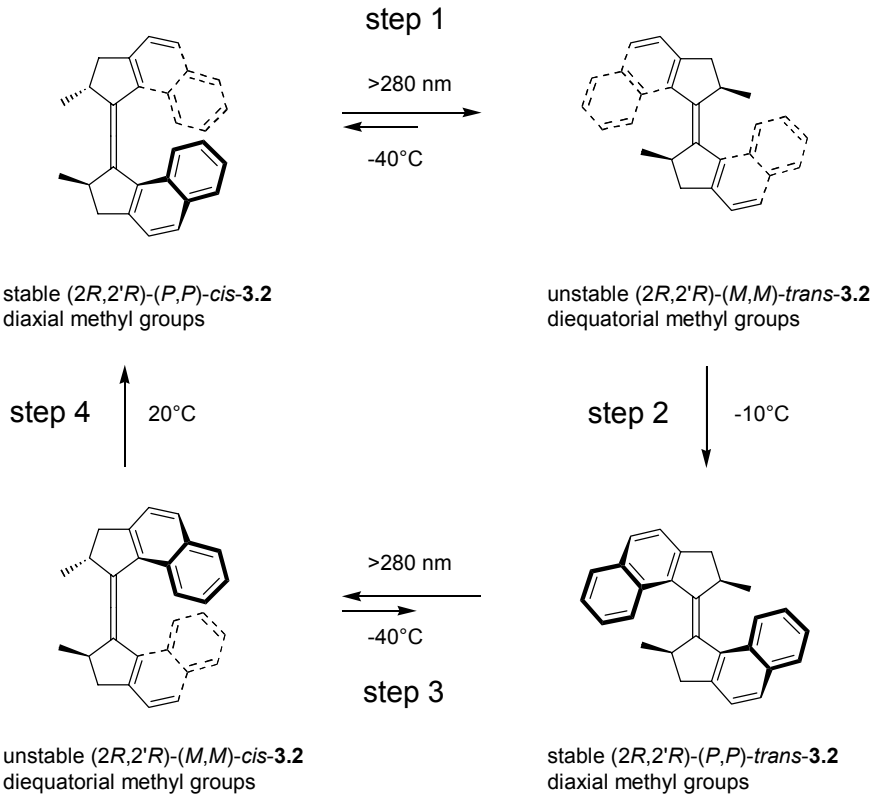

Scheme 3.7 *Photochemical and thermal isomerization processes during the 360° unidirectional rotary cycle of* ***3.2****.*

Photo-isomerization of a sample of (2*R*,2'*R*)-(*P*,*P*)-*cis*-**3.2** in *n*-hexane by irradiation ($\lambda \geq$ 280 nm, T= -40°C) was monitored by UV-Vis (figure 3.6a) and CD spectroscopy (figure 3.6b). The major band in the CD spectrum shifted from 270.0 nm for the initial (2*R*,2'*R*)-(*P*,*P*)-*cis*-**3.2** to 263.2 nm at the photostationary state (PSS) and changed sign from $\Delta\varepsilon$ = -172.2 to $\Delta\varepsilon$ = +13.1 (figure 3.6b). The change in sign of the CD signal is indicative for the helix inversion of the molecule going from a overall (*P*)-helicity in (2*R*,2'*R*)-(*P*,*P*)-*cis*-**3.2** to an (*M*)-helicity in the newly formed isomer, anticipated to be the energetically unstable (2*R*,2'*R*)-(*M*,*M*)-*trans*-**3.2** isomer with both methyl substituents in an equatorial orientation (step 1, scheme 3.7). The exact nature of this unstable *trans*-isomer was confirmed by low temperature ^{1}H NMR.[16] A solution of racemic stable *cis*-**3.2** **(**toluene-d_8), with methyl

substituents in an axial orientation, was irradiated ($\lambda \geq 280$ nm, $T = -78$°C) overnight. After irradiation, the signals of the methyl protons of stable (2R^*,2'R^*)-(P^*,P^*)-*cis*-**3.2** at δ 1.17-1.18 ppm shifted to higher field at δ 0.68-0.69 ppm as a result of the diequatorial orientation of the methyl groups in the unstable (2R^*,2'R^*)-(M^*,M^*)-*trans*-**3.2** formed. In the aromatic part of the spectrum, absorptions appeared at lower field, δ 7.70-7.72 and δ 7.95-7.97 ppm, indicative of the formation of a molecule with a *trans*-geometry. Heating of this sample showed a clean conversion of the unstable (2R^*,2'R^*)-(M^*,M^*)-*trans*-**3.2**, with equatorial methyl substituents, to the stable (2R^*,2'R^*)-(P^*,P^*)-*trans*-**3.2**, with axial methyl substituents. In combination with CD spectroscopy, these ^{1}H NMR experiments provide direct evidence for one half of the unidirectional movement of the molecule.

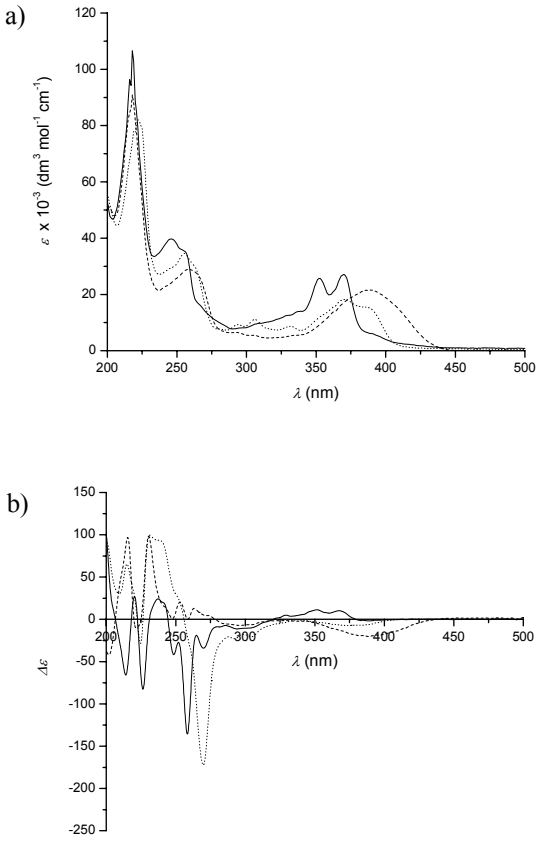

Figure 3.6 *UV-Vis (n-hexane) (a) and CD (n-hexane) spectra (b) obtained in the first half of the rotary cycle: pure (2R,2'R)-(P,P)-cis-**3.2** (dotted line), after step 1 (dashed line) and after step 2 (solid line) (c.f. scheme 3.7).*

Subsequently, the *n*-hexane solution containing a photostationary state mixture of (2*R*,2'*R*)-(*P*,*P*)-*cis*-**3.2** and (2*R*,2'*R*)-(*M*,*M*)-*trans*-**3.2** was kept at -10°C and the CD signal at 230 nm was monitored in time. An inversion of the CD spectrum was observed after complete conversion, indicating the overall inversion of helicity of the molecule (figure 3.6b and figure 3.7, trace a). This indicates that unstable (2*R*,2'*R*)-(*M*,*M*)-*trans*-**3.2** was converted to stable (2*R*,2'*R*)-(*P*,*P*)-*trans*-**3.2** (step 2, scheme 3.7). In (2*R*,2'*R*)-(*P*,*P*)-*trans*-**3.2**, the methyl substituents are back in their favored (pseudo-)axial orientation. From the change in CD monitored in time, the rate constant (k_t) at various temperatures was determined. Using the Eyring equation, the plot of ln (k·h)/(k_B·T) versus 1/T (figure 3.8a), the Gibbs energy ($\Delta^{\ddagger}G^{\theta}$ = 80±1 kJ·mol^{-1}), the enthalpy ($\Delta^{\ddagger}H^{\theta}$ = 73±1 kJ·mol^{-1}) and the entropy of activation ($\Delta^{\ddagger}S^{\theta}$ = -24±6 J·K^{-1}·mol^{-1}) of the process could be determined. The Gibbs energy of activation was then employed to calculate the half-life of the conversion of (2*R*,2'*R*)-(*M*,*M*)-*trans*-**3.2** to (2*R*,2'*R*)-(*P*,*P*)-*trans*-**3.2**. This thermal helix inversion has a half-life of only 18 s at room temperature (293.15 K) and is the fastest thermal helix inversion step observed for any motor molecule sofar.

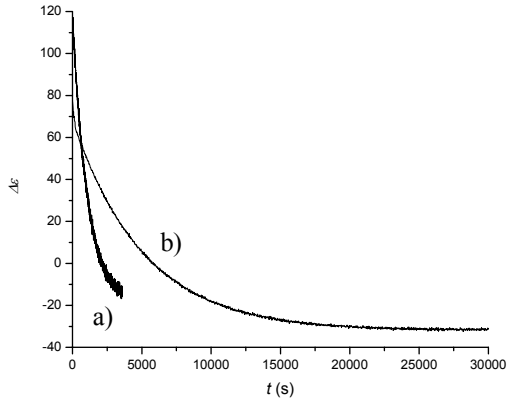

Figure 3.7 *CD absorption monitored in time for the two thermal helix inversion in the rotary process: a) conversion of (2R,2'R)-(M,M)-trans-**3.2** to (2R,2'R)-(P,P)-trans-**3.2** (Δε at 230 nm, -10°C, n-hexane; b) conversion of (2R,2'R)-(M,M)-cis-**3.2** to (2R,2'R)-(P,P)-cis-**3.2** (Δε at 279 nm, 20°C, n-hexane).*

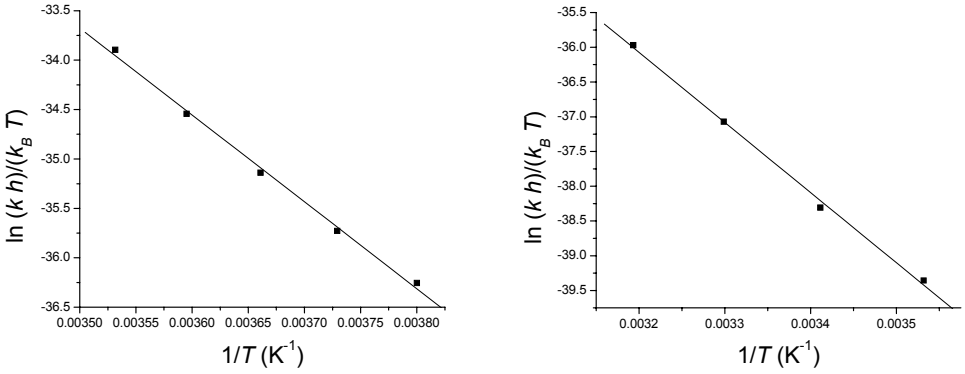

Figure 3.8 *Eyring plots for the thermal helix inversion of (2R,2'R)-(M,M)-trans-**3.2** to (2R,2'R)-(P,P)-trans-**3.2** on the left side and on the right side the thermal helix inversion of (2R,2'R)-(M,M)-cis-**3.2** to (2R,2'R)-(P,P)-cis-**3.2**.*

Due to the low stability of (2*R*,2'*R*)-(*M*,*M*)-*trans*-**3.2**, the photostationary state (PSS) ratio of the first photoequilibrium could not be determined directly. After the thermal helix inversion of (2*R*,2'*R*)-(*M*,*M*)-*trans*-**3.2** to (2*R*,2'*R*)-(*P*,*P*)-*trans*-**3.2**, the amount of stable (2*R*,2'*R*)-(*P*,*P*)-*trans*-**3.2** formed reflects the amount of unstable (2*R*,2'*R*)-(*M*,*M*)-*trans*-**3.2** present at the PSS. Using chiral HPLC analysis, the ratio of (2*R*,2'*R*)-(*P*,*P*)-*cis*-**3.2** and (2*R*,2'*R*)-(*M*,*M*)-*trans*-**3.2** in the PSS mixture was determined to be 22:78. The formation of (2*R*,2'*R*)-(*P*,*P*)-*trans*-**3.2** was confirmed by comparison of independent samples of racemic and enantiomerically pure (2*R*,2'*R*)-(*P*,*P*)-*trans*-**3.2**. From these data, the CD and UV-Vis spectra of unstable (2*R*,2'*R*)-(*M*,*M*)-*trans*-**3.2** could be calculated (figure 3.9).

The mixture of (2*R*,2'*R*)-(*P*,*P*)-*cis*-**3.2** and (2*R*,2'*R*)-(*P*,*P*)-*trans*-**3.2** (22:78 ratio) obtained after irradiation and heating of the original sample was used for further experiments. Irradiation of this sample ($\lambda \geq 280$ nm, T= -40°C), resulted in a shift of the major band in the CD spectrum from 258.4 nm to 279.0 nm and a change in sign from $\Delta\varepsilon$ = -135.6 to $\Delta\varepsilon$ = +59.1 (figure 3.10). This is indicative of the helix inversion taking place upon irradiation of (2*R*,2'*R*)-(*P*,*P*)-*trans*-**3.2** and (2*R*,2'*R*)-(*P*,*P*)-*cis*-**3.2** to (2*R*,2'*R*)-(*M*,*M*)-*cis*-**3.2** and (2*R*,2'*R*)-(*M*,*M*)-*trans*-**3.2**, respectively. After the irradiation, the CD signal of the sample was monitored in time at 279 nm at 20°C, during which an inversion of the CD signal was observed due to thermal helix inversions (figure 3.7, trace b). Due to the instability of the diequatorial compounds, the equilibrium ratio of the four forms present in the mixture could not be determined directly. Analogously for the first PSS, this equilibrium ratio was determined by conversion of the unstable isomers to the stable isomers. The ratio of stable *cis*-**3.2** and *trans*-**3.2** reflects directly the composition of the mixture at the PSS

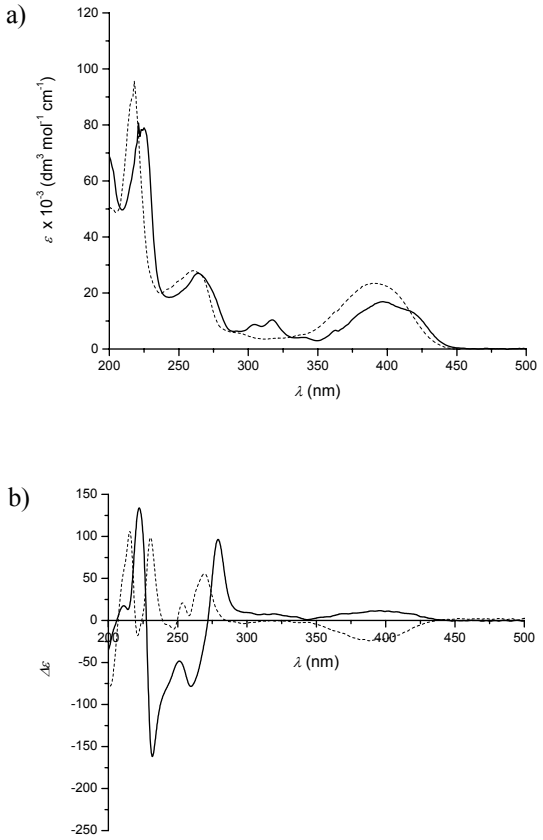

Figure 3.9 *Calculated UV-Vis (a) and CD (b) spectra of (2R,2'R)-(M,M)-trans-**3.2** (dashed line) and (2R,2'R)-(M,M)-cis-**3.2** (thick solid line).*

The equilibrium ratio at the second PSS of (2*R*,2'*R*)-(*P*,*P*)-*cis*-**3.2** and (2*R*,2'*R*)-(*P*,*P*)-*trans*-**3.2** was determined by HPLC to be 67:33. Taking into account the ratio established for the first photo-equilibrium, a PSS ratio of (2*R*,2'*R*)-(*P*,*P*)-*trans*-**3.2** and (2*R*,2'*R*)-(*M*,*M*)-*cis*-**3.2** of 21:79 for the second photo-equilibrium can be calculated. The ratio in the PSS was identical when determined independently by irradiation of a sample of pure (2*R*,2'*R*)-(*P*,*P*)-*trans*-**3.2** ($\lambda \geq$ 280 nm, T= -40°C). The barrier of the interconversion between the unstable (2*R*,2'*R*)-(*M*,*M*)-*cis*-**3.2** and (2*R*,2'*R*)-(*P*,*P*)-*cis*-**3.2** was determined by irradiation of a sample of (2*R*,2'*R*)-(*P*,*P*)-*trans*-**3.2** ($\lambda \geq$ 280 nm, T= –40°C) and subsequent heating at various temperatures. From the time-dependent CD measurements, the rate constants (k_c) of the first order process were obtained at various temperatures. These data were used to calculate both the Gibbs energy ($\Delta^{\ddagger}G^{\theta}$ = 93±1 kJ·mol^{-1}), the enthalpy ($\Delta^{\ddagger}H^{\theta}$ = 84±1 kJ·mol^{-1}) and the entropy of activation ($\Delta^{\ddagger}S^{\theta}$ = -31±7 J·K^{-1}·mol^{-1}) and the half-life of

this helix inversion at room temperature ($t_{½}$ = 78 min, 293.15K) (figure 3.8b). Using these data, the CD and UV-Vis spectra of unstable (2*R*,2'*R*)-(*M*,*M*)-*cis*-**3.2** could be calculated (figure 3.9).

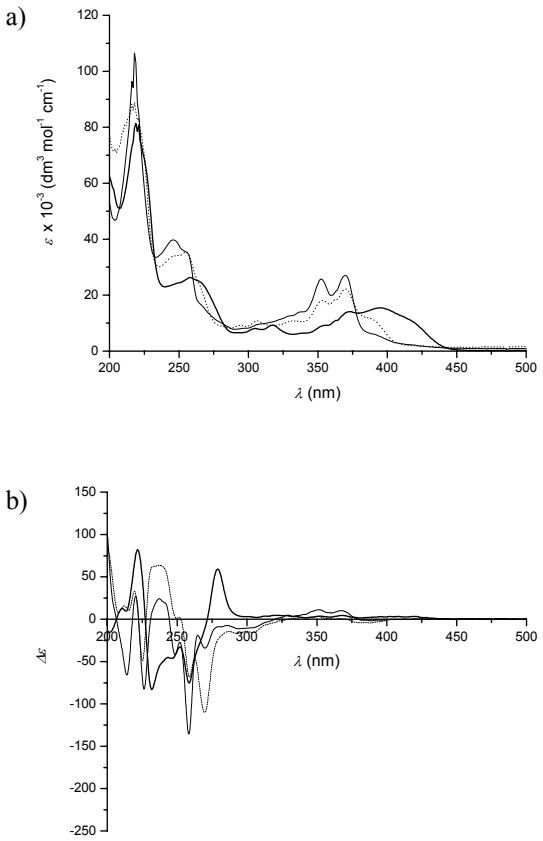

Figure 3.10 *UV-Vis (n-hexane) (a) and CD (n-hexane) (b) spectra obtained in the second half of the rotary cycle: after step 2 (solid line), step 3 (thick solid line) and step 4 (short dotted line).*

Confirmation of the structure of the racemic unstable (2R^*,2'R^*)-(M^*,M^*)-*cis*-**3.2** with equatorial methyl groups was performed by low temperature ^{1}H NMR.[16] A sample of racemic stable (2R^*,2'R^*)-(P^*,P^*)-*trans*-**3.2**, dissolved in toluene-d_8, was irradiated overnight ($\lambda \geq 280$ nm, T= –78°C). Due to a diequatorial orientation of the methyl groups in the unstable (2R^*,2'R^*)-(M^*,M^*)-*cis*-**3.2** formed, a new doublet appeared at lower field (δ 1.46-1.47 ppm) compared to the signals of the protons of the axial methyl groups of stable (2R^*,2'R^*)-(P^*,P^*)-*trans*-**3.2** (δ 1.26-1.27 ppm). In the aromatic region of the

spectrum, absorptions appeared at higher field, δ 6.49-6.52 and δ 6.75-6.78 ppm, which is indicative for the shielded protons due to the anisotropic ring current in a compound with *cis*-geometry. After heating of this sample a clean conversion of the unstable (2R^*,2'R^*)-(M^*,M^*)-*cis*-**3.2,** with equatorial methyl groups, to the stable (2R^*,2'R^*)-(P^*,P^*)-*cis*-**3.2** with axial methyl groups was observed. Also in this case, the ^{1}H NMR data provide additional evidence for the second half of the rotary cycle of the molecule.

The CD spectra of (2*R*,2'*R*)-(*P*,*P*)-*cis*-**3.2** (figure 3.5b) and (2*R*,2'*R*)-(*M*,*M*)-*cis*-**3.2** (figure 3.9b) and (2*R*,2'*R*)-(*P*,*P*)-*trans*-**3.2** (figure 3.5b) and (2*R*,2'*R*)-(*M*,*M*)-*trans*-**3.2** (figure 3.9b) nicely show the pseudo-enantiomeric relation between the stable and less stable isomers of both *cis*-**3.2** and *trans*-**3.2**. Comparing the CD spectra of both forms of the *cis*-**3.2** and *trans*-**3.2** isomers, there is a net inversion of the major absorptions. However, the stepwise inversion of the CD signals in the rotary cycle of the five-membered ring motor molecule are less pronounced than was the case for the six-membered ring motor molecule due to the less favorable photo-equilibria for the motor system **3.2** compared to those of the original motor **3.1** (see chapter 2). The intensity and the shape of the CD spectra of all four isomers are, however, sufficiently different to show the helix inversion in each step, as is shown in figures 3.6b and 3.10b.

3.1.5 Calculations[17]

In order gain more insight into the structural relation between the four isomers and especially between the stable (2*R*,2'*R*)-(*P*,*P*)-*cis*-**3.2** and stable (2*R*,2'*R*)-(*P*,*P*)-*trans*-**3.2** on one side and on the other side the unstable (2*R*,2'*R*)-(*M*,*M*)-*cis*-**3.2** and unstable (2*R*,2'*R*)-(*M*,*M*)-*trans*-**3.2**, calculations were performed. The structures were optimized by DFT using the b3lyp/6-31g(d)//b3lyp/3-21g(d) method. In order to be certain that an energy mimimum was reached for each of the four structures, the infrared spectra were calculated and only positive normal modes were found.

Table 3.1 *Results of the calculated structures and the experimentally determined data. For the numbering of the individual atoms see figures 3.3 and 3.4.*

	stable *trans*-**3.2**		unstable *trans*-**3.2**	stable *cis*-**3.2**		unstable *cis*-**3.2**
	DFT	X-ray	DFT	DFT	X-ray	DFT
ΔE (kJ·mol^{-1})	+11.0		+20.2	0.0		+26.5
C_1-C_1	1.354 Å	1.350 Å	1.363 Å	1.354 Å	1.365 Å	1.364 Å
C_2-C_1-C_{9b}	104.3°	104.2°	105.4°	104.8°	105.0°	105.9°
C_2-C_1-$C_{1'}$	125.6°	126.0°	126.6°	122.3°	121.6°	124.4°
C_{9b}-C_1-$C_{1'}$	126.6°	127.4°	127.2°	132.7°	133.2°	129.6°
C_2-C_1-$C_{1'}$-$C_{2'}$	-153.3°	-162.2°	145.5°	16.8°	11.0°	-30.7°
C_{9b}-C_1-$C_{1'}$-$C_{9b'}$	158.2°	155.8°	165.4°	-5.8°	-3.2°	-24.4°
C_2-C_1-$C_{1'}$-$C_{9'b}$	2.4°	-3.2°	-26.0°	-168.7°	-176.1°	152.5°
C_1-$C_{1'}$-$C_{9'b}$-$C_{9'a}$	48.1°	44.4°	-36.6°	34.2°	31.5°	-27.1°
C_1-$C_{1'}$-$C_{2'}$-$C_{2'ax}$	-120.9°	-116.2°	-22.0°	-93.6°	-96.4°	-34.1°

All structures were found to be C_2-symmetric. The most stable form, as was already anticipated during the synthesis, is the stable (2*R*,2'*R*)-(*P*,*P*)-*cis*-**3.2**. The unstable (2*R*,2'*R*)-(*M*,*M*)-*cis*-**3.2** was found to be the most unstable of the four isomers, relative to the stable *cis*-**3.2**, it lies 26.5 kJ·mol^{-1} higher in energy. It should be noted that this value does not reflect the rate of the thermal helix inversion since this rate is dependent on the activation barrier and not on the relative energies of the molecules. The stable (2*R*,2'*R*)-(*P*,*P*)-*trans*-**3.2** was found to be 11.0 kJ·mol^{-1} higher in energy than the stable (2*R*,2'*R*)-(*P*,*P*)-*cis*-**3.2**. The energy of the unstable (2*R*,2'*R*)-(*M*,*M*)-*trans*-**3.2** was 20.2 kJ·mol^{-1} relative to the stable (2*R*,2'*R*)-(*P*,*P*)-*cis*-**3.2** and hence the energy difference between the two *trans*-isomers is 9.2 kJ·mol^{-1}. By comparing the experimental results with the computational results, as is shown in table 3.1, it can be concluded that, using this methodology, adequate structures of the overcrowded alkenes can be obtained. Although this is less interesting for the stable forms of **3.2**, it is a valuable method for computing the structures of the unstable isomers of **3.2** and other structurally related molecules (*vide infra*).

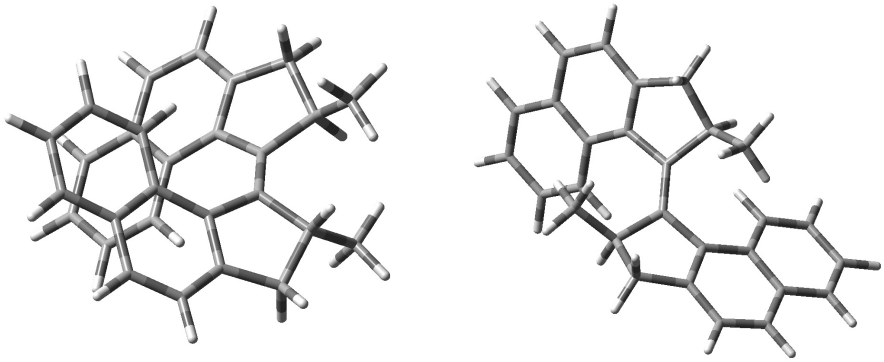

Figure 3.11 *The calculated structures of unstable cis-**3.2** (left) and unstable trans-**3.2** (right).*

From the calculated structures of the unstable forms depicted in figure 3.11 it is evident that both molecules have their methyl substituents in an equatorial orientation. The naphthalene moieties are on the opposite side with respect to the methyl substituents. Unstable *cis*- and *trans*-**3.2** conformers with an (*R*)-configuration at their stereocenters will have an (*M*,*M*)-helical structure as is evident from figure 3.11. The optimized structures described above were used for the calculation of the UV-Vis and CD spectra using time dependent DFT. The excitation energies and the rotatory strengths for each of the four isomers of **3.2** were

calculated using the b3lyp/6-31g(d) method. The experimentally and calculated UV-Vis and CD spectra of each isomer are depicted in figures 3.12 and 3.13, respectively.

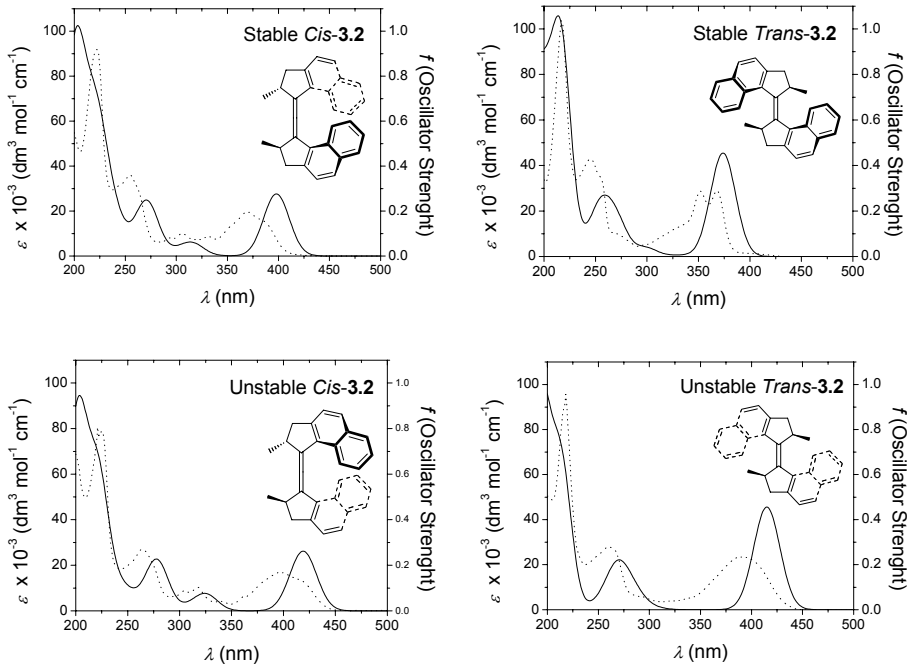

Figure 3.12 *The experimentally determined UV-Vis (dotted) and the calculated UV-Vis (solid) spectra of the four isomers of* ***3.2****.*

In general, the calculated UV-Vis spectra have roughly the same shape as the experimentally determined UV-Vis spectra. However, the calculated UV-Vis band of the lowest energy is consistently too much shifted to lower wavelengths. The red-shift in the UV-Vis spectra going from a stable to an unstable isomer is correctly predicted. The same holds for the calculated CD spectra; the Cotton effects have the right sign and overall shape, but their fine structure was in most cases not adequately calculated (see figure 3.13). Nevertheless, these results show that the computational method can be used to assign correctly the absolute configuration of the molecules.

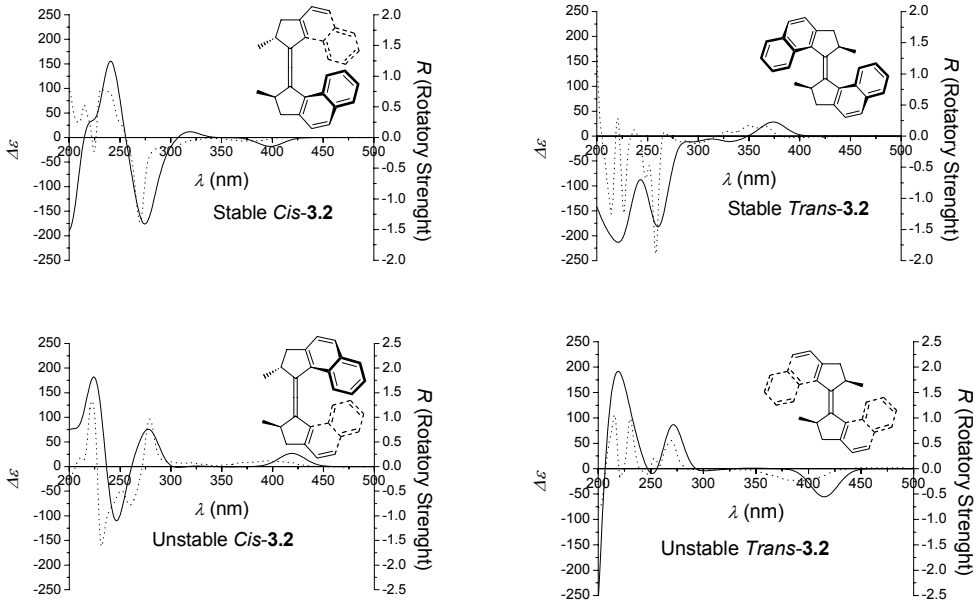

Figure 3.13 *The experimentally determined CD (dotted line) and the calculated CD (solid line) spectra of the four isomers of **3.2**.*

3.1.6 Discussion

The ratios of the PSS of the first step of the molecular motor **3.1**, going from stable *trans*-**3.1** to unstable *cis*-**3.1** and for the third step, going from stable *cis*-**3.1** to unstable *trans*-**3.1**, were 5:95 and 10:90, respectively. The corresponding ratios of the molecular motor **3.2** are 22:78 for the first step, going from stable *cis*-**3.2** to unstable *trans*-**3.2**, and 21:79 for the third step in the rotary process, going from stable *trans*-**3.2** to unstable *cis*-**3.2**. It should be emphasized that the slightly lower selectivity does not affect the unidirectional rotation as long as light energy is supplied and the temperature is sufficiently high to ensure thermal helix inversion. The thermal barriers, which are the rate determining steps in the rotary process, have decreased considerably. Molecular motor **3.2** can perform its 360° rotation readily at room temperature. This is a significant improvement compared to the first-generation molecular motor **3.1** which had to be heated at 60°C before a significant conversion of the unstable *trans*-isomer to the stable *trans*-isomer takes place. Even compared to most of the second-generation molecular motors, where the speed of rotation could be tuned by synthetic modification, the newly presented motor molecule **3.2** is very fast. There is only one molecule of the family of the non-symmetric six-membered ring molecular motors which can keep up with the speed of the current symmetrical five-membered motor molecule **3.2**. The unstable form of the fastest rotating second-generation motor molecule has an half-life of 40 min at room temperature, which is slightly faster than

the slowest step going from unstable *cis*-**3.2** to stable *cis*-**3.2** ($t_{½}$= 78 min), but much slower than the fastest step going from unstable *trans*-**3.2** to the stable *trans*-**3.2** ($t_{½}$=18 s). The fact that the symmetrical five-membered motor molecule **3.2** shows much faster rotary motion than the (symmetrical) six-membered molecules in the thermally driven helix inversions, is promising for the further development of even faster, new generations of motor molecules. Moreover, it is highly surprising that compound **3.2**, which has two nearly flat five-membered rings, can adopt two energetically distinct conformations and that the apparently rather small differences in orientation of its methyl substituents are sufficiently large to control the unidirectional rotation process.

3.2 Decreasing the Size of the Motor Molecules

In pursuit of faster molecular motors, two possible structural variations have been shown to be possible for the structurally related six-membered symmetrical molecular motors. Smaller atoms can be introduced in the six-membered ring (oxygen instead of carbon) and the size of the substituent next to the double bond can be altered. In this section, the first target towards further structural modifications is the molecular motor **3.25**, with an oxygen atom incorporated in the five-membered ring. This compound is to be synthesized from 2-naphthol **3.21** in a five step procedure as shown in scheme 3.8.

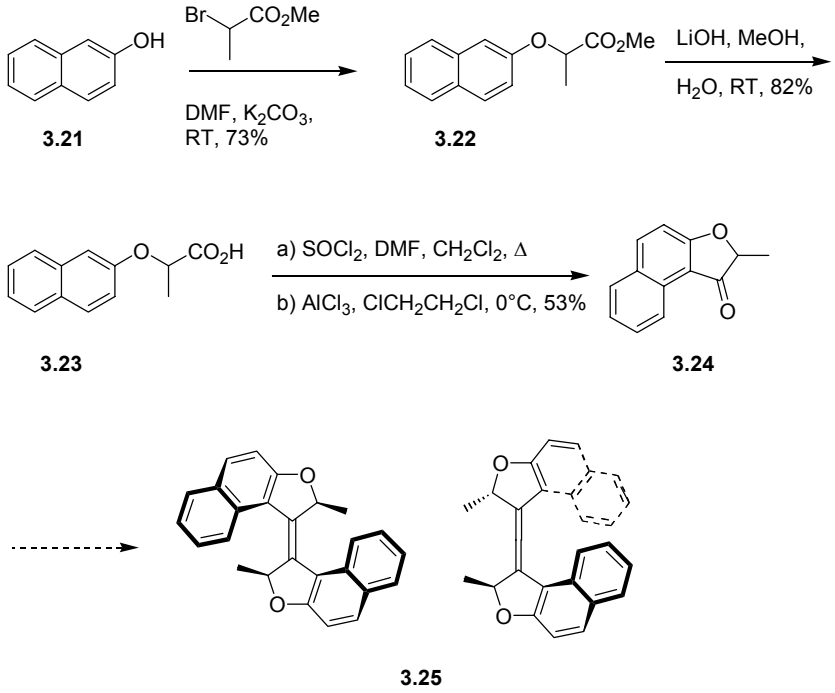

Scheme 3.8 *Attempted synthesis of oxygen containing molecular motor **3.25**.*

Reaction of 2-naphthol **3.21** with 2-bromopropionic acid methyl ester gave the methyl ester **3.22** in 73% yield. The methyl ester was then hydrolyzed by reaction with LiOH using standard conditions resulting in the acid **3.23** in moderate yield. This acid is slightly unstable, since the colorless product obtained after reaction turns yellow over time and the ^{1}H NMR spectrum reveals formation of decomposition products. Conversion of the acid **3.23** using standard Friedel-Crafts conditions gave the ketone **3.24** as a colorless oil in moderate yield. This oil proved to be quite unstable and turned brown overnight and formed a number of degradation products that were not further identified. Ketone **3.24** was therefore used immediately after purification in the final step of the reaction sequence: the reductive McMurry reaction. Using standard reaction conditions ($TiCl_4$/zinc powder) a complex mixture of products was obtained from which the desired alkene **3.25** could not be isolated. A possible explanation for failure of the reaction is the relatively high acidity of the α-proton, which might lead to a number of condensation products as well as the fact that the ketone **3.24** upon ketone-enol tautomerization yields an aromatic product.

3.3 Increasing the Size of the Substituent

The introduction of the more bulky *i*-propyl substituent revealed some interesting mechanistic details for the behavior of the motor molecules with two six-membered rings (chapter 2). The synthesis is, not unexpectedly, increasingly difficult going from the methyl, to the ethyl and finally the *i*-propyl substituents. The synthesis of the molecular motor with two five-membered rings **3.2** is much easier and the yields obtained in the McMurry reaction have improved dramatically. In view of these two observations, the choice was made to introduce two *t*-butyl groups onto the α-positions next to the double bond of a molecular motor with five-membered rings.

3.3.1 Synthesis

The synthesis of the molecule is straightforward and follows the general synthetic principles applied to the methyl substituted molecular motor **3.2** (scheme 3.9). The commercially available acid **3.26** was converted cleanly to ester **3.27** in good yield by reaction with methyl iodide in DMF in the presence of base. Deprotonation of the ester **3.27** using LDA in THF at low temperature and subsequent alkylation with **3.13** gave the desired ester **3.28** in moderate yield. This ester **3.28** could be cleaved only using harsh conditions, but **3.29** was obtained in good yield after refluxing for six days in a basic mixture containing KOH. This acid was then converted smoothly to the desired ketone **3.30** using the standard Friedel-Crafts procedure employing $SOCl_2$ and $AlCl_3$. Preliminary attemps to couple this ketone using the McMurry reaction with $TiCl_4$ and zinc powder resulted in the recovery of the starting material. However, using prolonged reaction times of nearly two weeks, the desired alkene **3.31** was obtained as a mixture of *cis*- and *trans*-isomers in an approximate 5:2 ratio in a combined yield of 19%. Since in the reaction mixture obtained after workup ketone **3.30** is still present, even longer reaction times might yield more product. The *cis*-isomer **3.31** was obtained pure by precipitation from heptane. The structures of both isomers were assigned by comparison of the ^{1}H NMR spectra with those

of the corresponding isomers of the methyl substituted five-membered ring molecular motor **3.2**.

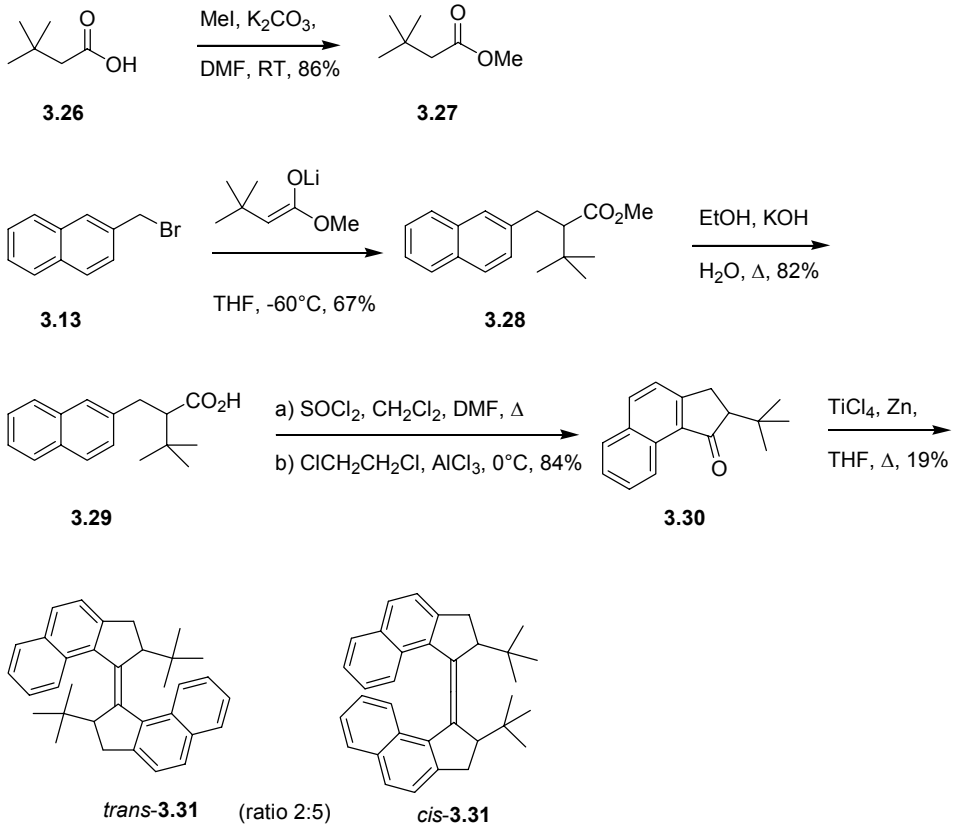

Scheme 3.9 *Synthesis of the t-butyl substituted molecular motor **3.31**.*

3.3.2 X-ray Crystallographic Analysis

Further evidence for the structural assignment was obtained by X-ray analysis of the *cis*-isomer of **3.31**. Sharp, colorless plateless of the *cis*-**3.31** suitable for X-ray crystallographic analysis were obtained by recrystallization from heptane (figure 3.14).

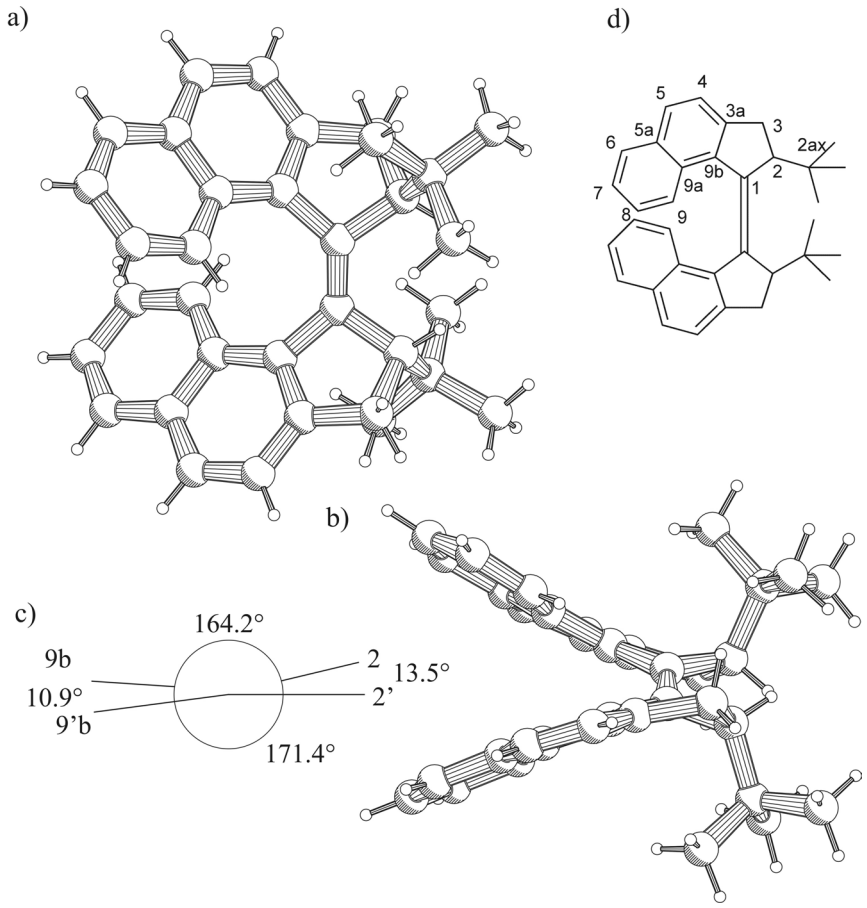

Figure 3.14 *PLUTO drawings of racemic (2S*,2'S*)-(P*,P*)-cis-(±)-2,2'-di-t-butyl-2,2',3,3'-tetrahydro-1,1'-bicyclopenta[a]naphthalenylidene (**3.31**) viewed perpendicular (a) to the central double bond and along (b) the central double bond. Newman projection of the configuration around the central double bond (c) as well as the numbering scheme adopted for the molecule (d) are depicted.*

The overall molecular shape of the *t*-butyl substituted *cis*-**3.31** shows only minor differences compared to the methyl substituted analogue *cis*-**3.2**. The structure of *cis*-**3.31**, which is C_2-symmetric in solution, deviates slightly from the preferred geometry due to crystal packing effects. The helical shape and the (pseudo-)axial orientation of the *t*-butyl substituents are the most noteworthy structural features. As was already observed for *cis*-**3.2**, the naphthalene moiety and the *t*-butyl substituent in each half of the molecule are found to be oriented in the same direction. The length of the double bond was found to deviate only slightly from literature values:[15] 1.353 Å. The geometry of *cis*-**3.31** around the central double bond (see also the Newman projection in fig. 3.14) is similar to that of *cis*-

3.2. The bond angles around C_1 and $C_{1'}$ are: C_2-C_1-C_{9b} = 104.1°, C_2-C_1-$C_{1'}$ = 124.2° and C_{9b}-C_1-$C_{1'}$ = 130.9° (average total angle around C_1 and $C_{1'}$= 359.8°). These values are averages of values in the two parts of the molecule since the structure is pseudo-C_2-symmetric. The values for the torsion angles around the double bond are: C_2-C_1-$C_{1'}$-C_2 = -13.5°, C_{9b}-C_1-$C_{1'}$-$C_{9'b}$ = 10.9° and C_2-C_1-$C_{1'}$-$C_{9'b}$ = 178.7° (average). Similarly to *cis*-**3.2**, the deviation from planarity of the alkene moiety in *cis*-**3.31** is relatively small compared to that in *trans*-**3.2**. Other parts of the structure, for *cis*-**3.31** compared to *cis*-**3.2**, showed a slightly larger change, *e.g.* the angle between the least-square planes of the atoms in both naphthalene moieties (48.1°), the torsion angle between the central double bond and the naphthalene moiety ($C_{1'}$-C_1-C_{9b}-C_{9a} = -44.8°) and the torsion angle to the *t*-butyl substituent (C_1-$C_{1'}$-$C_{2'}$-$C_{C2'ax}$ = 102.6°) The two five-membered rings in the molecule are relatively flat, the atoms C_1, C_2 and C_3 only slightly deviate from the least-square plane through C_1, C_2, C_3, C_{3a} and C_{9b}.

3.3.3 Photochemical Experiments

In order to investigate the photochemical behavior of **3.31**, enantiomerically pure material was needed. The stable *cis*-**3.31** could be resolved by chiral preparative HPLC using the Chiralcel OD column as the stationary phase and a mixture of heptane:*i*-propanol = 99.75:0.25 as the eluent. In order to determine the absolute configuration of the two fractions, the spectra of the first eluted fraction of *cis*-**3.31** and that of (2*R*,2'*R*)-(*P*,*P*)-*cis*-**3.2** were compared. As can be seen from figure 3.15, the UV-Vis and CD spectra are similar in shape. Noteworthy is the large difference in intensity of the absorption in the CD spectrum at 233.6 nm which has nearly doubled in magnitude. On the basis of this comparison, the absolute configuration of the first eluted fraction of the *t*-butyl substituted compound is assigned (2*R*,2'*R*)-(*M*,*M*)-*cis*-**3.31**.

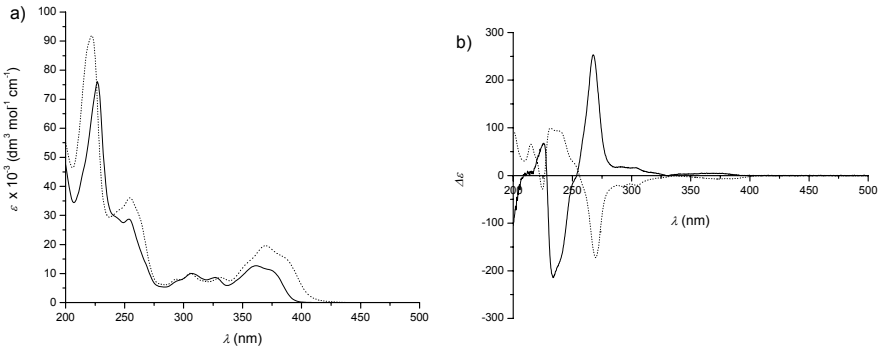

Figure 3.15 *UV-Vis (a) and CD (b) spectra of (2R,2'R)-(M,M)-cis-**3.31** (solid line) and (2R,2'R)-(P,P)-cis-**3.2** (dotted line) in n-hexane.*

Irradiation of a solution of (2*R*,2'*R*)-(*M*,*M*)-*cis*-**3.31** in *n*-hexane at low temperature ($\lambda \geq$ 280 nm, T= -25°C) gave complete conversion to another isomer of **3.31**, as was determined by

HPLC. The solution of (2*R*,2'*R*)-(*M*,*M*)-*cis*-**3.31**, which is colorless, turned rapidly orange upon irradiation and a band appeared as high as 480 nm in the UV-Vis spectrum. Coloration of the sample is observed in all cases for unstable forms, but never as intense and as red-shifted as for this sample. The UV-Vis and CD spectra of this new isomer are depicted in figure 3.16. The CD absorptions of the newly formed isomer are not as intense as for stable (2*R*,2'*R*)-(*M*,*M*)-*cis*-**3.31**. The most intense absorption is found at 223.0 nm ($\Delta\varepsilon$= -157.7), other signals at longer wavelengths are significantly less intense. Comparison of the CD spectrum of the new isomer of **3.31** with that of the unstable (2*R*,2'*R*)-(*M*,*M*)-*trans*-**3.2** or even unstable (2*R*,2'*R*)-(*M*,*M*)-*cis*-**3.2**, did not give decisive evidence for the formation of either unstable (2*R*,2'*R*)-(*P*,*P*)-*trans*-**3.31** or even unstable (2*R*,2'*R*)-(*P*,*P*)-*cis*-**3.31**, which is not supposed to form photochemically from the stable (2*R*,2'*R*)-(*M*,*M*)-*cis*-**3.31**. Upon heating the sample in *n*-hexane at 60°C, no decoloration was observed, pointing to the relative stability of this newly formed isomer. Only when a sample was dissolved in dodecane, allowing heating at elevated temperature (*e.g.* *T*= 90°C), decoloration of the sample was observed leading to the formation of (2*R*,2'*R*)-(*M*,*M*)-*trans*-**3.31**, as was confirmed by HPLC, UV-Vis and CD spectroscopy (see figure 3.16). The UV-Vis spectrum shows clearly the two absorptions at 350 and 360 nm, which are characteristic for (2*R*,2'*R*)-(*M*,*M*)-*trans*-**3.31**. Also in the case of (2*R*,2'*R*)-(*M*,*M*)-*trans*-**3.31**, the CD spectrum does not have the intense Cotton effects that were found for (2*R*,2'*R*)-(*P*,*P*)-*trans*-**3.2** (figure 3.9). The only obvious similarity between the two CD spectra are the absorptions in the CD at 259.2 nm ($\Delta\varepsilon$= +158.7) for stable (2*R*,2'*R*)-(*M*,*M*)-*trans*-**3.31** and at 258.0 nm ($\Delta\varepsilon$= -236.5) for the stable *trans*-**3.2**. The other Cotton effects in the CD spectrum are surprisingly small for such a twisted molecule.

As was indicated above, heating of a sample of the newly formed isomer of **3.31** in dodecane at elevated temperatures did lead to full conversion to the stable (2*R*,2'*R*)-(*M*,*M*)-*trans*-**3.31**. Since both stable (2*R*,2'*R*)-(*M*,*M*)-*trans*-**3.31** and (2*R*,2'*R*)-(*M*,*M*)-*cis*-**3.31** do not absorb light at 480 nm where the newly formed isomer of **3.31** has a strong absorption, an experiment was performed to determine the behavior of this molecule when irradiated at this absorption band. Direct excitation of a sample of the new isomer of **3.31** in *n*-hexane at this wavelength (λ= 436 nm, *T*= -25°C) gave after prolonged irradiation a complete conversion to the stable (2*R*,2'*R*)-(*M*,*M*)-*trans*-**3.31**. The long irradiation time (24h) needed is most probably due to the low intensity of the Xe-lamp at these wavelengths, but might also be due to a low quantum yield. Subsequent irradiation of the stable (2*R*,2'*R*)-(*M*,*M*)-*trans*-**3.31** ($\lambda\geq$ 280 nm, *T*= -25°C) gave within 15 min complete conversion to the same unknown isomer of **3.31** obtained after irradiation of stable (2*R*,2'*R*)-(*M*,*M*)-*cis*-**3.31**. Hence, the same UV-Vis and CD spectra were obtained after irradiation of either (2*R*,2'*R*)-(*M*,*M*)-*trans*-**3.31** and (2*R*, 2'*R*)-(*M*,*M*)-*cis*-**3.31**.

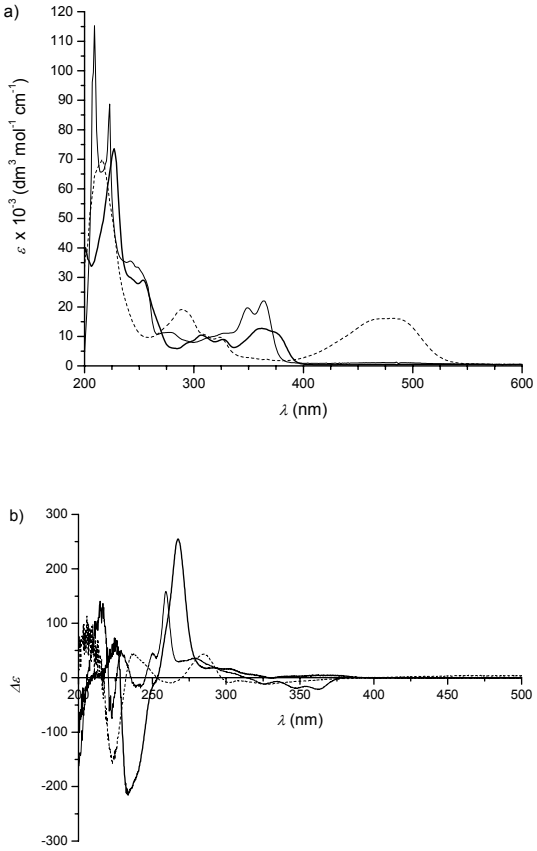

Figure 3.16 *UV-Vis (n-hexane) (a) and CD (n-hexane) (b) spectra of the isomers of t-butyl substituted olefin* ***3.31****. Stable (2R,2'R)-(M,M)-cis (thick solid line), unknown isomer (dashed line) and stable (2R,2'R)-(M,M)-trans (solid line).*

In order to quantify the height of the activation barrier for the conversion of the new isomer of **3.31** into the stable (2*R*,2'*R*)-(*M*,*M*)-*trans*-**3.31**, a sample of (2*R*,2'*R*)-(*M*,*M*)-*cis*-**3.31** in dodecane was irradiated ($\lambda \geq$ 280 nm, T= -25°C) to form this new isomer of **3.31**. The sample was then heated at various temperatures (70, 80, 90, 100°C) while the intensity of the CD-signal at 230 nm was monitored. The kinetic data revealed that a unimolecular process took place going from the new isomer of **3.31** to the stable (2*R*,2'*R*)-(*M*,*M*)-*trans*-**3.31**. Using an Eyring plot (figure 3.17), these data were used to calculate both the Gibbs energy ($\Delta^{\ddagger}G^{\theta}$ = 105±4 kJ·mol^{-1}), the enthalpy ($\Delta^{\ddagger}H^{\theta}$ = 76±4 kJ·mol^{-1}) and the entropy of activation ($\Delta^{\ddagger}S^{\theta}$ = -100±10 J·K^{-1}·mol^{-1}) and the half-life of the thermal helix inversion at room temperature ($t_{½}$ = 193h, 293.15K).

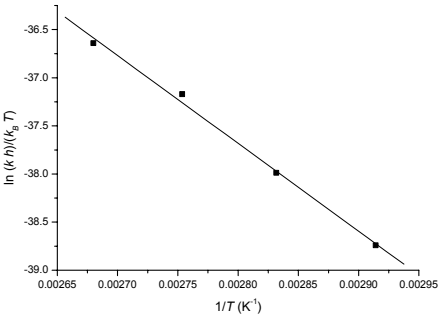

Figure 3.17 *Eyring plot for the thermal helix inversion of the new isomer of **3.31** to form the stable (2R,2'R)-(M,M)-trans-**3.31**.*

Unfortunately, the isomers of **3.31** are not as robust as the previously examined molecular motors. Upon prolonged (24 h) irradiation at $\lambda \geq$ 280 nm photodegradation took place to multiple products which precipitated from the solution.

3.3.4 Structural Determination of the Unknown Isomer

As stated above, the actual structure of new isomer could not be assigned by comparison with the UV-Vis and CD spectroscopic data from previously prepared switches or motor molecules. Therefore, irradiation experiments ($\lambda \geq$ 280 nm, T= 20°C) were performed with a mixture of stable *trans*-**3.31** and stable *cis*-**3.31** in toluene-d_8 and benzene-d_6 in order to generate quantitatively the unknown isomer of **3.31**. The assignment of the geometry of the unknown isomer of **3.31** on basis of ^{1}H NMR spectroscopy was difficult. The arene protons absorbing at relatively high field, δ 6.4 and δ 6.8 ppm, are normally indicative for molecules with a *cis*-geometry. The shift to higher field is due to the ring current anisotropy of a neighboring naphthalene moiety. At the same time, no absorption was observed at low field at approximately δ 8.0 ppm which would indicate a *trans*-geometry. However, in the NOE spectrum, a small interaction was observed between the protons of the *t*-butyl and the protons at C_9 of the naphthalene ring, which is usually observed for *trans*-isomers, but not for *cis*-isomers. Interestingly, while following the photochemical reaction by ^{1}H NMR spectroscopy, first the stable *trans*-**3.31** is converted completely to the unknown isomer of **3.31**, followed by a slower, complete conversion of *cis*-**3.31** to the unknown isomer of **3.31**. After prolonged irradiation, a number of decomposition products appear in the spectrum. One side product **3.32**, the result of photo-oxidation of **3.31**, could be isolated and characterized (figure 3.18). Sofar, these or similar side-products, have not been observed for either six-membered molecular motors as described in the previous chapter or for the five-membered molecular motor **3.2** as described in the present chapter. Conclusive evidence for structure of the unknown isomer of **3.31** could only be obtained by X-ray crystallography (*vide infra*).

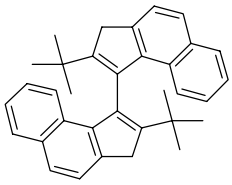

3.32

Figure 3.18 *Photodegradation products isolated from the ^{1}H NMR experiment.*

Heating of the unknown isomer of **3.31** at 100°C in a toluene-d_8 solution showed a fairly rapid conversion to the stable *trans*-**3.31**, followed by the very slow (days in boiling toluene-d_8) thermal conversion to the stable *cis*-**3.31**. The thermal interconversion of *cis* to *trans* isomers of alkenes is know for numerous compounds in literature, *e.g.* stilbenes.[18] However, the reverse, formation of a *cis*-isomer thermally from a *trans*-isomer could not be found in literature. This is another indication, apart from the preferred formation of the *cis*-**3.31** over *trans*-**3.31** in the synthesis, that *cis*-**3.31** is thermodynamically more stable than *trans*-**3.31**.

3.3.5 X-ray Crystallographic Analysis: Unstable Cis

The unknown isomer of **3.31** was generated by irradiation ($\lambda \geq$ 280 nm, T= 20°C) of a solution of stable (2R^*,2R^*)-(M^*,M^*)-*cis*-**3.31** and stable (2R^*,2R^*)-(M^*,M^*)-*trans*-**3.31** in toluene-d_8 and could be crystallized by slow diffusion of methanol in an *n*-hexane solution as an orange crystal suitable for X-ray crystallography. Surprisingly, the unknown isomer of **3.31** obtained after irradiation proved to be the (2R^*,2'R^*)-(P^*,P^*)-*cis*-**3.31**. The helicity of (2R^*,2'R^*)-(P^*,P^*)-*cis*-**3.31** is, compared to that of stable (2R^*,2'R^*)-(M^*,M^*)-*cis*-**3.31**, inverted. Although the X-ray structure of the unstable *cis*-**3.31** suggests that the compound is C_2-symmetric in the crystal, it is slightly distorted from its preferred C_2-symmetric geometry in solution as was evident from ^{1}H NMR. Another remarkable feature of the molecule is the twisted nature of the compound. Not only is the double bond severely twisted, but also the two naphthalene moieties are bent. This all in order to keep the *t*-butyl substituents in an axial position (torsion angle $C_{1'}$-C_1-C_2-C_{2ax} (average, 73.7°)). The central double bond is significantly longer, 1.379 Å, compared that of, for example, stable (2R^*,2'R^*)-(P^*,P^*)-*cis*-**3.2** (1.359 Å, average) and (2R^*,2'R^*)-(M^*,M^*)-*cis*-**3.31** (1.353 Å). The angles around the carbon atoms C_1 and $C_{1'}$ around the double bond are characterized as follows: C_2-C_1-C_{9b} (107.02°), C_2-C_1-$C_{1'}$ (120.87°), C_{9b}-C_1-$C_{1'}$ (132.11°), $C_{2'}$-$C_{1'}$-$C_{9'b}$ (107.03°), $C_{2'}$-$C_{1'}$-C_1 (119.86°) and $C_{9'b}$-$C_{1'}$-C_1 (133.10) giving total angles around C_1 of 360.0° and $C_{1'}$ of 360.0°. From the torsion angles C_2-C_1-$C_{1'}$-C_2 = -37.3°, C_{9b}-C_1-$C_{1'}$-$C_{9'b}$ = -39.6° and C_2-C_1-$C_{1'}$-$C_{9'b}$ = 141.58° (average), it can be seen that the central double bond is severely twisted. This is especially obvious from the Newman projection in figure 3.19 and by comparison with the torsion angles of stable (2R^*,2'R^*)-(M^*,M^*)-*cis*-**3.31**: C_2-C_1-$C_{1'}$-C_2 = 13.5°, C_{9b}-C_1-$C_{1'}$-$C_{9'b}$ = 10.9° and C_2-C_1-$C_{1'}$-$C_{9'b}$ = 178.7° (average). The torsion angle C_{9a}-C_{9b}-C_1-$C_{1'}$ is in the unstable (2R^*,2'R^*)-(P^*,P^*)-*cis*-**3.31** reduced to only 6.4° (average). In the stable *cis*-isomers, this torsion angle normally nicely refects the angle between the both naphthalene chromophores. Now, however, the central double bond is twisted to such

an extent that it no longer reflects this angle (42.0°) correctly. Also the naphthalene moieties themselves are bent. Whereas in each half of the molecule one aromatic ring is relatively flat (C_{5a}-C_6-C_7-C_8-C_9-C_{9a} and $C_{5'a}$-$C_{6'}$-$C_{7'}$-$C_{8'}$-$C_{9'}$-$C_{9'a}$) the remaining atoms in the naphthalene moiety are bent away to avoid steric hindrance. The deviations from the least-square planes through the planar aromatic rings are quite large: C_{3a} (-0.40 Å), C_4 (0.51 Å), C_5 (-0.26 Å), C_{9b} (0.02 Å), C_{3a} (-0.19 Å), $C_{4'}$ (0.28 Å), $C_{5'}$ (-0.15 Å) and $C_{9'b}$ (0.10 Å).

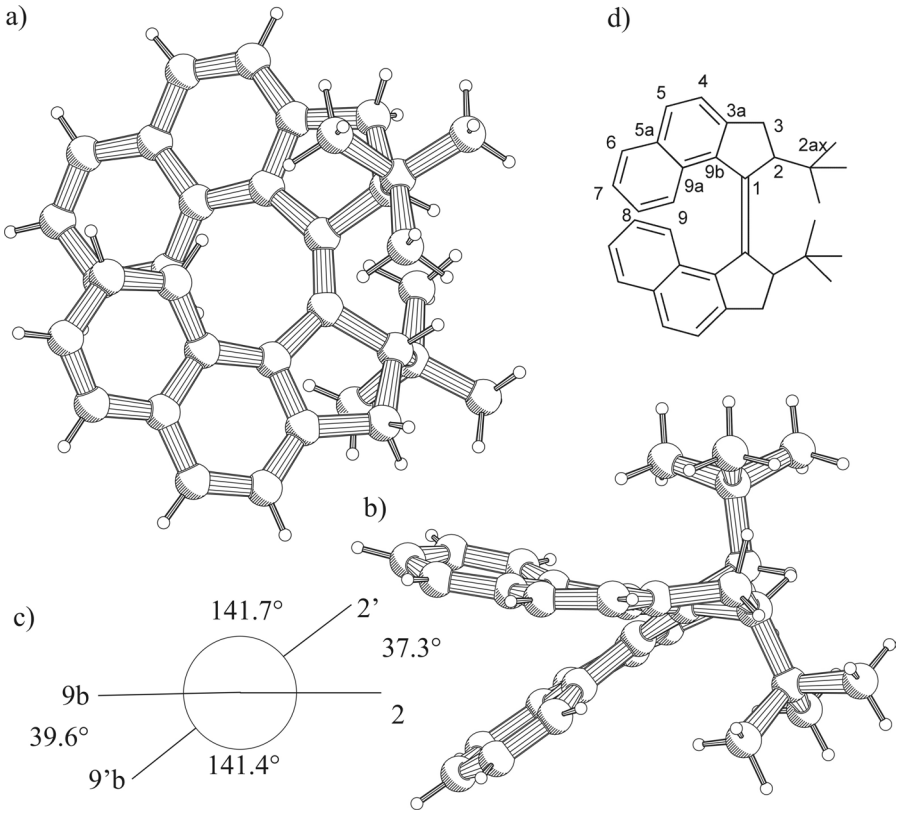

Figure 3.19 *PLUTO drawings of (2S*,2'S*)-(M*,M*)-cis-(±)-**3.31**; t-butyl substituted overcrowded alkene **3.31** viewed perpendicularly (a) and along (b) the central double bond. The Newman projection viewing along the central double bond (c) and the adopted numbering scheme (d).*

The five-membered rings are, compared to their stable counterparts, relatively flat and the deviations for C_1, C_2 and C_3 from the least-square plane through C_1-C_2-C_3-C_{3a}-C_{9b} are not larger than 0.11 Å. So by bending the naphthalene away rather than twisting the central double bond in the molecule, the steric bulk can be accommodated. Twisted and sterically distorted alkenes have been topic of interest for many decades. An excellent recent review

on organic molecules with abnormal geometric parameters has been written by Komarov.[19] Compared to the examples in literature, the unstable (2*R**,2'*R**)-(*P**,*P**)-*cis*-**3.31** possesses one of the most twisted double bonds. The only examples which could be found in the literature having a more twisted double bond are the alkenes **3.33**,[20] **3.34**[21] and its derivatives**, 3.35**[22] and **3.36**[22] (figure 3.20).

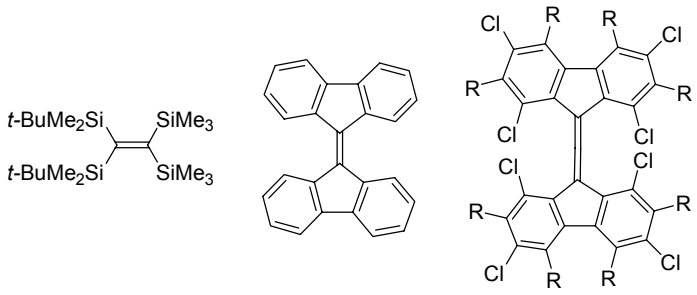

3.33: 50° **3.34**: up to 54° **3.35**, R=H: 55° **3.36**, R=Cl: 66°

Figure 3.20 *Alkenes **3.33** and **3.34-3.36** with a larger twist of the double bond than the less stable cis-**3.31**.*

3.3.6 Rotary Motion and Isomerization Pathways of the *t*-Butyl-Substituted Alkene

Summarizing the observations above, the following scheme can be drawn for the *t*-butyl substituted alkene **3.31** (see scheme 3.10). Photoirradiation of either stable (2*R**,2'*R**)-(*M**,*M**)-*trans*-**3.31** or stable (2*R**,2'*R**)-(*M**,*M**)-*cis*-**3.31** ($\lambda \geq$ 280 nm) leads to the formation of the unstable (2*R**,2'*R**)-(*P**,*P**)-*cis*-**3.31**. Heating at elevated temperatures of unstable (2*R**,2'*R**)-(*P**,*P**)-*cis*-**3.31** gives the stable (2*R**,2'*R**)-(*M**,*M**)-*trans*-**3.31**. The same reaction can also be performed by irradiation of the unstable (2*R**,2'*R**)-(*P**,*P**)-*cis*-**3.31** with light (λ= 436 nm). Further heating of stable (2*R**,2'*R**)-(*M**,*M**)-*trans*-**3.31** completes the cycle and reverts the system *via* a slow thermal isomerization to the starting point as the stable (2*R**,2'*R**)-(*M**,*M**)-*cis*-**3.31** is regenerated.

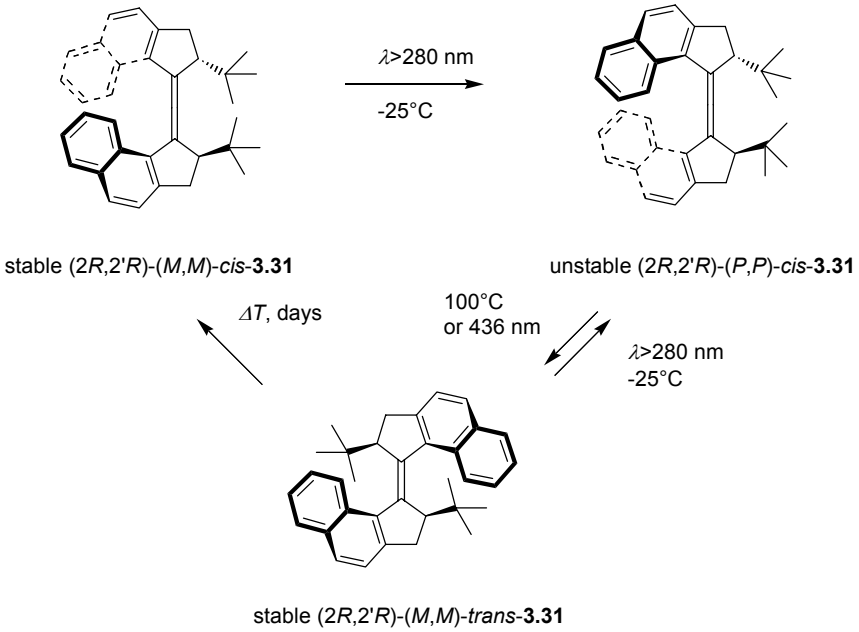

Scheme 3.10 *Photochemical and thermal isomerizations of t-butyl substituted alkene **3.31**.*

3.3.7 Calculations[17]

In the case of the methyl substituted molecular motor **3.2** the experimental results were accurately confirmed by DFT calculation using the b3lyp/6-31g(d)//b3lyp/3-21g(d) method. Not only the structures of the three experimentally observed isomers of **3.31** were calculated, but also the possibility was investigated whether an unstable *trans*-isomer of **3.31** could be located at an energy minimum. To ascertain wherther an energy minima had been reached for each of the four isomers of **3.31**, the infrared spectra were calculated and only positive normal modes were found. The relevant structural data are depicted in table 3.2. All structures were found to be C_2-symmetric. Analoguous to methyl substituted **3.2**, the stable *cis*-**3.31** is the most stable of the four isomers. Relative to the stable *cis*-**3.31**, the unstable *cis*-**3.31** lies 57.5 kJ·mol^{-1} higher in energy. The stable *trans*-**3.31** has an higher energy than the stable *cis*-**3.31**, with a value of 42.0 kJ·mol^{-1}. The unstable *trans*-**3.31**, which is indeed located at an energy minumum, is much more unstable than all the other isomers and the difference in energy relative to the stable *cis*-**3.31** is as high as 89.7 kJ·mol^{-1}. As is also the case for the calculations presented for the methyl substituted molecular motor **3.2**, these calculations reflect accurately the experimentally determined data obtained from X-ray crystallographic analyses. No statement can be made, however, concerning their kinetic stability since this depends on activation barriers, which were not calculated.

Table 3.2 *Results of the calculated structures for all four isomers and the experimentally determined data from X-ray crystallography.*

	stable *cis*-**3.31**		unstable *cis*-**3.31**		stable *trans*-**3.31**	unstable *trans*-**3.31**
	DFT	X-ray	DFT	X-ray	DFT	DFT
ΔE (kJ·mol^{-1})	0		+57.5		+42.0	+89.7
C_1-C_1	1.356 Å	1.353 Å	1.380 Å	1.379 Å	1.359 Å	1.374 Å
C_2-C_1-C_{9b}	104.4°	104.1°	107.4°	107.0°	104.1°	104.6°
C_2-C_1-$C_{1'}$	124.9°	124.2°	121.1°	120.4°	145.1°	129.9°
C_{9b}-C_1-$C_{1'}$	129.5°	130.9°	131.5°	132.6°	123.8°	104.6°
C_2-C_1-$C_{1'}$-$C_{2'}$	-19.0°	-13.5°	-40.2°	-37.3°	145.1°	-136.8°
C_{9b}-C_1-$C_{1'}$-$C_{9b'}$	9.6°	10.9°	-43.5°	-39.6°	-142.4°	143.0°
C_2-C_1-$C_{1'}$-$C_{9'b}$	175.3°	178.7°	138.1°	141.6°	1.3°	-40.1°
C_1-$C_{1'}$-$C_{9'b}$-$C_{9'a}$	-44.9°	-44.8°	-72.0°	-73.7°	-62.6°	-36.1°
C_1-$C_{1'}$-$C_{2'}$-$C_{2'C}$	-105.9°	102.6°	-7.9°	-6.4°	-130.5°	-24.6°

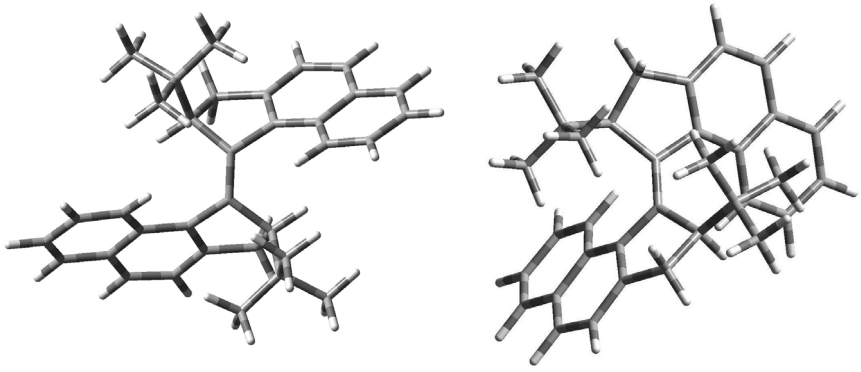

Figure 3.21 *Calculated structures of the stable and unstable trans isomers of **3.31**.*

The calculated structures of the stable and unstable *trans*-**3.31** isomers are depicted in figure 3.21. Both molecules have a helical shape and, as was observed experimentally for the *cis*-isomers of **3.31**, the *t*-butyl substitutents in both isomers of *trans*-**3.31** adopt an axial orientation. The central double bond in unstable *trans*-**3.31** is twisted to approximately the same extent as in the unstable *cis*-**3.31** (see table 3.2). The calculated structures of the *cis*-isomers of **3.31** show excellent agreement with the experimentally obtained data by X-ray analysis as can be seen from table 3.2. This is important to note, since it shows that using this methodology the structures of these highly strained molecules can accurately be predicted. The optimized structures described above were used for the calculation of the UV-Vis and CD spectra using the time dependent DFT method. The excitation energies and the rotatory strengths for each of the four isomers of **3.31** were calculated using the b3lyp/6-31g(d) method. The experimentally and calculated UV-Vis and CD spectra of each isomer are depicted in figures 3.22 and 3.23, respectively.

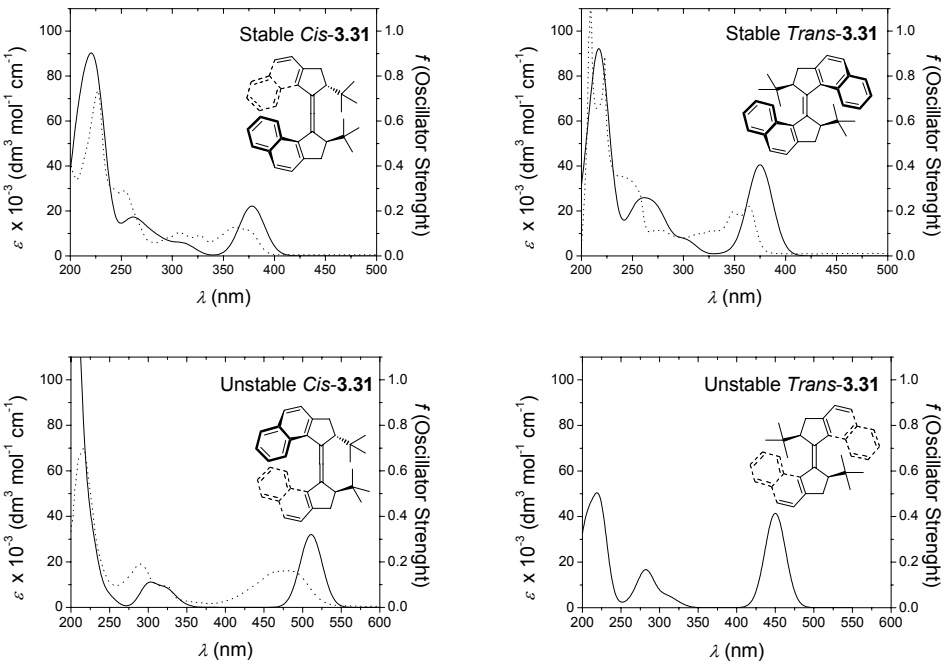

Figure 3.22 *The experimentally determined UV-Vis (dotted line) and the calculated UV-Vis (solid line) spectra of the four isomers of* ***3.31****.*

As was the case for **3.2**, the UV-Vis and CD spectra can be calculated quite accurately using this methodology. The calculated UV-Vis spectra show roughly the same absorption bands as the experimentally determined UV-Vis spectra, although most of the fine structure is missing (figure 3.22). However, the calculated UV-Vis band of the lowest energy is again consequently shifted to longer wavelengths compared to the experimentally determined band. The same observation can be made for the CD spectra (see figure 3.23). The large Cotton effects are accurately predicted in sign and size, but the fine structure of the spectra is not accurately reproduced by the calculation. It is important to note that the shape and sign of the Cotton effects is calculated correctly, since it is essential for the correct assignment of the absolute configuration of the isomers of alkene **3.31**.

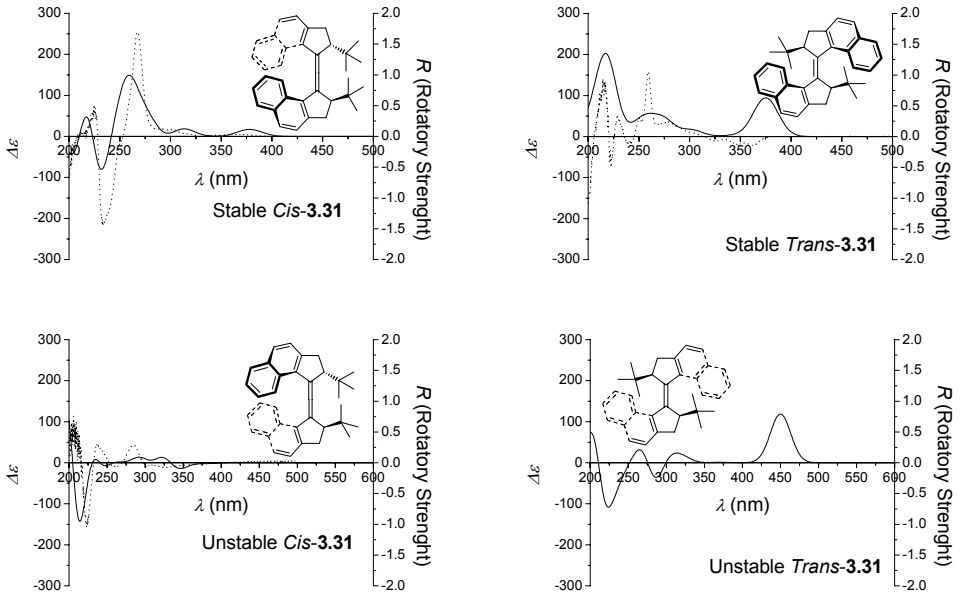

Figure 3.23 *The experimentally determined CD (dotted line) and the calculated CD (solid line) spectra of the four isomers of **3.31**.*

3.3.8 Discussion

The experimental observations described above for alkene **3.31** are different from all molecular motors described so far. Contrary to the usual rotary behavior of the overcrowded alkenes, no evidence for the formation of the unstable *trans*-**3.31** was found. The existence of the three other forms, stable and unstable *cis*-**3.31** and stable *trans*-**3.31** could be confirmed experimentally. Two important differences in the behavior of bis-*t*-butyl substituted alkene **3.31** compared to, for example, the bis-methyl substituted alkene **3.2** have to be noted. The first difference is that irradiation of a stable *cis*-isomer would normally lead to the formation of an unstable *trans*-isomer. In case of **3.31**, irradiation of the stable *cis*-**3.31** gives the unstable *cis*-**3.31** isomer. Apparently there is a preference after relaxation from the excited state for the pathway leading to formation of this unstable *cis*-**3.31**. From stable *cis*-**3.31** it is difficult to form the unstable *trans*-**3.31** because of the two very bulky *t*-butyl substituents which have to pass along each other. It is much easier for the two naphthalene moieties to flip along each other. Therefore, refolding in the excited state followed by relaxation to the ground state takes place along a pathway that eventually leads to the unstable *cis*-**3.31**. Although experimentally the unstable *trans*-**3.31** was not

observed, calculations indicate that this isomer is found at an energy minimum, but that it is significantly higher in energy than the other three isomers.

A second difference is that heating of an unstable *cis*- or *trans*-isomer normally would lead to the stable *cis*- or *trans*-isomeric counterparts. The thermal conversion of unstable *cis*-**3.31** to stable *trans*-**3.31** has no precedent in previously reported systems. This interconversion takes place at elevated temperatures at moderate speed. Other characteristics of alkene **3.31** have found precedent. For example, molecular motor **2.2** is able to switch selectively between the stable *cis*-**2.2** and the unstable *trans*-**2.2**. This switching behavior is described in chapter 2.[23] The present overcrowded alkene **3.31** could in principle also function as such a perfect chiroptical switch with full conversion in either way and simple read-out. A negative aspect is the production of various side-products upon prolonged irradiation of which **3.32** could be isolated and characterized. These side-products were, however, only obtained after prolonged irradiation times (hours) with polychromatic light ($\lambda \geq$ 280 nm). Upon irradiation of stable *trans*-**3.31** with light ($\lambda \geq$ 280 nm) the system completely switches to the unstable *cis*-**3.31**. Reversal of the process is accomplished by irradiation with blue light (λ= 436 nm). Probably irradiation of *trans*-**3.31** leads to the same exited state as irradiation of stable *cis*-**3.31**. Finally, the stable *trans*-**3.31** is thermally converted to the stable *cis*-**3.31**. Although so far no thermal conversion of a *trans*-isomer to *cis*-isomer has been reported, the opposite, thermal conversion of a *cis*-isomer to *trans*-isomer is a common process found in the literature,[18a] *e.g.* for stilbenes[18b] and azobenzenes.[24]

Also the overcrowded alkene **3.31** could function as a molecular motor. The unidirectional rotation can, however, not be proven unequivocally. The problem is that during the thermal conversion of stable *trans*-**3.31** to stable *cis*-**3.31**, the two halves of the molecule can either rotate clockwise or counterclockwise. Neither of the two pathways can be excluded and hence the unidirectionality of rotation of the system is not certain. However, the system performs its three-state cycle with high selectivity. Starting with the stable *cis*-**3.31**, irradiation in the first step of the rotary process leads to the unstable *cis*-**3.31**. Subsequent heating or irradiation of unstable *cis*-**3.31** gives stable *trans*-**3.31**. The system reverts to the original *cis*-**3.31** on prolonged heating of stable *trans*-**3.31** at high temperatures. The molecule is therefore a three-state switching system, since unidirectional rotation cannot be proven unequivocally.

3.4 Conclusion

The new molecular motor **3.2** presented in this chapter has a five-membered ring in both upper and lower halves connected by an olefinic bond, a structural feature distinct from all light-driven molecular motors reported sofar which contain either one or two six-membered rings. The new molecular motor **3.2** is synthesized far more efficiently as yields of up to 76% have been reached in the key coupling reaction. The increased synthetic accessibility of the molecular motors having a five-membered ring comes to expression in the synthesis of the molecular motor molecule **3.31** bearing *t*-butyl substituents instead of methyl substituents. For the original molecular motor it was nearly impossible to introduce the

relatively large *i*-propyl substituents next to the double bond let alone the sterically very demanding *t*-butyl substituents. Another remarkable finding is that, in contrast to the synthesis of the symmetrical molecular motor **3.1**, both *cis*-and *trans*-isomers of **3.2** and **3.31** are obtained. The *cis*-isomers of both five-membered ring molecular motors **3.2** and **3.31** are even obtained in excess, whereas during the preparation of the original motor molecule **3.1** no trace of a *cis*-isomer was found. Photo-isomerization studies with **3.2** revealed that the photochemical equilibria are less favorable compared to molecular motors with a six-membered ring. Both the five- and six-membered molecular motors have a similar geometry as far as the overall helicity and stereochemistry of the molecule is concerned. X-ray crystallographic analysis showed that the atoms in the five-membered ring have only a slight deviation from the least-square plane through the atoms of the five-membered ring. As a result there are only small conformational differences between the methyl substituents in a (pseudo-)axial and in a (pseudo-)equatorial orientation, but surprisingly the energy differences are still large enough to enable the molecule to rotate in a unidirectional fashion. The unidirectionality of the rotation has been shown by CD spectroscopy and ^{1}H NMR spectroscopy at low temperature. Compared to the symmetric first-generation molecular motor **3.1**, the newly presented motor **3.2** is considerably faster and only one second-generation molecular motor with a six-membered ring can keep up with the present molecular system. Because of the low thermal isomerization barriers, molecular motor (2*R*,2'*R*)-**3.2** is capable of a continuous rotation in a net clockwise fashion upon irradiation at room temperature. The slightly lower selectivity of both photoisomerizations does not affect the unidirectional rotary motion since the two thermal inversion steps shift both photoequilibria under conditions of continuous irradiation. The presented findings offer important guidelines for the design of more advanced rotary motors. The photochemical behavior of the *t*-butyl substituted molecular motor is completely different from that of the methyl substituted molecular motor. An important difference can be found in the stability of the both unstable forms. The unstable *cis*-**3.31** was found to be much more stable than the unstable *cis*-**3.2**, presumably due to steric hindrance. Unfortunately, the *trans*-isomer-**3.31** was too unstable and no experimental evidence for the existance of this isomer could be obtained by UV-Vis, CD or NMR spectroscopy. Despite the different behavior the molecule can perform a 360° rotation around its central double bond. However, the unidirectionality of this rotation cannot be established unequivocally. Also, the molecule in principle is able to function as a molecular switch by selective interconversion between the stable *trans*-**3.31** and the unstable *cis*-**3.31**. The selectivity for the individual photochemical steps in **3.31** is unprecedented in the motor systems, since both photoequilibria proceed with full selectivity to single isomers of **3.31**. The ratios obtained in for example motor **3.2** at the PSS are much less selective. In conclusion, the alkene **3.31** not only offers new insights in the behavior of the molecular motor, but also provides an interesting showcase for stereochemistry in general.

3.5 Experimental Section

General Remarks

See chapter 2 for general remarks concerning all experimental details in this section.

Computational Details

Prior to calculation of the excited states, the geometry of all the molecules was optimized in their ground states with the use of the b3lyp hybrid funcional and 3-21g(d) basis set.[25] That the calculated structures were found at an energy minimum was confirmed by a frequency analysis, for each case only positive eigenvalues were found. Additionally, for all minimum geometries single point energies at b3lyp/6-31g(d) level were calculated. Excitation energies, oscillator strengths and rotatory strengths were calculated using the time-dependent DFT method[26] at b3lyp/6-31g(d) level of theory. For each of the investigated molecules 35 excited states were calculated. The rotatory strengths (R) were calculated in the dipole length representation from equation:

$$R_{0i} = Im(\langle \Psi_0 | \hat{\mu} | \Psi_i \rangle \langle \Psi_0 | \hat{m} | \Psi_i \rangle) = |\vec{\mu}_{0i}| \bullet |\vec{m}_{0i}| \bullet \cos(\vec{\mu}_{0i}, \vec{m}_{0i})$$

All calculations were carried out with the Gaussian98 suite of programs.[27] The CD and UV-Vis spectra were simulated by overlapping Gaussian functions for each transition.[28]

Table 3.3 X-ray crystallographic data of (2R^*,2'R^*)-(P^*,P^*)-*trans*-(±)-**3.2** and (2R^*,2'R^*)-(P^*,P^*)-*cis*-(±)-**3.2**.

compound	stable *trans*-(±)-**3.2**	stable *cis*-(±)-**3.2**
formula	$C_{28}H_{24}$	$C_{28}H_{24}$
fw (g·mol^{-1})	360.50	360.50
crystal dimension (mm)	0.45 x 0.42 x 0.13	0.41 x 0.39 x 0.33
color	slightly yellow	colorless
habit	platelet	block
crystal system	orthorhombic	monoclinic
space group, no.	*Pbca* (61)	$P2_1$ (4)
a (Å)	9.3938 (5)	10.144 (1)
b (Å)	18.939 (1)	15.382 (2)
c (Å)	21.924 (1)	13.469 (2)
β (°)		106.173 (2)
V (Å^3)	3900.5 (3)	2018.5 (4)
Z	8	4
ρ (g·cm^{-3})	1.228	1.186
T (K)	100 (1)	100 (1)
μ (cm^{-1})	0.69	0.67)
number of reflections	4825	7768
number of refined parameters	349	546
final agreement factors:		
$wR(F^2)$	0.1175	0.2161
$R(F)$	0.0446	0.0824
GooF	1.029	1.046

Table 3.4 X-ray crystallographic data of (2*S**,2'*S**)-(*P**,*P**)-*cis*-(±)-**3.31** and (2*S**,2'*S**)-(*M**,*M**)-*cis*-(±)-**3.31**.

compound	stable *cis*-(±)-**3.31**	unstable *cis*-(±)-**3.31**
formula	$C_{34}H_{36}$	$C_{34}H_{36}$
fw ($g \cdot mol^{-1}$)	444.66	444.66
crystal dimension (mm)	0.35 x 0.29 x 0.11	0.50 x 0.38 x 0.31
color	colorless	orange
habit	needle	block
crystal system	orthorhombic	orthorhombic
space group, no.	*Pbca* (61)	$P2_12_12_1$ (19)
a (Å)	7.2761 (3)	9.7582 (6)
b (Å)	19.4524 (8)	14.4454 (8)
c (Å)	36.240 (1)	17.915 (1)
V ($Å^3$)	5129.3 (3)	2525.3 (3)
Z	8	4
ρ ($g \cdot cm^{-3}$)	1.152	1.169
T (K)	100 (1)	100(1)
μ (cm^{-1})	0.64	0.65
number of reflections	6334	4973
number of refined parameters	451	451
final agreement factors:		
$wR(F^2)$	0.1230	0.0838
$R(F)$	0.0475	0.0341
GooF	1.030	1.049

(2*R,2'*R**)-(*P**,*P**)-*trans*-(±)-2,2'-Dimethyl-2,2',3,3'-tetrahydro-1,1'-bicyclopenta[*a*]-naphthalenylidene-(3.2)**

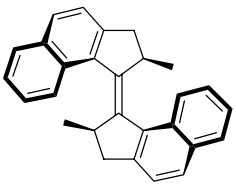

To a stirred suspension of zinc powder (1.34 g, 20.5 mmol) in THF (6 ml) was added slowly $TiCl_4$ (1.14 ml, 10.3 mmol) at 0°C. The resulting black slurry was then heated at reflux for 2h. A solution of ketone **3.3** (1.01 g, 5.15 mmol) in THF (4 ml) was added and the heating was continued for 3d. The reaction mixture was poured into a sat. aq. sol. of NH_4Cl (100 ml) and was extracted with ethyl acetate (3x 75ml). The combined organic layers were dried ($MgSO_4$) and the solvents were removed under reduced pressure to yield the impure product as a brown oil. Further purification was performed by column chromatography (SiO_2, heptane, R_f= 0.31) yielding the desired olefins as a yellowish oil (605 mg, 1.96 mmol, 76%) as a mixture of *cis*-**3.2** and *trans*-**3.2** in an approximate ratio of 5:2; *m/z* (EI, %) = 360 (M^+, 100); HRMS (EI): calcd. for $C_{28}H_{24}$: 360.1878, found 360.1866; *Trans*-**3.2** olefin could be recrystallized from ethyl acetate to provide beige crystals in 14% yield (m.p. 192.7-193.2°C); Stable (2*R**,2'*R**)-(*P**,*P**)-*trans*-**3.2**: ^{1}H (300 MHz, $CDCl_3$) δ 1.29-1.32 (d, *J*= 6.2 Hz, 6H, Me_{2ax}), 2.32-2.37 (d, *J*= 14.7 Hz, 2H, H_{3eq}), 2.93-3.00 (dd, *J*= 14.7, 5.5 Hz, 2H, H_{3ax}), 3.03-3.09 (m, 2H, H_{2eq}), 7.39-7.42 (d, *J*= 8.1 Hz, 2H, H_4), 7.44-7.49 (m, 2H, H_7), 7.52-7.57 (m, 2H, H_8), 7.75-7.78 (d, *J*= 8.1 Hz, 2H, H_5), 7.90-7.93 (d, *J*= 8.4 Hz, 2H, H_6), 8.25-8.27 (d, *J*= 8.4 Hz, 2H, H_9); ^{1}H (500 MHz, toluene-d_8, -20°C) δ 1.26-1.27 (d, *J*= 6.4 Hz, 6H), 2.04-2.07 (d, *J*= 14.6 Hz, 2H), 2.72-2.76 (dd, *J*= 14.6, 5.6 Hz, 2H), 3.07-3.10 (m, 2H), 7.18-7.20 (d, *J*= 8.2 Hz, 2H), 7.30-7.33 (m, 2H), 7.38-7.41 (m, 2H), 7.56-7.58 (d, *J*= 8.1 Hz, 2H), 7.72-7.74 (d, *J*= 8.1, 2H), 8.38-8.39 (d, *J*= 8.1 Hz, 2H); ^{13}C (50 MHz, $CDCl_3$) δ 19.3 (q), 41.3 (t), 43.1 (d), 124.1 (d), 124.7 (d), 125.0 (d), 126.7 (d), 127.7 (d), 128.4 (d), 130.2 (s), 132.9 (s), 138.5 (s), 141.4 (s), 141.8 (s); UV-Vis: (*n*-hexane) $\lambda_{max}(\varepsilon)$

217 (103600), 245 (42900), 352 (28700), 368 (29000); *Trans*-**3.2** isomer could be separated using a Chiralcel OD column as the stationary phase and a mixture of heptane : *i*-propanol in a ratio of 99.9 : 0.1 as the eluent at a rate of 1 ml·min^{-1}. The first eluted fraction (t= 12.2 min) contained (2*R*,2'*R*)-(*P*,*P*)-*trans*-**3.2**, the second eluted fraction (t= 14.4 min) contained (2*S*,2'*S*)-(*M*,*M*)-*trans*-**3.2**. Unfortunately, preparative HPLC separation failed using these conditions. Using a Chiralcel OD column as the stationary phase and a mixture of heptane : *i*-propanol in a ratio of 99.5 : 0.5 as the eluent both enantiomers of *trans*-**3.2** have the same retention time (t= 5.54 min) at a rate of 1 ml·min^{-1}. By irradiation of a solution containing enantiomerically pure (2*R*,2'*R*)-(*P*,*P*)-*cis*-**3.2** (see below) in *n*-hexane at –40°C and subsequent heating, a mixture of (2*R*,2'*R*)-(*P*,*P*)-*cis*-**3.2** and (2*R*,2'*R*)-(*P*,*P*)-*trans*-**3.2** was obtained which was separated using preparative HPLC (Daicel Chiralcel OD column as the stationary phase and a mixture of heptane : *i*-propanol in a ratio of 99.9 : 0.1 as the eluent at a rate of 1 ml·min^{-1}) into the individual compounds; (2*R*,2'*R*)-(*P*,*P*)-*trans*-**3.2**: CD: (*n*-hexane) $\lambda_{max}(\Delta\varepsilon)$ 214.0 (-156.4), 220.6 (36.0), 226.8 (-154.8), 236.6 (13.0), 248.4 (-85.7), 251.6 (-59.1), 258.0 (-236.5), 266.4 (8.5), 280.8 (-12.1), 285.8 (-8.9), 298.2 (-15.3), 330.0 (10.6), 351.8 (21.5), 366.6 (20.6).

(2*R,2'*R**)-(*P**,*P**)-*cis*-(±)-2,2'-Dimethyl-2,2',3,3'-tetrahydro-1,1'-bicyclopenta[*a*]-naphthalenylidene-(3.2)**

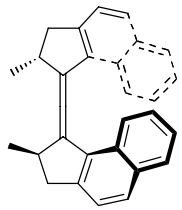

For the purification of the *cis*-**3.2** olefin obtained from the synthesis described above, multiple recrystallizations from ethyl acetate and ethanol were required before obtaining it pure as slightly yellow crystals; m.p. 178.6-179.9°C; Stable (2*R*,2'*R*)-(*P*,*P*)-*cis*-**3.2**: ^{1}H (300 MHz, $CDCl_3$) δ 1.22-1.24 (d, J= 6.6 Hz, 6H, Me_{2ax}), 2.66-2.71 (d, J= 14.7 Hz, 2H, H_{3eq}), 3.56-3.65 (m, 4H, H_{2eq}, H_{3ax}), 6.34-6.39 (m, 2H, H_8), 6.57-6.60 (d, J= 8.4 Hz, 2H, H_9), 6.94-6.99 (m, 2H, H_7), 7.47-7.50 (d, J= 8.1 Hz, 2H, H_4), 7.64-7.66 (d, J= 8.1 Hz, 2H, H_6), 7.70-7.72 (d, J= 8.1 Hz, 2H, H_5); ^{1}H (500 MHz, touene-d_8, -20°C) δ 1.17-1.18 (d, J= 6.5 Hz, 6H), 2.46-2.49 (d, J= 15.0 Hz, 2H), 3.38-3.42 (dd, J= 15.0, 6.0 Hz, 2H), 3.45-3.48 (m, 2H), 6.35-6.38 (m, 2H), 6.80-6.83 (m, 2H), 7.34-7.36 (d, J= 8.1 Hz, 2H), 7.50-7.51 (d, J= 8.1 Hz, 2H), 7.57-7.59 (d, J= 7.7 Hz, 2H); one aromatic proton (d) was not observed due to overlap with the solvent; ^{13}C (75 MHz, $CDCl_3$) δ 20.7 (q), 40.6 (t), 42.2 (d), 123.5 (d), 124.0 (2xd), 126.7 (d), 127.6 (d), 128.4 (d), 129.9 (s), 132.2 (s), 136.9 (s), 140.0 (s), 144.0 (s); UV-Vis: (*n*-hexane) $\lambda_{max}(\varepsilon)$ 222 (91900), 255 (36000), 294 (8100), 306 (10100), 332 (8600), 370 (19600); Resolution of *cis*-**3.2** was performed by chiral HPLC using a Daicel Chiralcel OD column as the stationary phase and a mixture of heptane : *i*-propanol in a ratio of 99.5 : 0.5 as the eluent at a rate of 1 ml·min^{-1}. The first eluted fraction (t= 4.89 min) of *cis*-**3.2** contained (2*R*,2'*R*)-(*P*,*P*)-*cis*-**3.2**, the second fraction (t= 6.12 min) contained (2*S*,2'*S*)-(*M*,*M*)-*cis*-**3.2**; (2*R*,2'*R*)-(*P*,*P*)-*cis*-**3.2**: CD: (*n*-hexane): $\lambda_{max}(\Delta\varepsilon)$ 209.4 (30.4), 214.8 (65.6), 224.6 (-28.4), 231.4 (99.5), 269.8 (-172.5), 373.0 (-7.3).

(2*R,2'*R**)-(*M**,*M**)-*trans*-(±)-2,2'-Dimethyl-2,2',3,3'-tetrahydro-1,1'-bicyclopenta[*a*]-naphthalenylidene-(3.2)**

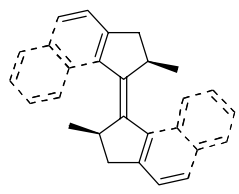

Irradiation ($\lambda \geq$ 280 nm) overnight of a solution of (2*R**,2'*R**)-(*P**,*P**)-*cis*-**3.2** in toluene-d_8 at -78°C provided a mixture of (2*R**,2'*R**)-(*P**,*P**)-*cis*-**3.2** and the desired (2*R**,2'*R**)-(*M**,*M**)-*trans*-**3.2**. The unstable *trans*-**3.2** could not be isolated in pure form due to its instability; Unstable (2*R**,2'*R**)-(*M**,*M**)-*trans*-**3.2**: ^{1}H (500 MHz, toluene-d_8, -20°C, spectral data derived from a mixture containing stable *cis*-**3.2**) δ 0.68-0.69 (d, J= 6.0 Hz, 6H), 2.76-2.81 (dd, J= 15.0, 7.7 Hz, 2H), 2.94-2.98 (dd, J= 15.0, 7.7 Hz, 2H),

3.45-3.48 (m, 2H), 7.24-7.26 (d, *J*= 7.7 Hz, 2H), 7.28-7.31 (m, 2H), 7.36-7.38 (m, 2H), 7.59-7.61 (d, *J*= 8.1 Hz, 2H), 7.71-7.73 (d, *J*= 7.7 Hz, 2H), 7.95-7.97 (d, *J*= 8.6 Hz, 2H); For the determination of the UV-Vis spectrum of the unstable *trans*-**3.2**, a sample of known concentration of stable *cis*-**3.2** was irradiated at –40°C with $\lambda \geq 280$ nm. The UV-Vis spectrum taken after irradiation is the sum of the absorptions of stable *cis*-**3.2** and unstable *trans*-**3.2**. After conversion of unstable *trans*-**3.2** to stable *trans*-**3.2**, *vide supra*, the ratio of both compounds and hence their concentrations were determined (HPLC, isosbestic point: 273 nm). Since both concentrations and the ε of stable *cis*-**3.2** are known, the UV-Vis spectrum of unstable *trans*-**3.2** can be calculated according to $A = \varepsilon_{\text{stable } cis} \cdot c_{\text{stable } cis} \cdot l + \varepsilon_{\text{unstable } trans} \cdot c_{\text{unstable } trans} \cdot l$; UV-Vis: (calc., *n*-hexane) $\lambda_{max}(\varepsilon)$ 218 (95600), 260 (27900), 392 (23400); The CD spectrum of the unstable *trans*-**3.2** has been calculated in a similar manner as the UV-Vis spectrum. A sample of known concentration of stable *cis*-**3.2** was irradiated at –40°C with $\lambda \geq 280$ nm. The CD spectrum taken after the irradiation is the sum of the CD spectra of stable *cis*-**3.2** and unstable *trans*-**3.2**. After conversion of unstable *trans*-**3.2** to stable *trans*-**3.2**, *vide supra*, the ratio of both compounds and hence their concentrations can be determined (HPLC, isosbestic point: 273 nm). Since both concentrations and the $\Delta\varepsilon$ of stable *cis*-**3.2** are known, the CD spectrum of the unstable *trans* compound can be calculated according to $\Theta = (3.3 \cdot 10^5 \ \Delta\varepsilon_{\text{stable } cis} \cdot c_{\text{stable } cis} \cdot l) / M + (3.3 \cdot 10^5 \cdot \Delta\varepsilon_{\text{unstable } trans} \cdot c_{\text{unstable } trans} \cdot l) / M$; CD: (calc., *n*-hexane) 215.6 (106.0), 221.2 (-18.1), 230.4 (98.6), 247.0 (-10.4), 253.4 (20.9), 258.0 (5.8), 269.2 (55.7), 297.6 (-3.9), 317.2 (-0.3), 388.4 (-24.2).

(2*R,2'*R**)-(*M**,*M**)-*cis*-(±)-2,2'-Dimethyl-2,2',3,3'-tetrahydro-1,1'-bicyclopenta[*a*]-naphthalenylidene-(3.2)**

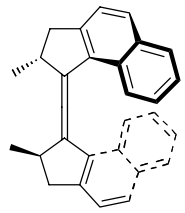

Irradiation ($\lambda \geq 280$ nm) overnight of a solution of (2*R**,2'*R**)-(*P**,*P**)-*trans*-**3.2** in toluene-d_8 at -78°C provided a mixture of (2*R**,2'*R**)-(*P**,*P**)-*trans*-**3.2** and the desired (2*R**,2'*R**)-(*M**,*M**)-*cis*-**3.2**. The unstable *cis*-**3.2** could not be isolated in pure form due to its instability; Unstable (2*R**,2'*R**)-(*M**,*M**)-*cis*-**3.2**: ^{1}H (500 MHz, toluene-d_8, -20°C, spectral data derived from a mixture containing stable *trans*-**3.2**) δ 1.46-1.47 (d, *J*= 6.0 Hz, 6H), 2.93-2.97 (dd, *J*= 15.6, 7.2 Hz, 2H), 3.07-3.14 (m, 2H), 3.58-3.63 (m, 2H), 6.49-6.52 (m, 2H), 6.75-6.78 (m, 2H), 7.26-7.29 (m, 4H), 7.41-7.43 (d, *J*= 8.1 Hz, 2H), 7.52-7.53 (d, *J*= 8.1 Hz, 2H); The UV-Vis spectrum of unstable *cis*-**3.2** was obtained in a similar way as for unstable *trans*-**3.2** (see above); UV-Vis: (calc., *n*-hexane) $\lambda_{max}(\varepsilon)$ 221 (80700), 264 (27100), 305 (8800), 317 (10400), 397 (16900); The CD spectrum of unstable *cis*-**3.2** was obtained in a similar way as for unstable *trans*-**3.2** (see above); CD: (calc., *n*-hexane) 222.2 (133.8), 231.8 (-161.9), 251.2 (-48.5), 259.8 (-78.6), 279.2 (96.4), 343.4 (0.9), 395.8 (11.7).

2-Methyl-2,3-dihydro-1*H*-cyclopenta[*a*]naphthalen-1-one (3.3)

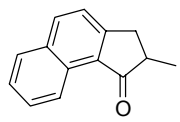

Method A: Ketone **3.4** (1.2 g, 6.5 mmol) in THF (40 ml) was deprotonated at low temperature (-80°) using a freshly prepared solution of LDA (7.0 mmol, 1.1 eq). The reaction mixture immediately turned deep red/brown. After 1h stirring at –60°C, an excess of methyl iodide was added (1.0 ml) and the reaction mixture was allowed to reach room temperature overnight. After the standard workup procedure, quenching with an aq. sol. of NH_4Cl (100 ml), extraction with ether (2x 50 ml), drying of the combined organic layers ($MgSO_4$) and evaporation of all volatiles, three compounds were found. These compounds could be separated by column chromatography (SiO_2, heptane:ethyl acetate= 16:1, R_f(**3.12**)= 0.56, R_f(**3.3**)= 0.43, R_f(**3.4**)= 0.25). The desired product was obtained in only low yield as a colorless oil (0.40 g, 2.0 mmol, 31%). Method B: Ketone **3.3** was prepared in a similar

fashion as is decribed below for the enantiomerically pure ketone *(R)*-**3.3** from acid chloride **3.16**. However, for the Friedel-Crafts reaction toluene was used instead of dichloroethane as the solvent.

(2*R*)-2-Methyl-2,3-dihydro-1*H*-cyclopenta[*a*]naphthalen-1-one ((*R*)-3.3)

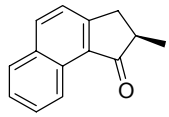

A mixture of acid **(*R*)-3.6** (0.55 g, 2.6 mmol) in a solution of $SOCl_2$ (1.3 ml), DMF (2 drops) and CH_2Cl_2 (50 ml) was refluxed for 1h. The volatiles were removed under reduced pressure and the remaining yellow oil was dissolved in dichloroethane (100 ml) and the solution cooled to 0°C. There was added quickly $AlCl_3$ (0.69 g, 5.2 mmol, 2 eq) and the reaction mixture was stirred for 45 min. Quenching with a sat. aq. sol. of $NaHCO_3$ (200 ml), extraction with CH_2Cl_2 (3x 50 ml) and drying over $MgSO_4$, gave ketone (*R*)-**3.3** as a slighly yellow oil (0.44 g, 2.2 mmol, 86%, HPLC: e.e.=99%); $[\alpha]_D^{20}$=-95.7° (*c*= 0.65, $CHCl_3$); ^{1}H (300 MHz, $CDCl_3$) δ 1.37-1.39 (d, *J*= 7.0 Hz, 3H), 2.77-2.87 (m, 2H), 3.44-3.53 (dd, *J*= 16.0, 8.1 Hz, 1H), 7.49-7.52 (d, *J*=8.4 Hz, 1H), 7.53-7.58 (m, 1H), 7.65-7.70 (m, 1H), 7.88-7.91 (d, *J*= 8.1 Hz, 1H), 8.03-8.06 (d, *J*= 8.4 Hz, 1H), 9.14-9.17 (d, *J*= 8.4 Hz, 1H); ^{13}C (75 MHz, $CDCl_3$) δ 16.1 (q), 34.7 (t), 41.8 (d), 123.38 (d), 123.43 (d), 126.0 (d), 127.6 (d), 128.2 (d), 129.0 (s), 129.5 (s), 132.1 (s), 135.1 (d), 156.1 (s), 209.2 (s); *m/z* (EI, %) = 196 (M^+, 100), 181 (83); HRMS (EI): calcd. for $C_{14}H_{12}O$: 196.0888, found 196.0898; determination of the e.e. was performed by HPLC using a Daicel Chiralcel OB-H column as the stationary phase and a mixture of heptane : *i*-propanol = 99:1 as the eluent at a rate of 0.5 ml·min^{-1}. The first eluted fraction (*t*= 19.3 min) contained (*S*)-**3.3** and the second fraction (*t*= 22.1 min) contained (*R*)-**3.3**.

2,3-Dihydro-1*H*-cyclopenta[*a*]naphthalen-1-one (3.4)

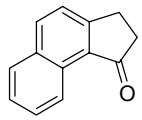

A solution of CH_2Cl_2 (25 ml) containing acid **3.7** (0.55 g, 2.8 mmol), $SOCl_2$ (1.5 ml, 2.5 g, 21 mmol)) and a drop of DMF heated at reflux for 1h. Cooling and removal of the volatiles under reduced pressure gave a slightly brown solid. This solid was dissolved in toluene (25 ml) and cooled to 0°C whereupon $AlCl_3$ (0.45 g, 3.4 mmol) was added. After stirring for 90 min, water was added and the mixture was extracted with ether, dried ($MgSO_4$) and after removal of the organic solvents, a brown solid was obtained. Using column chromatography, ketone **3.4** was obtained as a white solid (0.36 g, 2.0 mmol, 72%); m.p. 105.0-105.2°C (lit. 105°C)[4]; ^{1}H (300 MHz, $CDCl_3$) δ 2.79-2.82 (m, 2H), 3.20-3.24 (m, 2H), 7.50-7.58 (m, 2H), 7.65-7.70 (dt, *J*= 7.0, 1.1 Hz, 1H), 7.88-7.90 (d, *J*= 8.1 Hz, 1H), 8.02-8.05 (d, *J*= 8.4 Hz, 1H), 9.15-9.18 (d, *J*= 8.4 Hz, 1H); ^{13}C (75 MHz, $CDCl_3$) δ 25.6 (t), 36.3 (t), 123.3 (d), 123.5 (d), 126.0 (d), 127.6 (d), 128.2 (d), 128.8 (s), 130.3 (s), 132.0 (s), 135.0 (d), 157.9 (s), 206.8 (s); *m/z* (EI, %) = 182 (M^+, 100), 154 (43); HRMS (EI): calcd. for $C_{13}H_{10}O$: 182.0732, found 182.0733.

3-Naphthalen-2-yl-propionic acid (3.5)

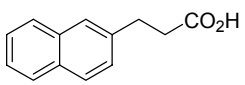

Boiling cyanide **3.10** (2.0 g, 11 mmol) overnight in an aq. sol. of 30% HCl (100 ml) gave after extraction with ether(3x 50 ml), drying of the combined organic layers ($MgSO_4$) and subsequent removal of all volatiles under reduced pressure, the acid **3.5** as a white solid (2.15 g, 10.8 mmol, 97%); m.p. 135.1-136.1°C (lit. 134-135°C)[7]; ^{1}H (300 MHz, $CDCl_3$) δ 2.76-2.81 (t, *J*= 7.7 Hz, 2H), 3.11-3.16 (t, *J*= 7.7 Hz, 2H), 7.33-7.37 (dd, *J*= 8.4, 1.5 Hz, 1H), 7.42-7.49 (m, 2H), 7.66 (s, 1H), 7.78-7.83 (m, 3H); ^{13}C (75 MHz, $CDCl_3$) δ 30.7 (t), 35.5 (t), 125.4 (d), 126.0 (d), 126.4 (d),

126.8 (d), 127.5 (d), 127.6 (d), 128.2 (d), 132.2 (s), 133.5 (s), 137.5 (s), 179.2 (s); *m/z* (EI, %) = 200 (M^+, 71), 141 (100); HRMS (EI): calcd. for $C_{13}H_{12}O_2$: 200.0837, found 200.0843.

2-Methyl-3-naphthalen-2-yl-propionic acid (3.6)

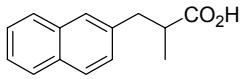

A mixture of ester **3.15** (1.72 g, 7.5 mmol), KOH (6.0 g), ethanol (30 ml) and water (30 ml) was heated at reflux overnight. Acidification of the reaction mixture with an aq. sol. of 30% HCl and extraction with ether (3x100 ml), washing of the combined organic layers with water (3x 100 ml) followed by drying over $MgSO_4$ gave after removal of the solvent acid **3.6** as a white solid (1.4 g, 6.5 mmol, 87%); m.p. 87.4-88.4°C.

(2*R*)-2-Methyl-3-naphthalen-2-yl-propionic acid ((*R*)-3.6)

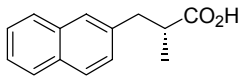

In a mixture of THF and water (4:1, 125 ml) was dissolved **3.18** (6.20 g, 16.6 mmol). To the stirred, ice cooled solution was then added dropwise H_2O_2 (30% aq. sol., 7.0 ml, 70 mmol). After 5 min a solution of LiOH (0.65 g, 27 mmol) in water (5 ml) was added slowly and the reaction mixture was subsequently stirred for 90 min. A solution of Na_2SO_3 (9.0 g, 69 mmol) in water (25 ml) was added and stirring was continued for 45 min at room temperature. The major part of the THF was removed under reduced pressure and the basic solution was extracted with CH_2Cl_2 (3x 100 ml) to remove the chiral auxiliary. Acidification with an aq. sol. of 10% HCl and extraction with CH_2Cl_2 (3 x 100 ml) gave after drying over Na_2SO_4 and removal of the organic solvents the acid (*R*)-**3.6** as a white solid (3.24 g, 15.1 mmol, 90%); m.p. 82.8-83.8°C; $[\alpha]_D^{20}$= -26.1° (*c*= 1.75, $CHCl_3$); ^{1}H (300 MHz, $CDCl_3$) δ 1.21-1.24 (d, *J*= 7.0 Hz, 3H), 2.81-2.93 (m, 2H), 3.23-3.29 (m, 1H), 7.32-7.35 (dd, *J*= 8.4, 1.5 Hz, 1H), 7.42-7.50 (m, 2H), 7.65 (s, 1H), 7.77-7.84 (m, 3H); ^{13}C (75 MHz, $CDCl_3$) δ 16.5 (q), 39.3 (t), 41.1 (d), 125.4 (d), 126.0 (d), 127.3 (d), 127.4 (d), 127.5 (d), 127.6 (d), 128.0 (d), 132.2 (s), 133.4 (s), 136.5 (s), 182.8 (s); *m/z* (EI, %) = 214 (M^+, 58), 141 (100); HRMS (EI): calcd. for $C_{14}H_{14}O_2$: 214.0994, found 214.1010.

2-Naphthalen-2-yl-ethanol (3.8)[5]

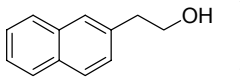

Prepared according to a literature procedure: ^{1}H (300 MHz, $CDCl_3$) 1.43 (s, 1H), 3.02-3.07 (t, *J*= 6.4 Hz, 2H), 3.94-3.98 (m, 2H), 7.35-7.39 (dd, *J*= 8.4, 1.8 Hz, 1H), 7.42-7.50 (m, 2H), 7.69 (s, 1H), 7.79-7.83 (m, 3H); ^{13}C (75 MHz, $CDCl_3$) δ 39.0 (t), 63.0 (t), 125.1 (d), 125.8 (d), 127.1 (d), 127.2 (d), 127.3 (d), 127.4 (d), 127.8 (d), 132.0 (s), 133.3 (s), 135.9 (s); *m/z* (EI, %) = 172 (M^+, 48), 141 (100), 115 (16); HRMS (EI): calcd. for $C_{12}H_{12}O$: 172.0888, found 172.0890.

2-(2-Bromoethyl)naphthalene (3.9)

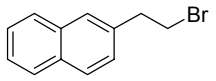

Alcohol **3.8** (8.4 g, 49 mmol) in ether (50 ml) was added slowly to a solution of PBr_3 (1.5 ml, 24 mmol) in ether (100 ml) at 0°C. The mixture was then heated at reflux for 2h and after a standard workup procedure the bromide **3.9** was obtained as a white solid (8.1 g, 34.5 mmol, 70%) which was used immediately in the following reaction; m.p. 59.1-62.2°C (lit. 64.5-65.5°)[5]; ^{1}H (300 MHz, $CDCl_3$) δ

3.32-3.37 (t, *J*= 7.5 Hz, 2H), 3.65-3.70 (t, *J*= 7.5 Hz, 2H), 7.33-7.36 (d, *J*= 8.8 Hz, 1H), 7.45-7.52 (m, 2H), 7.81 (s, 1H), 7.83-7.85 (m, 3H); ^{13}C (75 MHz, $CDCl_3$) δ 32.7 (t), 39.2 (t), 125.4 (d), 125.9 (d), 126.6 (d), 127.0 (d), 127.4 (d), 127.5 (d), 128.0 (d), 132.2 (s), 133.3 (s), 136.1 (s); *m/z* (EI, %) = 236 (M^+, 46), 234 (M^+, 45), 141 (100); HRMS (EI): calcd. for $C_{12}H_{11}{}^{79}Br$: 234.0044, found 234.0046.

3-Naphthalen-2-yl-propionitrile (3.10)

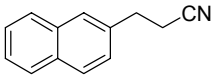

A mixture of bromide **3.9** (3.95 g, 16.8 mmol), KCN (8.1 g, 125 mmol) and DMSO (50 ml) was stirred for 4h at 80°C. The reaction mixture was poured into 1*N* aq. NaOH (100 ml) and extracted with ether (3x 100 ml). The organic layers were washed with water (6x 200 ml) and then with brine (2x 100 ml). Drying over $MgSO_4$ and evaporation of the organic layers gave the crude product which was purified by column chromatography (SiO_2, heptane:ethyl acetate= 16:1, R_f=0.24) to yield **3.10** as a white solid (2.48 g, 13.7 mmol, 82%); m.p. 78.1-78.6°C (lit. 78-78.5°C)[6]; ^{1}H (300 MHz, $CDCl_3$) δ 2.69-2.74 (t, *J*= 7.5 Hz, 2H), 3.11-3.16 (t, *J*= 7.5 Hz, 2H), 7.33-7.36 (dd, *J*= 8.4, 1.5 Hz, 1H), 7.45-7.52 (m, 2H), 7.69 (s, 1H), 7.80-7.85 (m, 3H); ^{13}C (75 MHz, $CDCl_3$) δ 18.4 (t), 30.9 (t), 118.8 (s), 125.4 (d), 125.8 (d), 125.9 (d), 126.3 (d), 127.17 (d), 127.21 (d), 128.0 (d), 131.9 (s), 133.0 (s), 135.2 (s); *m/z* (EI, %) = 181 (M^+, 36), 141 (100); HRMS (EI): calcd. for $C_{13}H_{11}N$: 181.0892, found 181.0894.

2,2-Dimethyl-2,3-dihydro-cyclopenta[*a*]naphthalen-1-one (3.11)

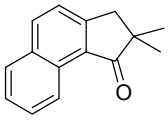

This product was isolated as a side product from the alkylation of **3.4** and was obtained as a colorless oil, which solidified upon standing; m.p.< 50°C; ^{1}H (300 MHz, $CDCl_3$) δ 1.30 (s, 6H), 3.10 (s, 2H), 7.47-7.50 (d, *J*= 8.4 Hz, 1H), 7.53-7.70 (m, 2H), 7.88-7.90 (d, *J*= 8.1 Hz, 1H), 8.04-8.07 (d, *J*= 8.1 Hz, 1H), 9.14-9.16 (d, *J*= 8.4 Hz, 1H); ^{13}C (75 MHz, $CDCl_3$) δ 25.2 (q), 42.9 (t), 45.4 (s), 123.7 (d), 123.8 (d), 126.2 (d), 127.9 (d), 128.5 (d), 128.7 (s), 129.6 (s), 132.5 (s), 135.5 (d), 155.0 (s), 211.6 (s); *m/z* (EI, %) = 210 (M^+, 52), 195 (100); HRMS (EI): calcd. for $C_{15}H_{12}O$: 210.1045, found 210.1087.

2-(Bromomethyl)naphthalene (3.13)[8]

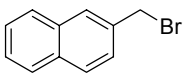

Prepared according to a literature procedure: 2-methylnaphthalene (14.3 g, 101 mmol), NBS (17.5 g, 101 mmol) dibenzoylperoxide (0.1 g, 0.4 mmol) in CCl_4 (150 ml) were heated at reflux for 18 h. The cooled solution was filtered and the solvent removed under reduced pressure. The brown solid was recrystallized from pentane giving white crystals of 2-(bromomethyl)naphthalene (15.8 g, 71 mmol, 71%); ^{1}H NMR (300 MHz, $CDCl_3$) δ 4.68 (s, 2H), 7.48-7.53 (m, 3H), 7.81-7.86 (m, 4H).

2-Methyl-3-naphthalen-2-yl-propionic acid methyl ester (3.14)

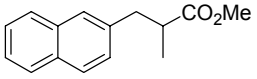

A LDA solution in THF (100 ml) was prepared at –50°C by adding *n*-BuLi (10 ml, 16 mmol) to di-*i*-propylamine (2.25 ml, 16 mmol) followed by stirring for 15 min at –50°C. Subsequently, methyl propionate (1.53 ml, 16 mmol) was added dropwise at –60°C and the resulting mixture was stirred for 1h at approximately –60°C. The bromide **3.13** (3.9 g, 17.6 mmol) dissolved in THF

(20 ml) was added slowly and the reaction mixture was allowed to warm overnight to room temperature. Addition of sat. aq. sol. of NH_4Cl (200 ml) and extraction with ether (2x 100 ml), drying of the organic layers ($MgSO_4$) and evaporation of the solvent gave a yellow oil. Purification by column chromatography (SiO_2, heptane:ethyl acetate=16:1, R_f=0.4) provided ester **3.14** as a colorless oil (1.75 g, 7.6 mmol, 48%).

(2*R*)-2-Methyl-3-naphthalen-2-yl-propionic acid methyl ester ((*R*)-3.14))

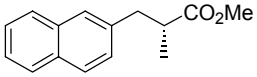

A mixture of acid (*R*)-**3.6** (15 mg, 70 μmol), methyl iodide (0.25 ml, 4.0 mmol), K_2CO_3 (110 mg, 0.80 mmol) in DMF (2 ml) was stirred overnight at room temperature. After addition of ether (25 ml) the reaction mixture was washed with water (5x 25 ml). The organic layer was dried ($MgSO_4$) and the solvent removed under reduced pressure to give the ester (*R*)-**3.14** as a colorless oil (14 mg, 61 μmol, 87%); HPLC: e.e.>99%; ^{1}H (300 MHz, $CDCl_3$) δ 1.18-1.20 (d, *J*= 6.2 Hz, 3H), 2.79-2.89 (m, 2H), 3.16-3.19 (m, 1H), 3.64 (s, 3H), 7.29-7.32 (d, *J*= 8.4 Hz, 1H), 7.42-7.48 (m, 2H), 7.61 (s, 1H), 7.73-7.79 (m, 3H); ^{13}C (75 MHz, $CDCl_3$) δ 16.6 (q), 39.6 (t), 41.1 (d), 51.3 (q), 125.1 (d), 125.7 (d), 127.1 (2xd), 127.3 (d), 127.4 (d), 127.8 (d), 132.0 (s), 133.3 (s), 136.6 (s), 176.1 (s); *m/z* (EI, %) = 228 (M^+, 38), 141 (100); HRMS (EI): calcd. for $C_{15}H_{16}O_2$: 228.1150, found 228.1141; Determination of the e.e. of the sample was performed by HPLC using a Daicel Chiralcel OB-H column as the stationary phase and a mixture of heptane : *i*-propanol = 99:1 as the eluent at a rate of 0.5 ml·min^{-1}. The first eluted fraction (t = 23.6 min) contained (*R*)-**3.14** and the second eluted fraction (t=26.3 min) contained (*S*)-**3.14**.

2-Methyl-3-naphthalen-2-yl-propionyl chloride (3.15)

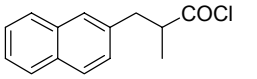

A mixture of acid **3.6** (0.51 g, 2.4 mmol), $SOCl_2$ (2.0 ml), DMF (2 drops) and CH_2Cl_2 (20 ml) was heated at reflux for 1h. All volatiles were distilled off under reduced pressure yielding the acid chloride **3.15** as a yellow oil (0.55 g, 2.4 mmol, 98%) which was used immediately in the subsequent reaction; ^{1}H (300 MHz, $CDCl_3$) δ 1.31-1.33 (d, *J*= 6.6 Hz, 3H), 2.89-2.96 (ddd, *J*= 13.6, 6.3, 1.8 Hz, 1H), 3.23-3.39 (m, 2H), 7.30-7.33 (dd, *J*= 8.4, 1.8 Hz, 1H), 7.43-7.49 (m, 2H); 7.65 (s, 1H), 7.79-7.84 (m, 3H).

(4*S*)-4-Benzyl-3-propionyl-oxazolidin-2-one (3.17)

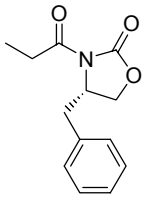

This compound was prepared according to a literature procedure.[14] Starting from **3.16** (9.4 g, 53 mmol), **3.17** was obtained as a colorless oil (11.3 g, 49 mmol, 92%); ^{1}H (300 MHz, $CDCl_3$) δ 1.12-1.16 (t, *J*= 7.3 Hz, 3H), 2.69-2.76 (dd, *J*= 13.2, 9.5 Hz, 1H), 2.79 (m, 2H), 3.17-3.23 (dd, *J*= 13.2, 3.3 Hz, 1H), 4.05-4.14 (m, 2H), 4.56-4.62 (m, 1H), 7.13-7.29 (m, 5H); ^{13}C (75 MHz, $CDCl_3$) δ 8.0 (q), 28.8 (t), 37.4 (t), 54.7 (d), 65.9 (t), 126.9 (d), 128.5 (d), 129.1 (d), 135.1 (s), 153.2 (s), 173.6 (s); *m/z* (EI, %) = 233 (M^+, 35), 142 (39), 57 (100); HRMS (EI): calcd. for $C_{13}H_{15}NO_3$ 233.1052, found 233.1065.

(4*S*)-4-Benzyl-3-((2*R*)-2-methyl-3-naphthalen-2-yl-propionyl)-oxazolidin-2-one (3.18)

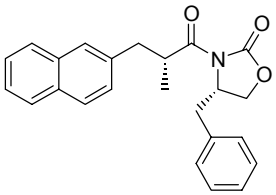

Freshly prepared LDA (44 mmol) in THF (150 ml) was cooled to -80°C. A solution of **3.17** (8.85 g, 39.7 mmol) in THF (50 ml) was slowly added at –80°C and the mixture was kept at this temperature for 2h. The temperature was slowly raised to 0°C and bromide **3.13** (20 g, 90 mmol) dissolved in THF (50 ml), was added and the reaction mixture was allowed to stir overnight. After quenching with a sat. aq. sol. of NH_4Cl (300 ml), the reaction mixture was extracted with ether (2x 100 ml), the combined organic layers were dried ($MgSO_4$) and the solvents removed under reduced pressure. The crude product was purified by flash column chromatography (SiO_2), first with a mixture of heptane : ethyl acetate = 16:1 to remove the excess bromide **3.13** and then with a heptane:ethyl acetate = 8:1 mixture. The resulting colorless solid was recrystallized from a heptane:ethyl acetate mixture giving the desired product **3.18** diastereomerically pure as white fluffy crystals (7.95 g, 21.3 mmol, 54%); m.p. 134.9-135.1°C; $[\alpha]_D^{20}$= +15.4° (*c*= 4.05, $CHCl_3$); ^{1}H (300 MHz, $CDCl_3$) δ 1.22-1.24 (d, *J*= 7.0 Hz, 3H), 2.46-2.49 (dd, *J*= 13.6, 9.2 Hz, 1H), 2.80-2.87 (dd, *J*= 13.2, 7.7 Hz, 1H), 3.06-3.11 (dd, *J*= 13.6, 3.3 Hz, 1H), 3.30-3.37 (dd, *J*= 13.2, 7.3 Hz, 1H), 4.06-4.28 (m, 3H), 4.64-4.72 (m, 1H), 6.96-7.00 (m, 2H), 7.18-7.21 (m, 3H), 7.40-7.49 (m, 3H), 7.72 (s, 1H), 7.78-7.82 (m, 3H); ^{13}C (75 MHz, $CDCl_3$) δ 16.6 (q), 37.5 (t), 39.4 (d), 39.9 (t), 54.9 (d), 65.7 (t), 125.3 (d), 125.8 (d), 127.1 (d), 127.4 (d), 127.5 (d), 127.6 (d), 127.7 (d), 127.8 (d), 128.6 (d), 129.1 (d), 132.1 (s), 133.3 (s), 134.9 (s), 136.6 (s), 152.9 (s), 176.3 (s); *m/z* (EI, %) = 373 (M^+, 93), 168 (93), 141 (100); HRMS (EI): calcd. for $C_{24}H_{23}NO_3$: 373.1678, found 373.1675.

(4*S*)-4-Benzyl-3-((2*S*)-2-methyl-3-naphthalen-2-yl-propionyl)-oxazolidin-2-one (3.20)

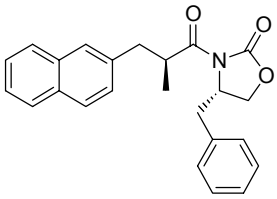

To a solution of oxazolidinone **3.17** (0.35 g, 2.0 mmol) in THF (10 ml) was added at –80°C *n*-BuLi (1.25 ml, 2.0 mmol). After stirring for 15 min, a solution of acid chloride **3.15** (0.55 g, 2.4 mmol) in THF (10 ml) was added slowly while keeping the temperature at –80°C. The reaction mixture was allowed to warm to room temperature. Workup following standard procedures gave a mixture of the two diastereomers **3.18** and **3.20** as a white solid. The isomers were separated using column chromatography (SiO_2, heptane:ethyl acetate= 8:1, R_f((*S*,*S*)-**3.20**)=0.14, R_f((*R*,*S*)-**3.18**)=0.08) giving the (*S*,*S*)-**3.20** diastereomer as a white solid (0.21 g, 0.56 mmol, 56%); m.p. 117-112.1°C; $[\alpha]_D^{20}$= +109.5(*c*= 0.95, $CHCl_3$); ^{1}H (300 MHz, $CDCl_3$) δ 1.28-130 (d, *J*= 6.6 Hz, 3H), 2.71-2.78 (dd, *J*= 13.3, 9.7 Hz, 1H), 2.83-2.90 (dd, *J*= 13.3, 7.1 Hz, 1H), 3.18-3.27 (m, 2H), 3.81-3.87 (t, *J*= 8.4 Hz, 1H), 4.02-4.06 (dd, *J*= 9.2, 2.2 Hz, 1H), 4.18-4.23 (m, 1H), 4.45-4.50 (m, 1H), 7.18-7.45 (m, 8H), 7.66 (s, 1H), 7.75-7.80 (m, 3H); ^{13}C (75 MHz, $CDCl_3$) δ 17.1 (q), 37.8 (t), 39.5 (d), 39.9 (t), 55.2 (d), 65.8 (t), 125.4 (d), 125.9 (d), 127.3 (d), 127.46 (d), 127.52 (d), 127.57 (d), 127.9 (d), 128.9 (d), 129.4 (d), 132.1 (s), 133.3 (s), 135.2 (s), 136.7 (s), 152.9 (s), 176.3 (s); one carbon atom (d) was not observed; *m/z* (EI, %) = 373 (M^+, 100), 197 (44), 168 (87), 141 (87); HRMS (EI): calcd. for $C_{24}H_{23}NO_3$: 373.1678, found 373.1672. The (*R*,*S*)-**3.18** diastereomer was obtained as a white fluffy solid with identical properties as the compound prepared enantiomerically pure (0.26, 0.69 mmol, 69%).

2-(Naphthalen-2-yloxy)-propionic acid methyl ester (3.22)

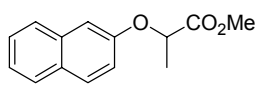

A mixture of 2-naphthol **3.21** (1.58 g, 11 mmol), 2-bromopropionic acid methyl ester (1.5 g, 9.0 mmol), K_2CO_3 (2.0 g, 14 mmol) in DMF (25 ml) was stirred overnight at 80°C. Addition of ether (100 ml) and repetitive washing with water (6 x 100 ml), followed by drying of the etheral layer (Na_2SO_4) and subsequent removal of all volatiles provided the ester **3.22** as a slightly colored oil (1.42 g, 6.6 mmol, 73%); ^{1}H (300 MHz, $CDCl_3$) δ 1.68-1.70 (d, *J*= 6.6 Hz, 3H), 3.76 (s, 3H), 4.89-4.96 (q, *J*= 6.6 Hz, 1H), 7.05-7.06 (d, *J*= 2.2 Hz, 1H), 7.18-7.22 (dd, *J*= 8.8, 2.2 Hz, 1H), 7.32-7.37 (m, 1H), 7.41-7.46 (m, 1H), 7.69-7.72 (d, *J*= 8.1 Hz, 1H), 7.75-7.78 (d, *J*= 8.8 Hz, 2H); ^{13}C (75 MHz, $CDCl_3$) δ 18.2 (q), 51.9 (q), 72.2 (d), 107.4 (d), 118.5 (d), 123.7 (d), 126.1 (d), 126.6 (d), 127.3 (d), 129.1 (s), 129.4 (d), 134.0 (s), 155.2 (s), 172.2 (s); *m/z* (EI, %) = 230 (M^+, 100), 171 (72), 144 (84); HRMS (EI): calcd. for $C_{14}H_{14}O_3$: 230.0943, found 230.0938.

2-(Naphthalen-2-yloxy)-propionic acid (3.23)

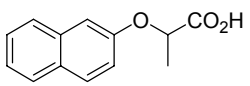

A mixture of ester **3.22** (0.39 g, 1.70 mmol), LiOH (0.50 g, 21 mmol), methanol (10 ml) and water (3 ml) was stirred overnight. Water (50 ml) was added and mixture was acidified to pH 1 and subsequently extracted with ether (2x 50 ml). The organic layer was washed with brine, dried over Na_2SO_4 and removal of the all volatiles gave a slightly colored solid (0.30 g, 1.3 mmol, 82%); m.p. 111.6-112.0°C; ^{1}H (300 MHz, $CDCl_3$) δ 1.71-1.74 (d, *J*= 7.0 Hz, 3H), 4.92-4.99 (q, *J*= 7.0 Hz, 1H), 7.10 (s, 1H), 7.18-7.22 (dd, *J*= 8.8, 2.2 Hz, 1H), 7.34-7.39 (m, 1H), 7.42-7.47 (m, 1H), 7.70-7.72 (d, *J*= 8.1 Hz, 1H), 7.76-7.79 (d, *J*= 8.8 Hz, 2H); ^{13}C (75 MHz, $CDCl_3$) δ 18.3 (q), 71.8 (d), 107.7 (d), 118.6 (d), 124.0 (d), 126.4 (d), 126.8 (d), 127.5 (d), 129.3 (s), 129.7 (d), 134.1 (s), 155.0 (s), 178.3 (s); *m/z* (EI, %) = 216 (M^+, 78), 144 (100); HRMS (EI): calcd. for $C_{13}H_{12}O_2$: 216.0786, found 216.0795.

2-Methyl-naphtho[2,1-*b*]furan-1(2*H*)-one (3.24)

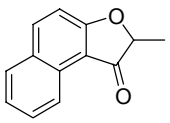

A mixture of acid **3.23** (0.27 g, 1.25 mmol), $SOCl_2$ (0.25 ml, 0.40 g, 3.42 mmol), DMF (1 drop) and CH_2Cl_2 (10 ml) was refluxed for 1h. All volatiles were removed under reduced pressure and the yellow oil obtained was dissolved in dichloroethane (20 ml). The mixture was cooled to 0°C and $AlCl_3$ (0.20 g, 1.5 mmol) was added whereupon the reaction mixture turned almost immediately black. Stirring was continued for 45 min at 0°C. Quenching the reaction mixture with water (100 ml) gave after extraction with ethyl acetate (3x 50 ml), drying of the combined organic layers (Na_2SO_4) and removal of all volatiles a black oil. Purification was performed by flash column chromatography (SiO_2, heptane:ethyl acetate=16:1) to give a nearly colorless oil which solidified upon standing (0.13 g, 0.66 mmol, 53%); m.p. 90.2-92.5°C; ^{1}H (300 MHz, $CDCl_3$) δ 1.60-1.62 (d, *J*= 7.3 Hz, 3H), 4.72-4.79 (q, *J*= 7.3 Hz, 1H), 7.23-7.26 (d, *J*= 8.8 Hz, 1H), 7.44-7.50 (m, 1H), 7.64-7.69 (m, 1H), 7.82-7.85 (d, *J*= 8.1 Hz, 1H), 8.06-8.09 (d, *J*= 9.2 Hz, 1H), 8.74-8.77 (d, *J*= 8.1 Hz, 1H); ^{13}C (75 MHz, $CDCl_3$) δ 16.3 (q), 82.6 (d), 112.1 (s), 113.8 (d), 122.9 (d), 125.1 (d), 128.3 (d), 128.9 (s), 129.1 (s), 129.6 (d), 139.7 (d), 174.8 (s), 201.8 (s); *m/z* (EI, %) = 198 (M^+, 100), 155 (39), 126 (47); HRMS (EI): calcd. for $C_{13}H_{10}O_2$: 198.0681, found 198.0693.

3,3-Dimethylbutyric acid methyl ester (3.27)

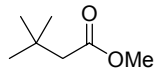

A mixture of 3,3-dimethyl-butyric acid **3.26** (24 g, 0.21 mol), DMF (150 ml), methyl iodide (20 ml) and K_2CO_3 (25 g) was stirred overnight at room temperature. Addition of ether (100 ml) and subsequent thorough washing with water (6x 200 ml) gave after drying ($MgSO_4$) and removal of the ether the crude ester. For further purification ester **3.27** was distilled at atmospheric pressure to yield a colorless liquid (23 g, 0.18 mol, 86%); b.p. 129-132°C (lit. 124-128°C)[29]; ^{1}H (300 MHz, $CDCl_3$) δ 1.02 (s, 9H), 2.2 (s, 2H), 3.65 (s, 3H); ^{13}C (75 MHz, $CDCl_3$) δ 29.5 (q), 30.5 (s), 47.6 (t), 50.9 (q), 172.6 (s).

3,3-Dimethyl-2-naphthalen-2-ylmethyl-butyric acid methyl ester (3.28)

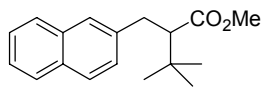

A freshly prepared solution of LDA (16 mmol) in THF (50 ml) was cooled to –70°C and neat methyl 3,3-dimethylbutanoate (1.95 g, 15 mmol) was added. The mixture was stirred for 45 min while maintaining the temperature at approximately –70°C. A solution of the bromide **3.13** (6.6 g, 30 mmol) dissolved in THF (30 ml) was added at –70°C and allowed to react while stirring overnight. After quenching with an aq. sat. sol. of NH_4Cl (100 ml), the reaction mixture was extracted with ether (3x 75 ml). The combined organic layers were washed with water and the solid remaining after evaporation of all volatiles was purified using column chromatography (SiO_2, heptane:ethyl acetate=50:1, R_f= 0.24) yielding the ester **3.28** as a colorless solid (2.7 g, 10 mmol, 67%); m.p. 69.6-70.5°C; ^{1}H (300 MHz, $CDCl_3$) δ 1.12 (s, 9H), 2.59-2.64 (dd, *J*= 11.7, 3.7 Hz, 1H), 2.97-3.14 (m, 2H), 3.47 (s, 3H), 7.29-7.32 (dd, *J*= 8.4, 1.5 Hz, 1H), 7.41-7.49 (m, 2H), 7.62 (s, 1H), 7.75-7.82 (m, 3H); ^{13}C (75 MHz, $CDCl_3$) δ 27.7 (q), 33.0 (t), 34.0 (s), 50.5 (q), 58.4 (d), 125.1 (d), 125.7 (d), 126.8 (d), 127.1 (d), 127.3 (d), 127.4 (d), 127.8 (d), 132.0 (s), 133.4 (s), 137.6 (s), 174.7 (s); *m/z* (EI, %) = 270 (M^+, 67), 214 (41), 181 (71), 141 (100); HRMS (EI): calcd. for $C_{18}H_{22}O_2$: 270.1620, found 270.1614.

3,3-Dimethyl-2-naphthalen-2-ylmethyl-butyric acid (3.29)

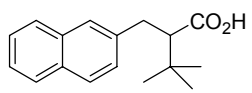

A mixture of ester **3.28** (2.7 g, 10 mmol), ethanol (50 ml) water (50 ml) and KOH (5.0 g, 89 mmol) was refluxed for 6d. Acidification with an aq. sol. of 30% HCl solution, subsequent extraction with ether (3x 50 ml) and washing of the combined organic layers with water, gave after drying ($MgSO_4$) and evaporation of all volatiles acid **3.29** as a yellow, impure solid. This solid was recrystallized from a mixture of heptane:ethyl acetate=50:1 to give the desired acid **3.29** as a white solid (2.1 g, 8.2 mmol, 82%); m.p.113.9-115.2°C; ^{1}H (300 MHz, $CDCl_3$) δ 1.09 (s, 9H), 2.56-2.61 (dd, *J*= 9.0, 5.3 Hz, 1H), 2.99-3.03 (m, 2H), 7.26-7.43 (m, 3H), 7.61 (s, 1H), 7.70-7.75 (m, 3H); ^{13}C (75 MHz, $CDCl_3$) δ 27.7 (q), 32.8 (t), 33.9 (s), 58.3 (d), 125.1 (d), 125.7 (d), 126.9 (d), 127.1 (d), 127.5 (2xd), 127.9 (d), 132.1 (s), 133.5 (s), 137.4 (s), 179.7 (s); *m/z* (EI, %) = 256 (M^+, 51), 200 (34), 141 (100); HRMS (EI): calcd. for $C_{17}H_{20}O_2$: 256.1463, found 256.1470.

2-*t*-Butyl-2,3-dihydro-1*H*-cyclopenta[*a*]naphthalen-1-one (3.30)

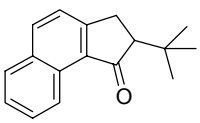

A mixture of acid **3.29** (1.96 g, 7.7 mmol), $SOCl_2$ (2.1 ml, 29 mmol) and DMF (2 drops) in CH_2Cl_2 (100 ml) was refluxed for 1h. All volatiles were then removed under reduced pressure and the yellow oil remaining was

dissolved in 1,2-dichloroethane (75 ml) and cooled to 0°C. $AlCl_3$ (2.0 g, 15 mmol) was added portionwise and the reaction mixture turned deep green. After stirring for 1h, the reaction was quenched by addition of an aq. sol. of 1*N* HCl (100 ml) followed by extraction with CH_2Cl_2 (2x 50 ml). The oil remaining after removal of all volatiles under reduced pressure was purified by using a short column (SiO_2, heptane:ethyl acetate=16:1, R_f=0.50). The ketone **3.30** was obtained as a slightly yellow oil which solidified upon standing (1.53 g, 6.4 mmol, 84%); m.p.= 71.9-73.2°C; ^{1}H (300 MHz, $CDCl_3$) δ 1.10 (s, 9H), 2.58-2.62 (dd, *J*= 7.3, 3.7 Hz, 1H), 3.04-3.11 (dd, *J*= 17.9, 3.7 Hz, 1H), 3.23-3.32 (dd, *J*= 17.9, 7.3 Hz, 1H), 7.49-7.57 (m, 2H), 7.64-7.69 (m, 1H), 7.87-7.90 (d, *J*= 8.1 Hz, 1H), 8.01-8.04 (d, *J*= 8.4 Hz, 1H), 9.16-9.19 (d, *J*= 8.4 Hz, 1H); ^{13}C (75 MHz, $CDCl_3$) δ 27.5 (q), 30.1 (t), 33.7 (s), 56.8 (d), 123.6 (d), 123.8 (d), 126.2 (d), 128.0 (d), 128.6 (d), 129.2 (s), 131.5 (s), 132.5 (s), 135.3 (d), 156.3 (s), 208.3 (s); *m/z* (EI, %) = 238 (M^+, 18), 182 (100); HRMS (EI): calcd. for $C_{17}H_{18}O$: 238.1358, found 238.1371.

(2*S,2'*S**)-(*P**,*P**)-*cis*-(±)-2,2'-Di-*t*-butyl-2,2',3,3'-tetrahydro-1,1'-bicyclopenta[*a*]-naphthalenylidene (3.31)**

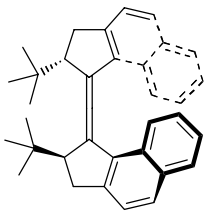

To a stirred suspension of zinc powder (1.0 g, 15.3 mmol) in THF (10 ml) was added carefully at 0°C under an argon atmosphere $TiCl_4$ (0.85 ml, 1.5 g, 7.7 mmol). The resulting black slurry was refluxed for 2h. Ketone **3.30** (0.92 g, 3.87 mmol) was added and reflux was continued for 13d. The reaction mixture was then poured into a sat. aq. sol. of NH_4Cl (100 ml) and extracted with ethyl acetate (3x 50 ml). The organic layers were dried ($MgSO_4$) and the solvents were removed under reduced pressure giving a yellow oil. This oil was further purified by column chromatography (SiO_2, heptane, R_f= 0.30) providing the *cis* and *trans* alkenes **3.31** as a yellow solid in an approximate *cis* : *trans* ratio of 5:2 (160 mg, 0.36 mmol, 19%); *m/z* (EI, %) = 444 (M^+, 64), 387 (49), 331 (100); HRMS (EI): calcd. for $C_{34}H_{36}$: 444.2817, found 444.2809. The *cis*-**3.31**-isomer was obtained pure as an amorphous white solid by precipitation from heptane. Crystals suitable for X-ray analysis were obtained as thin colorless plateless by recrystallization from heptane; m.p. 223.5-224.2°C; Stable (2*S**,2'*S**)-(*P**,*P**)-*cis*-**3.31**: ^{1}H (300 MHz, $CDCl_3$) δ 0.79 (s, 18H), 2.91-2.96 (d, *J*= 15.4 Hz, 2H), 3.39-3.45 (dd, *J*= 15.4, 5.9 Hz, 2H), 3.60-3.62 (d, *J*= 5.9 Hz, 2H), 6.28-6.38 (m, 4H), 6.84-6.89 (m, 2H), 7.41-7.44 (d, *J*= 8.1 Hz, 2H), 7.52-7.55 (d, *J*= 8.4 Hz, 2H), 7.61-7.64 (d, *J*= 8.1 Hz, 2H); ^{1}H (400 MHz, toluene-d_8) δ 0.81 (s, 18H, tBu$_{2ax}$), 2.80-2.83 (d, *J*= 15.2 Hz, 2H, H_{3ax}), 3.30-3.36 (dd, *J*= 15.2, 5.8 Hz, 2H, H_{3eq}), 3.62-3.64 (d, *J*= 5.8 Hz, 2H, H_{2eq}), 6.30-6.34 (m, 2H, H_8), 6.60-6.62 (d, *J*= 8.1 Hz, 2H, H_9), 6.72-6.76 (m, 2H, H_7), 7.28-7.31 (d, *J*= 8.1 Hz, 2H, H_4), 7.40-7.42 (d, *J*= 8.1 Hz, 2H, H_6), 7.53-7.55 (d, *J*= 8.1 Hz, 2H, H_5); ^{1}H (400 MHz, benzene-d_6, spectral data derived from a mixture containing *trans*-**3.31**) δ 0.82 (s, 18H), 2.80-2.84 (d, *J*= 15.4 Hz, 2H), 3.31-3.37 (dd, *J*=15.4, 6.2 Hz, 2H), 3.63-3.65 (d, *J*= 6.2 Hz, 2H), 6.37-6.41 (m, 2H), 6.69-6.71 (d, *J*= 8.1 Hz, 2H) 6.75-6.79 (m, 2H), 7.31-7.33 (d, *J*= 8.1 Hz, 2H), 7.45-7.47 (d, *J*= 8.1 Hz, 2H), 7.56-7.58 (d, *J*= 8.1 Hz, 2H); ^{13}C (75 MHz, $CDCl_3$) δ 28.7 (q), 34.5 (s), 35.1 (t), 58.8 (d), 122.3 (d), 123.8 (d), 123.9 (d), 126.2 (d), 127.4 (d), 128.1 (d), 128.4 (s), 132.1 (s), 139.1 (s), 140.1 (s), 144.0 (s); UV-Vis: (*n*-hexane) $\lambda_{max}(\varepsilon)$ 227 (76100), 254 (28700), 307 (10000), 327 (8600), 362 (12700); Resolution of stable *cis*-**3.31** was performed by chiral HPLC using a Daicel Chiralcel OD column as the stationary phase and a mixture of heptane : *i*-propanol in a ratio of 99.75 : 0.25 as the eluent at a rate of 1 ml·min^{-1}. The first eluted fraction (t= 4.08 min) of *cis*-**3.31** contained (2*S*,2'*S*)-(*P*,*P*)-*cis*-**3.31**, the second fraction (t= 4.92 min) contained (2*R*,2'*R*)-(*M*,*M*)-*cis*-**3.31**; (2*S*,2'*S*)-(*P*,*P*)-*cis*-**3.31**: CD: (*n*-hexane) $\lambda_{max}(\Delta\varepsilon)$ 225.8(+68.1), 233.6 (-214.8), 267.6 (+253.4), 376.4 (+4.6).

(2*S,2'*S**)-(*P**,*P**)-*trans*-(±)-2,2'-Di-*t*-butyl-2,2',3,3'-tetrahydro-1,1'-bicyclopenta[*a*]-naphthalenylidene (3.31)**

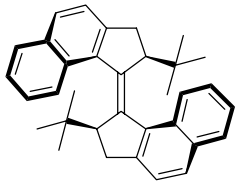

Not obtained in pure form from synthesis as described above. The stable *trans*-**3.31** was obtained pure *via* photochemical isomerization methods. This involves either irradiation ($\lambda \geq$ 280 nm, T=0°C) of (2*S*,2'*S*)-(*M*,*M*)-*cis*-**3.31** in *n*-hexane to form the unstable (2*S*,2'*S*)-(*P*,*P*)-*cis*-**3.31** followed by irradiation with a different wavelength ($\lambda \geq$ 436 nm, T=0°C) or by irradiation ($\lambda \geq$ 280 nm, T=0°C) of (2*S*,2'*S*)-(*M*,*M*)-*cis*-**3.31** in dodecane to form the unstable (2*S*,2'*S*)-(*P*,*P*)-*cis*-**3.31** which is then converted to the stable (2*S*,2'*S*)-(*P*,*P*)-*trans*-**3.31** by heating at elevated temperatures; ^{1}H (300 MHz, $CDCl_3$, spectral data derived from a mixture containing *cis*-**3.31**) δ 0.81 (s, 18H), 2.39-2.44 (d, J= 15.0 Hz, 2H), 2.52-2.59 (dd, J= 15.0, 5.5 Hz, 2H), 2.99-3.01 (d, J= 5.5 Hz, 2H), 7.24-7.26 (d, J= 7.3 Hz, 2H), 7.41-7.55 (m, 4H), 7.66-7.69 (d, J= 8.4 Hz, 2H), 7.85-7.87 (d, J= 8.1 Hz, 2H), 8.50-8.53 (d, J= 8.1 Hz, 2H); ^{1}H (400 MHz, benzene-d_6, spectral data derived from a mixture containing *cis*-**3.31**) δ 0.88 (s, 18H), 2.19-2.23 (d, J= 15.0 Hz, 2H), 2.45-2.50 (dd, J= 15.0, 5.5 Hz, 2H), 3.17-3.19 (d, 5.5 Hz, 2H), 7.06-7.08 (d, J= 8.1 Hz, 2H), 7.24-7.28 (m, 2H), 7.39-7.44 (m, 2H), 7.51-7.53 (d, J= 8.1 Hz, 2H), 7.68-7.70 (d, J= 8.1 Hz, 2H), 8.71-8.73 (d, J= 8.4 Hz, 2H); ^{1}H (400 MHz, toluene-d_8) δ 0.86 (s, 18H, tBu$_{2ax}$), 2.20-2.23 (d, J= 15.0 Hz, 2H, H$_{3ax}$), 2.44-2.49 (dd, J= 15.0, 5.5 Hz, 2H, H$_{3eq}$), 3.13-3.14 (d, J= 5.5 Hz, 2H, H$_{2eq}$), 7.04-7.06 (d, J= 8.1 Hz, 2H, H$_4$), 7.22-7.26 (m, 2H, H$_7$), 7.37-7.40 (m, 2H, H$_5$), 7.47-7.50 (d, J= 8.4 Hz, 2H, H$_8$), 7.63-7.65 (d, J= 8.4 Hz, 2H, H$_6$), 8.66-8.68 (d, J= 8.4 Hz, 2H, H$_9$); ^{13}C (75 MHz, $CDCl_3$) δ 29.7 (q), 34.0 (s), 34.7 (t), 57.7 (d), 122.9 (d), 124.6 (d), 124.7 (d), 127.2 (d), 127.9 (d), 128.3 (d), 129.0 (s), 132.9 (s), 140.9 (s), 141.3 (s), 143.0 (s); UV-Vis: (*n*-hexane) $\lambda_{max}(\varepsilon)$ 209 (115000), 223 (88700), 235 (35700), 239 (35100), 276 (11300), 349 (19700), 364 (22100); Resolution of stable *trans*-**3.31** was performed by chiral HPLC on a analytical scale using a Daicel Chiralcel OD column as the stationary phase and a mixture of heptane : *i*-propanol in a ratio of 99.75 : 0.25 as the eluent at a rate of 1 ml·min^{-1}. The first eluted fraction (t= 4.41 min) of *trans*-**3.31** contained (2*S*,2'*S*)-(*P*,*P*)-*trans*-**3.31**, the second fraction (t= 5.39 min) contained (2*R*,2'*R*)-(*M*,*M*)-*trans*-**3.31**; (2*S*,2'*S*)-(*P*,*P*)-*trans*-**3.31**: CD: (*n*-hexane): λ_{max} ($\Delta\varepsilon$) 216,6 (+136.4), 222.8 (-74.8), 229.0 (+50.4), 242.0 (-19.0), 250.2 (+46.0), 252.6 (+35.0), 259.2 (+158.7), 268.0 (+28.9), 278.6 (36.3), 326.6 (-11.8), 334.4 (-6.4), 346.6 (-19.6), 354.6 (-15.8), 362.2 (-21.8).

(2*S,2'*S**)-(*M**,*M**)-*cis*-(±)-2,2'-Di-*t*-butyl-2,2',3,3'-tetrahydro-1,1'-bicyclopenta[*a*]-naphthalenylidene (3.31)**

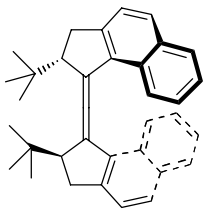

The compound was obtained pure by photochemical conversion and was not obtained from the synthesis. Preparation was performed by irradiation of the either pure (2*S*,2'*S*)-(*P*,*P*)-*cis*-**3.31** in *n*-hexane ($\lambda \geq$ 280 nm, T=0°C), or a mixture of racemic *cis*-**3.31** or *trans*-**3.31** in benzene-d_6 and toluene-d_8 at room temperature; ^{1}H (400 MHz, $CDCl_3$) δ 0.97 (s, 18H), 3.24-3.34 (m, 4H), 3.62-3.64 (d, J=7.0 Hz, 2H), 6.46-6.51 (m, 2H), 7.03-7.07 (m, 2H), 7.28-7.30 (d, J= 8.1 Hz, 2H), 7.42-7.44 (d, J= 8.1 Hz, 2H), 7.64-7.66 (d, J= 7.7 Hz, 2H), 7.70-7.72 (d, J= 8.1 Hz, 2H); ^{1}H (400 MHz, toluene-d_8) δ 0.96 (s, 18H), 3.17-3.20 (m, 4H), 3.60-3.62 (m, 2H), 6.39-6.44 (m, 2H), 6.83-6.87 (m, 2H), 7.24-7.26 (d, J= 8.1 Hz, 2H), 7.48-7.50 (d, J= 8.4 Hz, 2H), 7.54-7.56 (d, J= 8.1 Hz, 2H), 7.62-7.64 (d, J= 8.1 Hz, 2H); ^{1}H (400 MHz, benzene-d_6) δ 0.98 (s, 18H, t-Bu$_{2eq}$), 3.19-3.22 (m, 4H, H$_{3ax}$, H$_{3eq}$), 3.61-3.64 (m, 2H, H$_{2ax}$), 6.42-6.47 (m, 2H, H$_8$), 6.85-6.90 (m, 2H, H$_7$), 7.26-7.29 (d, J= 8.1 Hz, 2H, H$_4$), 7.53-7.56 (d, J= 8.1 Hz, 2H, H$_5$), 7.59-7.61 (d, J= 8.1 Hz, 2H, H$_6$), 7.73-7.75 (d, J= 8.4 Hz, 2H, H$_9$); ^{13}C (100 MHz,

$CDCl_3$) δ 27.9 (q), 29.8 (s), 30.2 (t), 55.6 (d), 123.1 (d), 124.8 (d), 124.9 (d), 129.0 (d), 130.2 (s), 133.9 (s), 139.2 (s), 143.9 (s), 148.2 (s); the spectrum was contaminated with a small amount of some hydrocarbon and two (d) were missing due to overlap with the toluene-d_8; *m/z* (EI, %) = 444 (M^+, 43), 387 (45), 331 (100). UV-Vis: (*n*-hexane) $\lambda_{max}(\varepsilon)$ 227 (70000), 289 (19100), 324 (9700), 481 (16100); The retention time of unstable (2*S*, 2'*S*)-(*M*,*M*)-*cis*-**3.31** is *t*= 11.36 min using a Daicel Chiralcel OD column as the stationary phase and a mixture of heptane : *i*-propanol in a ratio of 99.75 : 0.25 as the eluent at a rate of 1 ml·min^{-1}; (2*S*,2'*S*)-(*M*,*M*)-*cis*-**3.31**: CD: (*n*-hexane): λ_{max} ($\Delta\varepsilon$) 205.8 (+113.5), 223.0 (-157.7), 236.6 (+44.6), 262.4 (-9.5), 284.6 (+43.5), 303.0 (-8.8), 307.6 (-4.7), 327.0 (-12.5).

2,2'-Di-*t*-butyl-3*H*,3'*H*-[1,1']bi[cyclopenta[*a*]naphthalenyl] (3.32)

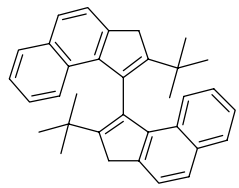

This compound was isolated after the photochemical reaction of olefin **3.31**; ^{1}H (400 MHz, $CDCl_3$) δ 1.14 (s, 18H), 3.68-3.74 (d, *J*= 23.1 Hz, 2H), 3.78-3.84 (d, *J*= 23.1 Hz, 2H), 6.95-6.99 (m, 2H), 7.20-7.24 (m, 2H), 7.65-7.68 (m, 4H), 7.77-7.80 (d, *J*= 8.4 Hz, 2H), 7.93-7.95 (d, *J*= 8.4 Hz, 2H); ^{1}H (400 MHz, toluene-d_8) δ 1.12 (s, 18H), 3.42-3.48 (d, 23.1 Hz, 2H), 3.55-3.61 (d, *J*= 23.1 Hz, 2H), 6.75-6.79 (m, 2H), 7.49-7.51 (d, *J*= 8.2 Hz, 2H), 7.57-7.59 (d, *J*= 8.2 Hz, 2H), 7.61-7.63 (d, *J*= 7.3 Hz, 2H), 8.19-8.21 (d, *J*= 8.8 Hz, 2H); one (m, 2H) was not observed due to overlap with the solvent. ^{13}C (100 MHz, $CDCl_3$) δ 29.7 (q), 31.0 (t), 109.7 (d), 121.9 (d), 123.8 (d), 125.0 (d), 125.1 (d), 128.4 (d), no (s) were observed due to small amount of material obtained. *m/z* (EI, %) = 442 (M^+, 100), 427 (47); HRMS (EI): calcd. for $C_{34}H_{34}$: 442.2661, found 442.2653.

3.6 References

1) N. Koumura, R. W. J. Zijlstra, R. A. van Delden, N. Harada, B. L. Feringa, *Nature* **1999**, *401*, 152-155.

2a) N. Koumura, E. M. Geertsema, A. Meetsma, B. L. Feringa, *J. Am. Chem. Soc.* **2000**, *122*, 12005-12006; b) N. Koumura, E. M. Geertsema, M. B. van Gelder, A. Meetsma, B. L. Feringa, *J. Am. Chem. Soc.* **2002**, *124*, 5037-5051; c) R. A. van Delden, A. Meetsma, B. L. Feringa, *Org. Bioorg. Chem.* **2003**, *1*, 33-35.

3) E. M. Geertsema, N. Koumura, M. K. J. ter Wiel, A. Meetsma, B. L. Feringa, *Chem. Commun*. **2002**, 2962-2963.

4) O. Kruber, *Ber.* **1933**, *66*, 1382-1396.

5) E. Campaigne, B. G. Heaton, *J. Org. Chem.* **1964**, *29*, 2372-2378.

6) S. Inaba, R. D. Rieke, *Synthesis*, **1984**, 842-844.

7) E. Fischer, J. Hagen, R. Jung, W. Knies, C. Kohl, F. Listmann, W. Neugebauer, T. Schulte, *Ber.* **1922**, *55*, 1833-1859.

8) W. Adcock, M. J. S. Dewar, R. Golden, M. A. Zeb, *J. Am. Chem. Soc*. **1975**, *97*, 2198-2205.

9a) M. K. J. ter Wiel, N. Koumura, R. A. Van Delden, A. Meetsma, N. Harada, B. L. Feringa, *Chirality* **2000**, *12*, 734-741; b) M. K. J. ter Wiel, N. Koumura, R. A. van Delden, A. Meetsma, N. Harada, B. L. Feringa, *Chirality* **2001**, *13*, 336.

10) D. A. Evans, M. D. Ennis, D. J. Mathre, *J. Am. Chem. Soc.* **1982**, *104*, 1737-1739.

11) D. A. Evans, J. M. Takacs, L. R. McGee, M. D. Ennis, D. J. Mathre, J. Bartroli, *Pure Appl. Chem.* **1981**, *53*, 1109-1127.

12) a) D. Enders, B. B. Lohray, *Angew. Chem.* **1987**, *99*, 359-360; b) D. Enders, H. Kipphardt, P. Fey; *Organic Synthesis*; Ed. E. Vedejs, Wiley, New York, **1987**, *65*, 183-202.
13) J. R. Gage, D. A. Evans; *Organic Synthesis*; Ed. J. P. Freeman, Wiley: New York, **1993**, Coll. Vol. VIII, 528-531; see chapter 2 for experimental data.
14) J. R. Gage, D. A. Evans; *Organic Synthesis*; Ed. J. P. Freeman, Wiley: New York, **1993**, Coll. Vol. VIII, 339-343.
15) *CRC Handbook of Chemistry and Physics **1993-1994***; Ed. D. R. Lide, CRC Press, Boca Raton, Florida, **1993**, 74, p 9-4.
16) Dr. A. J. R. L. Hulst is gratefully acknowledged for his help in performing the low temperature NMR studies.
17) These calculations were performed by Dr. M. G. Kwit.
18a) See for a general introduction concerning the stereochemistry of alkenes: E. L. Eliel, S. H. Wilen in: *Stereochemistry of Organic Compounds, Chapter 9: Stereochemistry of Alkenes*, Wiley, **1994**; b) For the case of stilbene: J. Saltiel, S. Ganapathy, C. Werking, *J. Phys. Chem.* **1987**, *91*, 2755-2758.
19) I. V. Komarov, *Russ. Chem. Rev.* **2001**, *70*, 991-1016.
20) H. Sakurai, H. Tobita, Y. Nakadaira, C. Kabuto, *J. Am. Chem. Soc.* **1982**, *104*, 4288-4289.
21a) S. C. Nyburg, *Acta Cryst.* **1954**, *7*, 779-780; b) N. A. Bailey, S. E. Hull, *Acta Cryst. B* **1978**, *34*, 3289-3295; c) N. A. Bailey, S. E. Hull, *Chem. Commun.* **1971**, 960-961.
22) E. Mollins, C. Miravitlles, E. Espinosa, M. Ballester, *J. Org. Chem.* **2002**, *67*, 7175-7178.
23) R. A. van Delden, M. K. J. ter Wiel, B. L. Feringa, *Chem. Commun*. **2004**, 200-201.
24) H. Suginome; *CRC Handbook of Photochemistry and Photobiology*, Eds. W. M. Horspool, P.-S. Song, Chapter 66: *E,Z-Isomerization of Imines, Oximes, and Azo Compounds*; CRC Press, Boca Raton, **1995**, 824-840.
25) A. D. Becke, *J. Chem. Phys*. **1993**, *98*, 5648-5652.
26a) R. Bauernschmitt, R. Ahlrichs, *Chem. Phys. Lett*. **1996**, *256*, 454-464; b) M. E. Casida, C. Jamorski, K. C. Casida, D. R. Salahub, *J. Chem. Phys*. **1998**, *108*, 4439-4449.
27) Gaussian 98, Revision A.10, M. J. Frisch, G. W. Trucks, H. B. Schlegel, G. E. Scuseria, M. A. Robb, J. R. Cheeseman, V. G. Zakrzewski, J. A. Montgomery Jr., R. E. Stratmann, J. C. Burant, S. Dapprich, J. M. Millam, A. D. Daniels, K. N. Kudin, M. C. Strain, O. Farkas, J. Tomasi, V. Barone, M. Cossi, R. Cammi, B. Mennucci, C. Pomelli, C. Adamo, S. Clifford, J. Ochterski, G. A. Petersson, P. Y. Ayala, Q. Cui, K. Morokuma, P. Salvador, J. J. Dannenberg, D. K. Malick, A. D. Rabuck, K. Raghavachari, J. B. Foresman, J. Cioslowski, J. V. Ortiz, A. G. Baboul, B. B. Stefanov, G. Liu, A. Liashenko, P. Piskorz, I. Komaromi, R. Gomperts, R. L. Martin, D. J. Fox, T. Keith, M. A. Al-Laham, C. Y. Peng, A. Nanayakkara, M. Challacombe, P. M. W. Gill, B. Johnson, W. Chen, M. W. Wong, J. L. Andres, C. Gonzalez, M. Head-Gordon, E. S. Replogle, J. A. Pople, Gaussian, Inc., Pittsburgh PA, **2001**.
28) C. Diedrich, S. Grimme, *J. Phys. Chem. A* **2003**, *103*, 2524-2539.
29) D. G. Botteron, G. P. Shulman, *J. Org. Chem.* **1962**, *17*, 1059-1061.